

**Fundamentals of process design and control of Anaerobic Sequencing Batch
Gas-Lift Reactor regarding the mixing process**

Von der Fakultät für Umwelt und Naturwissenschaften
der Brandenburgischen Technischen Universität Cottbus-Senftenberg
zur Erlangung des akademischen Grades eines
Doktor der Ingenieurwissenschaften

genehmigte Dissertation
vorgelegt von

MSc. Ing. Isabel Cristina Pulgarín Monsalve
aus Medellín, Colombia

Gutachter: Prof. Dr. rer. nat. habil Marion Martienssen

Gutachter: Prof. Dr. rer. nat. habil Birgit Kamm

Tag der mündlichen Prüfung: 23.04.2021

Acknowledgements

I thank Professor em. Dr. Ing. Habil. Busch for giving me the opportunity to be part of the group of students of the chair of waste management (Bioenergy), for allowing me to come to Germany to learn under his leadership about the world of bioenergy (Biogas and Biomethane), a topic that is still unknown in many Latin American countries, despite the fact that there is a high potential for utilization.

I would also like to thank Professor Dr. Ing Wagener - Lohse for his valuable contribution during his leadership of the chair, from his leadership in the FEE and his interest in realizing projects in Colombia.

To Professor Dr. rer. nat. habil Marion Martienssen and Prof. Dr. rer. nat. habil Birgit Kamm for agreeing to be the evaluators of this thesis.

To my office colleagues Dipl. Ing Heike Bischof and Dr. Ing. Jeannette Buschmann for their support and also for their leadership of the project before the FNR. To Dr. Ing. Marko Burkhard for his academic contributions and ideas as well as to Mandy.

To Ms. Nickel for her analytical rigor in the laboratory. And the experts in electromechanics Herr Klopchs and Martin for all their support in the construction and operation of the different reactors and equipment of this research.

To my student friends at the BTU in Cottbus for encouraging me and being part of this university experience and above all because they are still part of my life. Also, to the students who contributed to this research with the results of their Bachelor and Master projects.

To my angels in Germany, Mr. and Mrs. Eberhart and Ingrid Oettel for showing me their technical rigor, the true value of a German family and being my angels upon arrival, during my stay and departure from Germany.

To Christian, his father and family, to Sybille and her friends, for the experiences lived in the German culture.

To my great friends in Colombia to be always aware of the distance sending me their best energies.

To EPM/Colfuturo for the financing of my studies abroad. Finally, and most importantly to my family in Colombia, my parents and sister for so many years of absence abroad and their unconditional support in the most difficult moments.

List of content

1	Introduction and problem definition	10
2	Objectives and scientific innovation	16
3	State of science and technology	18
3.1	Anaerobic degradation of organic compounds	19
3.1.1	Biogas production	23
3.1.2	Biochemistry	24
3.2	Process control or Bioreactor types	26
3.2.1	Anaerobic Sequencing Batch Reactor (ASBR).....	26
3.2.2	Air/Gas Lift system.....	28
3.2.3	Dry/wet fermentation in two-stage-two-phase systems - hydrolysed production	35
4	Process principles.....	36
4.1	Stirring systems.....	36
4.1.1	Axial stirrers	36
4.1.2	Radial stirrers.....	39
4.1.3	Tangential stirrers	42
4.2	Stirring performance.....	44
4.2.1	Effect of the tank geometry.....	45
4.2.2	Reynolds number.....	47
4.3	Mixing times and homogenization	50
4.3.1	KCL tracer test.....	51
4.3.2	Colorimetric measurements - Fluorescent tracers	54

4.4	Rheology	55
5	Methodical approach.....	57
5.1	Analytical parameters.....	57
5.1.1	μ Viscosity	57
5.1.2	TS and OTS.....	59
5.1.3	COD (Chemical Oxygen Demand).....	59
5.1.4	PH.....	59
5.1.5	T°C	60
5.2	Operational variables	60
5.2.1	OLR	60
5.2.2	Hydraulic retention time (HRT)	61
5.2.3	Productivity (MBR CH ₄) and Methane Yield (Y CH ₄)	61
5.3	Mathematical models in ARL/GLR reactors hydrodynamics	62
6	Experimental design	64
6.1	Experimental configuration.....	65
6.1.1	Traditional stirred ASBR - single-stage processes.....	65
6.1.2	ASBR, ASBR+B and CSTR.....	67
6.1.3	Air/ Gas lift reactors	70
6.1.4	Mechanical stirring ST-ASBR	76
6.1.5	Comparison between KG-ASBR and ST-ASBR	77
6.2	Substrate Characterization.....	80
6.2.1	Substrate characterization – Organic food waste.	80
6.2.2	Substrate characterization - Hydrolysate of maize and grass silage produced at the GICON biogas plant.	82

6.2.3	Substrate characterization - Hydrolysate of maize silage produced at the BTU.....	83
6.3	Performance of the experimental execution	85
6.3.1	The ASBR – food waste cycle	85
6.3.2	The ASBR, ASBR+B and CSTR cycle.....	86
6.3.3	The KG – ASBR and ST – ASBR cycle	87
6.3.4	The ALR hydrodynamic flows characterization.....	88
6.4	Description of mathematical model in ALR.....	89
7	Results and discussion	95
7.1	ASBR Performance - single-stage processes	95
7.2	ASBR, ASBR+B, CSTR Performance – Methanation stage.....	96
7.3	ALR reactors performance	99
7.3.1	ARL hydrodynamic flows characterization	99
7.3.2	Homogenization and mixing time.....	100
7.3.3	Rheology performance in ALR.....	110
7.3.4	Performance mathematical simulation model	111
7.4	Comparison ST-ASBR and KG-ASBR reactors	119
7.4.1	Performance of operational and evaluation parameters	119
7.4.2	Comparison Mixing strategy	122
8	Conclusions and recommendations	125
9	Summary	128
	REFERENCES.....	129
	List of figures	136
	List of tables	138
	Annexes	139

Annex 1	KCl calibration curve.....	139
Annex 2	Uranine Video. For references please contact the author.....	141
Annex 3	Mathematical model.....	141
Annex 4	Graphics characterization flow in ALR.....	149
Annex 5	Conductivity and Homogenization data/graphics.....	152
Annex 6	Reactors comparison methane and productivity yield.....	163
Annex 7	Dynamic viscosity database	163
Annex 8	Reactors comparison OTS and TS database	163

List of symbols and abbreviations [Unit]

ALR:	Air Lift Reactor
ASBR:	Anaerobic Sequencing Batch Reactor
BTU:	Brandenburgische Technische Universität /Brandenburg University of Technology Cottbus – Senftenberg
<i>Cb</i> :	Bottom clearance [cm]
CCH ₄ :	Methane concentration
cm:	centimetre
COD:	Chemical Oxygen Demand
CSTR:	Continuous stirred-tank reactor
<i>Ct</i> :	Top clearance [cm]
d:	Days
<i>D</i> :	Reactor Diameter [cm]
<i>Dt</i> :	Draft tube diameter [cm]
D/T:	Impeller diameter to tank diameter ratio
EBA:	European Biogas Association
EEG:	Erneuerbare-Energien-Gesetzes/ German energy transition policy
FNR:	Fachagentur Nachhaltende Rohstoffe/Agency for Renewable Resources
GHG:	Greenhouse Gases
GLR:	Gas Lift Reactor
<i>HDt</i> :	Height of Draft tube [cm]
Ho:	Homogenisation
hp:	Horsepower ranges
HRT:	Hydraulic Retention Time [d]
KCL:	Potassium chloride
KG-ASBR:	Gas Lift - Anaerobic Sequencing Batch Reactor/ Kleingas ASBR
kg:	Kilogram

I:	Liter
LCFAs:	Long Chain Fatty Acids
m:	Meter
mg:	Milligram
MBR_{CH_4} :	Methane Productivity [$Nm^3_{CH_4}/(m^3_R \cdot d)$]
MC:	Methyl Cellulose
NI:	Normalized liters
O ₂ :	Oxygen
OLR/BR:	Organic Loading Rate/Organic Volume Load [$kg_{DM} m^{-3}d^{-1}$ or $kg_{COD} m^{-3}d^{-1}$]
OPEX:	Operating expense
oTS_{FM}	Organische Trockensubstanz/ Organic Dry Matter fresh mass
SDGs:	Sustainable Development Goals
ST-ASBR:	Traditional Stirred - Anaerobic Sequencing Batch Reactor
TS:	Trockensubstanz / Dry matter
VDt :	Draft tube volume [cm^3]
VDw :	Downcomer volume [cm^3]
$VolCb$:	Bottom clearance volume [cm^3]
$VolCt$:	Top clearance volume [cm^3]
VFAs:	Volatile Fatty Acids
W:	Impeller blade width
Y_{CH_4} :	Methane gas yield [normalized liters NI/($kg_{DS} \cdot d$) or NI/($kg_{COD} \cdot d$)]
Z:	Liquid depth
Z/D:	Liquid depth to tank diameter ratio
ρ :	Fluid density [g/cm^3]
μ :	Dynamic viscosity [$g/cm \cdot s$]
u :	Linear velocity [cm/s]
Re_{Dt} :	Reynolds number in Draft tube
δ :	Fixed value of deviation from homogeneity
\mathfrak{R}_s :	Region of scrutiny
C_T :	Concentration of tracer, mol/ m^3

1 Introduction and problem definition

In recent years, the consumption of fossil fuels has increased in such a way that the sustainability of the global energy system has been put at risk. For this reason, various international cooperation initiatives have been created that seek to encourage the increase of renewable energy projects and at the same time reduce the greenhouse gases (GHG) that are the main cause of global climate change; a concrete example of them is the Paris agreement or agreement on the United Nations framework convention for combating climate change, whose objectives are to keep the increase in global average temperature well below 2 °C, reduce the emission of GHG (mainly Methane CH₄ and Carbon Dioxide CO₂), as well as the increase in clean energy sources. As of March 2019, 195 states and the European Union have signed the Agreement (including Latin American countries such as Colombia)¹², establishing public policies that seek to diversify the global energy matrix in the coming years to the use of renewable energies.

Likewise, different research centres and academic institutions carry out scientific research to create new forms of energy through biotechnology, hydrogen conversion, CO₂ conversion, creation and optimisation of energy storage systems, use of new substitute materials and creation of bioenergy such biogas and biomethane. Germany is a leading country in the development of these and in the establishment of public policies that will make it possible to achieve this in the short, medium and long term as established by the latest Renewable Energy Sources Act 2017 (Erneuerbare-Energien-Gesetz -EEG) or German energy transition policy that includes strengthening German companies through innovation in the energy sector.

¹ "Paris Agreement". United Nations Treaty Collection.
https://treaties.un.org/pages/ViewDetails.aspx?src=TREATY&mtdsg_no=XXVII-7-d&chapter=27&clang=_en
march 2019.

² "European 20-20-20 Targets". Retrieved 13 April 2019.

It is also the European country with excellent development in bioenergy³, and with the highest number of biogas and biomethane plants installed, according to the latest report of the European Biogas Association (EBA) - statistical report 2018⁴.

For biogas and biomethane to be competitive with other renewable energy technologies that predominate worldwide, such as photovoltaics and wind power, and to survive the auctions of the energy market, it is necessary to continue working on the optimization of biogas production processes based on the anaerobic digestion of biomass, in order to make it an increasingly efficient and cheaper process. Biogas production processes can be used for production of heat or electricity, generation of biomethane as a substitute for fossil natural gas or to increase the production of biomethane with the same CO₂ content of biogas using Power-to-Methane (P2M) technology.

Thus, in the waste department of the Brandenburg University of Technology BTU – Cottbus Senftenberg, research is being carried out on biogas and biomethane to optimize processes and achieve better efficiency and lower costs. Specifically, this research sought to evaluate the mixing optimization process of an Anaerobic Sequencing Batch Reactor (ASBR) that has existed for more than 25 years patented by (Dague, R, 1993), but which is widely used on an industrial scale mainly for the anaerobic digestion of domestic wastewater treatment plants, food processing plants, pharmaceuticals and other biotechnological industries.

There are numerous scientific papers describing the operating conditions of ASBR reactors, normally associated with mechanical mixing; while pneumatic mixing processes have been sparsely studied, as it is not very common to find them at the industrial level in existing plants; but is also possible be done pneumatically by

³ RENEWABLES 2019 GLOBAL STATUS REPORT

https://www.ren21.net/gsr2019/chapters/chapter_03/chapter_03/ (accessed 25/06/19)

⁴ EBA Statistical Report 2018 http://biogas.org.rs/wp-content/uploads/2018/12/EBA_Statistical-Report-2018_European-Overview-Chapter.pdf (accessed 26/06/19)

pumping in biogas or by using the autonomously generated gas pressure for pump work (SCHÖNFETER, R *et al.* 2007).

Due to the above, the Waste Management Chair of the BTU works in cooperation with the planning and consulting company GICON GmbH as it was done previously in other investigations with successful results, for example, in the double-stage solid–liquid biogas process from solid waste and biomass. In this process, due to the strong separation of hydrolysis and methanation, the process is extremely stable and stirrers or other agitation equipment are not necessary; only liquids are pumped and therefore the energy consumption lowered. (BUSCH, G.; *et al.* 2009).

In this research focuses especially on the optimization of mixing processes in ASBR reactors, since mixing at an industrial level is one of the processes that consumes most economic resources in the operation and maintenance of biogas plants currently installed (BUSCH, G.; *et al.* 2009, KOWALCZYK, A.; *et al.* 2013). Optimization enhancement of this method is also very important in order to stabilize the process, to ensure that there are no disturbances in microbial development, homogenize the mixture and promote high levels of biogas production, high productivity and methane yield, and also, to achieve a desired energy efficiency in renewable energy plants from biomass.

The following is a summary of the experiments carried out at the laboratory level, using different types of ASBR reactors in three phases of the research:

In the first phase of the research, the performance of a traditional ASBR reactor mechanically mixed was tested in the liquid single stage fermentation of organic food waste, using domestic wastewater as inoculum of the process and simulating the substrate as the typical composition of municipal organic waste from the city of Medellín in Colombia.

In 2015 Colombia adopted the 17 Sustainable Development Goals (SDGs), because of this the United Nations Development Programme - UNDP supports the country in its effort to achieve them through the use of integrated solutions with the collaboration of government, private sector, civil society and citizens. Hence, in 2018

the Colombian government defined 169 aims to achieve these objectives by 2030. Goal No. 07 seeks to promote affordable and clean energy, so the government has decided to encourage the growth of non-conventional energy projects, which by the end of 2014 only represented less than 2% of total energy produced in the country⁵, the rest was equivalent to the production of energy with huge hydroelectric projects 70% and 30% in thermoelectric power generation. However, in 2016-2017, the country faced threats of rationing and power cuts in the cities due to a prolonged climatic phenomenon called "El Niño" that cause severe drought conditions which took the response capacity of the interconnected system to the limit. It is therefore essential to have additional capacity of renewable energy that is based on non-conventional sources, which are counter-cyclical in periods of drought.

In 2014, the government issued Law 1715 through which it regulates the integration of non-conventional renewable energy to the national energy system (including energy from biomass, solar, wind, tidal, geothermal and small hydro plants), which is why in 2019 made the first energy auction in the country to ensure clean energy in the coming years, with a goal of increasing from 22.4 MW in 2018 to 1,500 MW of clean energy by 2022.

Taking into account the great opportunities that the country has in terms of available biomass (not only for the organic urban waste sector but also for all the energy potential of the residual biomass in Colombia's agricultural and livestock sector), the exploitation scenarios are increasingly close, not only for the opportunities to generate bioenergy but also for the possibilities of obtaining biofuels for sustainable mobility, developing employment for the region and having the possibility of producing renewable natural gas (biomethane) as a substitute for fossil natural gas.

⁵ Source: Colombian National Planning Department (DNP – Departamento Nacional de Planeación) and Mining-Energy Planning Unit (UPME – Unidad de Planeación Minero Energética). hydroelectric power plants above 10 MW are excluded.
http://www.upme.gov.co/Estudios/2015/Integracion_Energias_Renovables/INTEGRACION_ENERGIAS_RENOVANLES_WEB.pdf

To materialize this goal, the government has incorporated actions in the national development plan (for the years 2018-2022) to increase the participation of bioenergy (biofuels, biogas, among others) in the country's energy matrix.

In the specific case of Medellín, in the next four years (2020-2023), priority will be given to renewable energy projects in the city. For this reason, this research included a pilot biogas production project with an ASBR using a substrate that is compositionally comparable to the municipal organic waste produced in the large food markets that supply the city; although in this first phase it used an ASBR reactor with a traditional mixing system and single-stage process that does not have scientific purposes that can provide criteria for comparison for the following phases of this research, it serves to provide criteria for analysing the potential of this type of substrate and possible future cooperation between Germany and Colombia for the development of projects in the fields of bioenergy, energy efficiency, circular economy and sustainable mobility.

In order to compare obtained data with other data obtained in projects that the waste management chair has carried out previously, in the second phase of this research the substrate was changed to maize silage since it has been widely studied and therefore there are elements of scientific comparison, just as the research was concentrated in a process where the stages of biogas production are separated in different vessels.

The second phase of the research, compared the methanation of the hydrolysate maize silage (obtained in a double-stage solid-liquid process) in three reactors: the first with the traditional design of an ASBR, the second reactor is the same ASBR with addition of packaging material (expanded clay) and the third reactor with the traditional design, but operated as a Continuous Stirred-Tank Reactor CSTR.

In the third phase, the topic of main scientific interest of this research was developed, comparing the methanation of the hydrolysate maize silage⁶ in two reactors operated simultaneously. The first so called traditional stirred (ST-ASBR) reactor mixed with mechanical agitation while the second reactor mixed with innovative pneumatic agitation with a concentric draught tube (internal loop configuration) and using the same biogas produced in a Gas Lift Reactor (KG-ASBR). Frequency, time and mixing velocity were compared in order to analyse the influences on biogas production, productivity and methane yield (MBR_{CH_4} , Y_{CH_4}), hydraulic retention time (HRT), organic loading rate (OLR), as well as some energy consumption associated with each type of mixture. Finally, a hydrodynamic analysis of the pneumatically mixing was performed in a new Air-Lift Reactor -ALR, on a larger scale but with the same innovative design of KG-ASBR, to analyse the operation of the system with a Newtonian fluid (air-water system) and a non-Newtonian fluid (air- Methyl Cellulose MC) in order to gather parameters and patterns of rheological behaviour required in the further industrial scale-up to be carried out by GICON GmbH.

The following chapters present the objectives of this scientific research, the state of the art or theoretical foundations with emphasis on ASBR reactors, Air/Gas Lift systems and on the hydrodynamic analysis of the mixing processes, followed by the methodology and detailed description of the experiments including the design of each reactor. Results of the three segment mentioned above, including a mathematical model that simulates the performance of the reactor with the innovative pneumatic mixing system will be elaborated afterwards. Finally, the conclusions and recommendations of the research are presented.

⁶ Also obtained in the same double-stage solid-liquid process of the second phase.

2 Objectives and scientific innovation

The aim of the research is the creation of bases for the design and process control of an Anaerobic Sequencing Batch Reactor on a laboratory scale in order to find the optimal operating regime and optimize the process of mixing.

Scientific and technical objectives of the research include the developing innovative solutions for mixing the reactor ASBR (gaslift system with a concentric draught tube configuration which enables the gas may be sparged either the draught tube or the annulus), achieving homogenization of the mixture with less energy consumption.

The mixing in the ASBR gaslift reactor is influenced by heavy turbulence and the hydraulic conditions of the system. If the innovative mixing technology works as optimal, back to the conversion of traditional Biogas plants under the continuously stirred tank reactor (CSTR) concept can be easily modified without changing major infrastructure to gaslift system. In contrast to the known technique of agitation (mechanical agitation), in this research is desired to study the vertical movement (axial) of the liquid from the bottom to the upper end of the riser. Therefore, the sedimented biomass and undigested solids may rise quickly and mixed with the feed substrate.

This study also includes the analyse of the hydrodynamic performance of the Air Lift system by means of gas flow determination in the riser, the evaluation of the liquid circulation velocity in the downcomer and the influence of the vertical draft tube and the effect of top and bottom clearance. The hydrodynamic parameters developed in this research will be mathematical modelled with the aim of valid the mixing optimization processes in this type of reactor.

For scientific analysis purposes, experiments of the mixing process in ASBR reactors will be performed using a substrate that has been extensively studied in the BTU waste management chair in previous dissertations, as is the case of maize silage.

It is already known that the process works optimally by separating the hydrolysis and methanization phases in a solid - liquid fermentation (Buschamann, J. 2015), so this research will use the same process to obtain the maize hydrolysate and concentrate in the mixing phase of the methanization stage.

However, in the initial phase of the design of experiments, an analysis of the performance of the traditional ASBR reactor mechanically mixed with a substrate that simulates the composition of organic waste from the city of Medellín in Colombia will be included, due to the fact that never before had experiments been carried out to find solutions at the laboratory level to use the organic biomass of food waste from this city using an ASBR reactor and to test if it is feasible to implement projects that allow solutions to be proposed to the problem of final waste disposal that it possesses.

3 State of science and technology

Thousands of oil platforms exist globally, which provides the oil for about 50000kWh of energy per year. Yearly, around US\$10 bn are spend in drilling for new oilfields to secure the supply of oil and hence the basis for industrial growth in the future (DEUBLEIN, D, *et al.* 2014). However, as with all fossil resources, the quantity of oil is limited and will not last forever. With the declining quantity of fossil fuels, it is critical today to focus on sustained economic use of existing limited resources and on identifying new technologies and renewable resources, for example, biomass, for future energy supply.

There is a lot of projections for energy supply in the future scenarios, different companies like Shell International has published a projection for different energy sources for the years from 1990 up to 2100 (from primary energy sources from 100.000 TWh/a to 450.000 TWh/a respectively). Further, by 2020 the technologies around renewable sources are spectated to have reached the potential for full economic use. Shell foresees fast grow for these future alternatives and has projected that by 2050 the regenerative energy resources will provide 50% of the total energy consumption worldwide. Another projection of energy supply in the future was made by the IPCC (International Panel on Climate Change) expects a threefold higher energy consumption by 2100 (referring back to 1990), providing a high demand. With sustained economic use of energy, calculations suggest that almost 30% of the total global primary energy consumption in 2050 will be covered by regenerative energy sources. In 2075, the percentage will be 50%, and it is expected to increase continuously up to 2100. According to the IPCC report, biomass is going to play the most important role, projected to deliver 50000 TWh in

2050, 75000 TWh in 2075, and 89000 in 2100, in line with the calorific value derived from the combustion of more than 16 bn Mg of wood. .⁷

Germany and government initiative such as Fachagentur Nachwachsende Rohstoffe e. V. (FNR - The Agency for Renewable Resources) works to optimize the processes of obtaining renewable energy, including the obtaining of biogas and biomethane from the anaerobic degradation of organic materials. These programs are necessary to achieve the government's objectives of producing 80% of energy from renewable energy by 2050 (EEG Law).

To achieve these goals, it is important to continue working on the optimization of biogas production from biomass and understand well its biochemistry and formation from the anaerobic degradation of organic compounds such as food waste and maize silage.

3.1 Anaerobic degradation of organic compounds

Anaerobic treatment is one type of biological treatment potentially applicable to organic compounds. This treatment has considerable advantages such as low energy requirements and nutrients, low amount of sludge, small reactor volumes, odors reduction and diminution of total solids by converting part of the volatile solids into biogas (RIOS, A. 2015)

The anaerobic degradation of organic compounds to methane is also known as methanation and takes place in four stages. In this process, fats, carbohydrates and proteins are broken down into low molecular substances by special microorganisms. The gas mixture that results from these biological processes usually consists of 50-75 volume % methane (CH₄), 25-50 volume % carbon dioxide (CO₂) and small proportions of trace gases, nitrogen and oxygen. Figure 1 shows the four steps of

⁷ <https://www.shell-wollishofen.ch/div/weltenergieverbrauch.htm>; https://www.wsa.rwth-aachen.de/uploads/tx_inetfiles/skript_ft_kap2_20-11-06.pdf 2006. Deublein, D, et al. 2011.

anaerobic degradation of organic compounds: hydrolysis, acidification, acetogenesis and methanogenesis. (FNR, 2018)

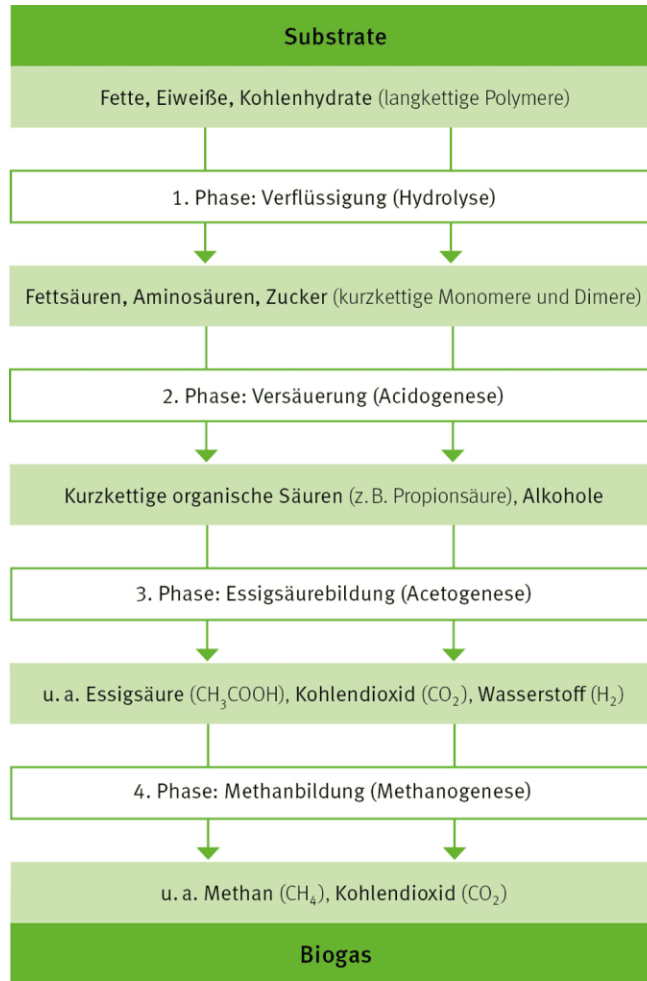


Figure 1 Representation of the fermentation process.
Source FNR Web site 2018.

Some authors describe five steps for solid organic substrates. (MANJUSHA, *et al.* 2016). This classification describes the five main biochemical steps (involving biological enzymes) in an anaerobic digester. It starts with disintegration, followed by hydrolysis, acidogenesis, acetogenesis and methanogenesis. The process can be described by the following steps Figure 2:

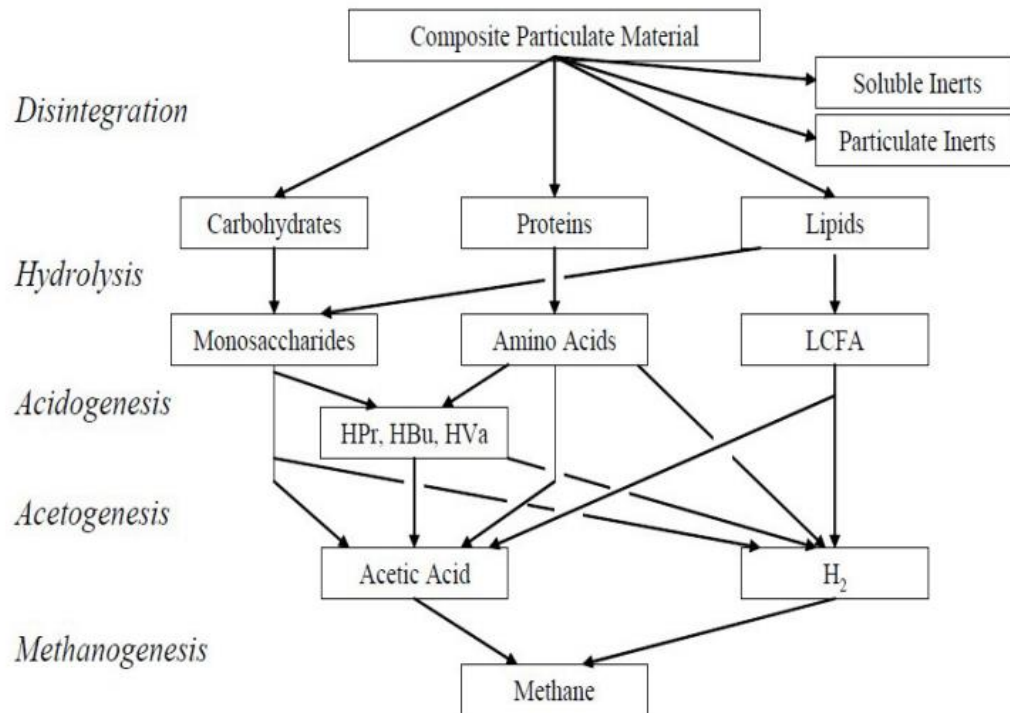


Figure 2 Biochemical steps in an anaerobic digester
 Source (MANJUSHA, *et al.* 2016)

In the **disintegration** step, complex biomass molecules are broken down to lipids (e.g. fats), carbohydrates and proteins.

There are many reasons for adding disintegration devices to a normal biomass fermentation plant, but there are some reasons against it. Some advantages are: The disintegration is helpful above all, if biomasses are difficult to destroy because increase the degree of decomposition and decrease the amount of sewage sludge (inoculum), increase the biogas yield (also after a thermal disintegration of 55°C), the products of disintegration can serve as a hydrogen source or electron donor for the denitrification of waste water, also the sedimentation behaviour of the sludge is improved, the formation of foaming and floating sludge in the reactor can be considerable reduce and sometimes even completely avoid, finally disintegration lower the viscosity of the sludge. (DEUBLEIN, D, *et al.* 2011)

However, disintegration have some disadvantages like the affects the dehydratability and increase the demand of flocculants in this process and increase the filtration resistance and the power consumption.

In the first phase of this research a mechanical disintegration process was made to the substrate of organic municipal solid waste, the substrate was sliced into cubes of no more than 0.5 cm in length. This size pre-condition was necessary to ensure a high amount of surface readily available for microorganisms to settle and thus enhance degradation per volume unit.

In **hydrolysis**. Molecules of carbohydrates, lipids and proteins are broken down to long chain fatty acids (LCFAs), amino acids and sugars. This decomposition is converted by hydrolytic bacteria, which release certain enzymes, in a biochemical process.

Long-chain carbohydrates present in insoluble structures such cellulose, hemicellulose, and starch are broken down by hydrolases, resulting in short chain sugars; proteins are broken down into amino acids by proteases; fats are broken down into fatty acids and glycerine by lipases.

The hydrolysis of carbohydrates take place within a few hours and the hydrolysis of proteins and lipids within a few days. The facultative anaerobic microorganisms use up the oxygen dissolved in the water, thus including the low redox potential required by obligatorily anaerobic microorganism. The enzymes derive from both facultative and obligatory anaerobic bacteria.

In **acidogenesis**, these LCFAs, amino acids and sugars are broken down to volatile fatty acids (VFAs), namely propionate, valerate, butyrate, some acetate and acetic acid, as well as hydrogen and carbon dioxide. Alcohols and lactic acids are also produced here in small quantities. (MANJUSHA, *et al.* 2016)

The monomers formed in the hydrolytic phase are taken up by different facultative and obligatory anaerobic bacteria and are degraded in the second, acidogenic, phase to short chain organic acids (VFAs). The concentration of the intermediately

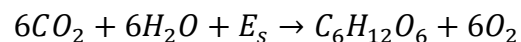
formed hydrogen ions affects the kind of fermentation products. The higher the partial pressure of hydrogen, the fewer reduced compounds, such as acetate, are produced. (DEUBLEIN, D, *et al.* 2011)

These VFAs are then transformed into acetate in the **acetogenesis**. In the acetic acid-forming stage, the acidification products are further broken down into acetic acid, hydrogen and carbon dioxide. This reaction is carried out by acetogenic bacteria. Hydrogen partial pressure can be of great importance in this context. If the hydrogen content is too high, this can prevent the reaction of acidogenesis intermediates for energy reasons. In conclusion, organic acids (e.g. capronic and propionic acids) would accumulate and inhibit methane formation. This means that the hydrogen-forming acetogenic bacteria must be in a suitable, optimised biocoenosis with the methanogenic archaeae (hydrogen-consuming).

In the **methanogenesis** the acetate is finally transformed into methane gas and carbon dioxide. In methane formation, the methanogenic archaeae use carbon dioxide as well as hydrogen, which ensures that acetic acid-forming bacteria have acceptable environmental conditions. (BUHLE, 2016; DEUBLEIN, D, *et al.* 2011; MANJUSHA, *et al.* 2016).

3.1.1 Biogas production

Biogas results from the microbial degradation of biomass, formed by photosynthesis by solar power E_s :



carbon dioxide + water + "sun" solar energy → sugar(glucose) + oxygen

Metabolic process in the plants transforms the following compounds into precursor products:

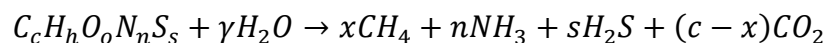
- Carbohydrates: Starch, inulin, cellulose, sugar, pectin

- Fat: fat, fatty acids, oil, phosphatides, waxes, carotene
- Protein: Protein, nucleoprotein, phosphoprotein
- Others: vitamins, enzymes, resins, toxins, essential oils.

During the metabolism of the sugar, the plants releases energy, when necessary, to the environment, so that the possible energy yield from plants may vary greatly.

3.1.2 Biochemistry

With the help of an approximate equation from Buswell in 1936, the theoretical maximum yield of methane can be estimated taking the elementary composition as a base. The formation of methane from biomass follows in general the equation (SPYRIDON, *et al.* 2016 and DEUBLEIN, D, *et al.* 2011):



Where

$$x = 1/8(4c + h - 2o - 3n - 2s)$$

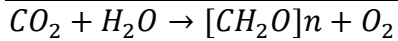
$$\gamma = 1/4(4c - h - 2o + 3n + 2s)$$

The secondary products include the following:

- Carbohydrates: $C_6 H_{12} O_6 \rightarrow 3 CH_4 + 3 CO_2$
- Fat: $C_{12} H_{24} O_6 + 3 H_2 O \rightarrow 7.5 CH_4 + 4.5 CO_2$
- Protein: $C_{13} H_{25} O_7 N_3 S + 6 H_2 O \rightarrow 6.5 CH_4 + 3 NH_3 + H_2 S + 6.5 CO_2$

The result in general is biogas composition of $CH_4:CO_2 = 71\%:29\%$. The ratio of CO_2 to CH_4 is determined by the reduction ratio of the organic raw material.

The energy balance can be calculated as first the organic material, which is built up by photosynthesis:



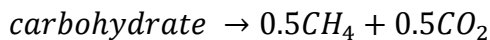
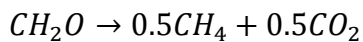
carbon dioxide + water + "sun" energy → carbohydrate + oxygen

Contains the energy

$$(-394kJ) + (-237kJ) + (Gibbs\ free\ energy\ \Delta G'_f/mol) \rightarrow (-153\ kJ) + 0kJ$$

$$\Delta G'_f = 478\ kJmol^{-1}\ at\ pH = 7$$

Second the degradation of the organic material to biogas

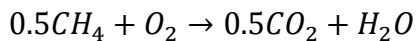


Results in release of energy:

$$(-153kJ) \rightarrow 0.5(-51\ kJ) + 0.5(-394\ kJ)$$

$$\Delta G'_f = -70\ kJmol^{-1}$$

Third on combusting methane, CO₂ and H₂O are formed, which can serve for photosynthesis



$$0.5(-51kJ) + 0kJ \rightarrow 0.5(-394\ kJ) + (-237\ kJ)$$

$$\Delta G'_f = -408\ kJmol^{-1}$$

and finally, the energy cycle is closed. Overall, any of the substances is thus enriched or lost.

When 1 kmol glucose is degraded to CO_2 and H_2O , 478 kJ kmol^{-1} of carbon can be gained as free energy, while the burning of 0.5 kmol of methane results in 408 kJ kmol^{-1} . Thus, the methane produced contains 85% of energy content of glucose. As shown by energy balances, very little heat is released with the anaerobic bioreaction. Therefore, bioreactors must be heated and well insulated.

However, the heat energy which is produced during the biogas production is not completely used, and the conversion to biogas is not complete. The volume of biogas which can be gained from substrates that is gain depends of the fraction of the material with high energy content in the organic mass, the content of the ODM in the total dry biomass, the DM content of the substrate, methane content of the biogas and the degree of decomposition of the respective biogas plant.

3.2 Process control or Bioreactor types

3.2.1 Anaerobic Sequencing Batch Reactor (ASBR)

The Anaerobic Sequencing Batch Reactor (ASBR) operates by sequential batches, has been studied as an alternative treatment for different systems because of their versatility. Introduced by Dague in 1991, operates in a single vessel on a fill-and-draw basis in a sequential manner. The ASBR is applicable for the conversion of a wide variety of organic wastewaters to methane and carbon dioxide (biogas). In the process, both biological contact and solids and liquid separation take place in one vessel, which facilitates the conversion to methane and carbon dioxide (Dague, R. 1993).

The principal advantages of the ASBR technology compared to other reactor systems are the relatively simple operation, the flexibility, a high biomass retention and the correspondingly high efficiency as well as a low investment expenditure for single-stage process control by implementing a sequential sequence of different

processes in one reactor. The ASBR process also has the potential to revitalise the process in the event of faults due to overloading of the reactor (Buschmann, J. 2015).

There are also other advantages, such as work under a wide range of mesophilic or thermophilic temperature range, are a good removal of biodegradable substances, high biogas production, and relatively low running costs, due to the lack of a forced aeration system (Rios, A. 2015).

The main factors affecting the overall performance of the ASBR are: agitation, Substrate/Biomass ratio, geometric configuration of the reactor and the feeding strategy, among others (FARINA, R *et al.* 2004).

The ASBR cycle or sequence is divided in four steps: feeding, intermittent mixing (react), settling time (settle), and effluent withdrawal (decant). In the feed stage, a specific amount of substrate is fed to the reactor, usually simultaneously to mixing. Secondly, during the reacting step, the reactor contents are mixed intermittently, so that the feed is in contact with the sludge; this is the most important step for the conversion to biogas and also the longest one. Thirdly, the settle step involves no mixing, so that the biomass sediments and a separation of liquid above and sludge below exists, making it easier for the decantation of the supernatant at the top (Riffat, R. 2013, Rios, A. 2015). These steps can be visualized in Figure 3:

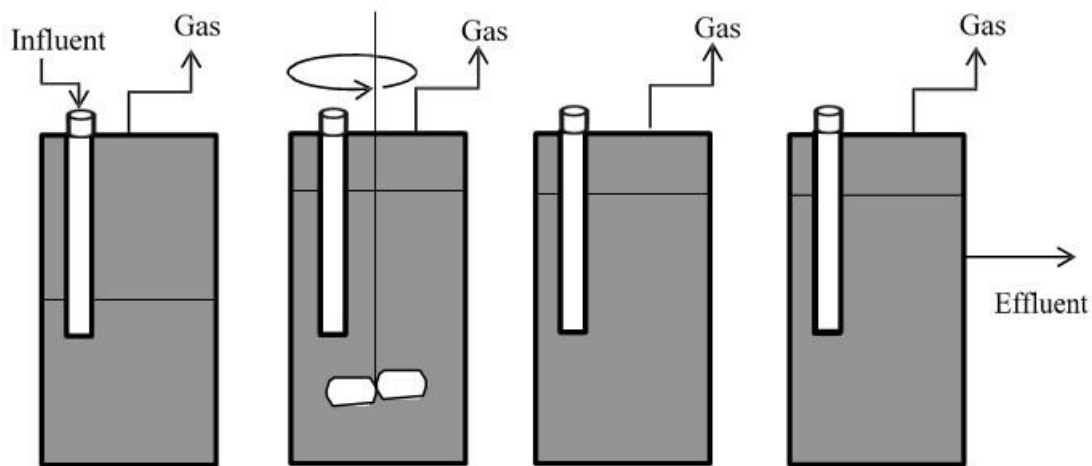


Figure 3 The four steps of an ASBR: feeding, intermittent mixing, settling time, and withdrawal.

Source (Rios, A. 2015).

Continuous mixing in the reactor is unnecessary, and it has been proven that intermittent mixing yields the same or better results than continuous mixing. An effective mixing system, however, is crucial, since it provides contact between the substrate and microorganisms, minimizes inhibitory reaction intermediaries, and in general stabilizes environment conditions (Dague, R. 1993; Rios, A. 2015).

This research investigates the change from the traditional mechanical mixing used in ASBR reactors to a pneumatic mixing mechanism, the strategy agitation is carried out by use of a gaslift system coupled to an ASBR with a concentric draught tube (internal loop configuration). The gaslift consist of a liquid pool divided into two distinct zones. The part of the reactor containing the gas-liquid upflow is the raiser and the region containing the downflowing fluid is known as the downcomer. The theoretical operating principle of these systems is described in detail below.

3.2.2 Air/Gas Lift system

The term air lift reactor (ALR) cover a wide range of gas-liquid or gas-liquid-solid pneumatic contacting devises that are characterized by the fluid circulation in a define cyclic pattern through channels built specifically for this purpose. In ALR, the content is pneumatically agitated by a stream of air or sometimes by other gases in those cases, the name gas lift reactors have been used gas lift reactor (GLR). In addition to agitation the gas stream has the important function of facilitating exchange of material between gas phase and the medium. (Merchuk, J.C.; *et al.* 1999). The GLR is a further development of the simple bubble column reactor and uses the principle of the "mammoth pump". Here, the flow of the liquid is generated by a gas. However, the flow follows a prescribed path and circulation is forced. (

The first clearly defined air-lift reactor was that patented by Le Francois in 1955. Initially, the device was mainly applied for large-scale microbiological processes,

such as single cell protein production. The reason for the suitability of the air-lift reactor for cell cultures is the relative mildness and uniformity of the turbulence in the air-lift system, compared with conventional bubble columns (which are also pneumatically agitated in a simple vessel into which gas is injected, usually at the bottom, and random mixing is produced by ascending bubbles) and continuous stirred tank reactors (CSTR). The characteristics of the flow in a properly designed ALR minimize the shear related damage to the cells. (Le Francois.; *et al.* 1955; Wood, L.A.; *et al.* 1987 and LeMerchuk, J.C.; *et al.* 1988).

Low shear fields, good mixing and extended aseptic operation made possible by elimination of stirrer shafts, seals and bearings are important advantages of ALR in fermentation applications, a wide variety of biological and chemical process. Continuous production of beer, vinegar, citric acid, and biomass from yeasts, bacteria and fungi has been carried out in airlift vessels. (CHISTI, M, *et al.* 1987)

In the ALR, the major patterns of fluid circulation are determined by the design of the reactor, which has a channel for gas-liquid up flow (the riser) and a separate channel for the downflow. The two channels are linked at the bottom and at the top to form a closed loop (Figure 4). The gas is usually injected near the bottom of the riser. The extent to which the gas disengages at the top, in the section termed the gas separator, is determined by the design of this section and the operating conditions. The fraction of the gas that does not disengage but is entrapped by the descending liquid and taken into the downcomer, has a significant influence on the fluid dynamics in the reactor and hence on the overall reactor performance. (MERCHUK, J.C.; *et al.* 1999).

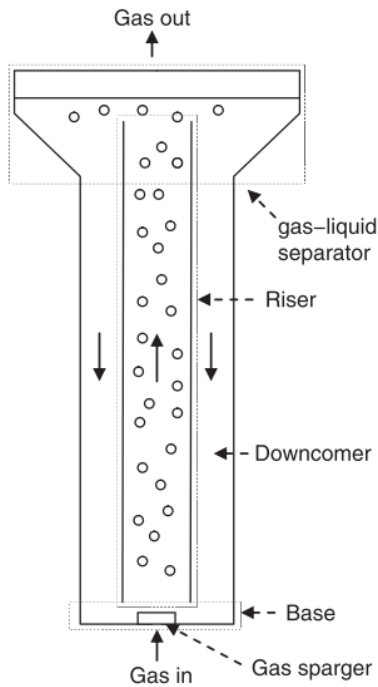


Figure 4 ALR configuration
Source: (MERCHUK, J.C.; *et al.* 1999).

Airlift reactors can be divided into two main types of reactors on the basis of their structure Figure 5: external loop vessels, in which circulation takes place through separate and distinct conduits; and baffled (or internal-loop) vessels, in which baffles placed strategically in a single vessel create the channels required for the circulation. The designs of both types can be modified further, leading to variations in the fluid dynamics, in the extent of bubble disengagement from the fluid, and in the flow rates of the various phases. (MERCHUK, J.; *et al.* 2010).

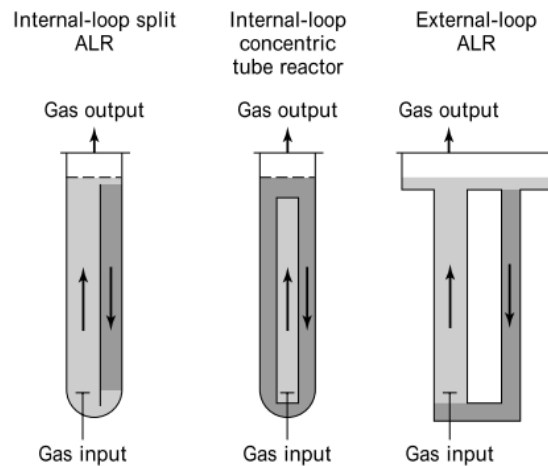


Figure 5 Different types of ALR

Source: (MERCHUK, J.; *et al.* 2010).

All ALRs, regardless of the basic configuration (external loop or baffled vessel), comprise four distinct sections with different flow characteristics:

Riser. The gas is injected at the bottom of this section, and the flow of gas and liquid is predominantly upward.

Downcomer. This section, which is parallel to the riser, is connected to the riser at the bottom and at the top. The flow of gas and liquid is predominantly downward. The driving force for recirculation is the difference in mean density between the downcomer and the riser; this difference generates the pressure gradient necessary for liquid recirculation.

Base. In the vast majority of airlift designs, the bottom connection zone between the riser and downcomer is very simple. It is usually believed that the base does not significantly affect the overall behavior of the reactor, but the design of this section can influence gas holdup, liquid velocity, and solid phase flow.

Gas separator. This section at the top of the reactor connects the riser to the downcomer, facilitating liquid recirculation and gas disengagement. Designs that allow for a gas residence time in the separator that is substantially longer than the

time required for the bubbles to disengage will minimize the fraction of gas recirculating through the downcomer. (MERCHUK, J.; *et al.* 2010).

Pneumatically agitated bioreactors take advantage of the injection of a gaseous stream (often air) to provide mixing and mediate transfer of gaseous substances (i.e., O₂ and CO₂) with the liquid phase. However, unlike in classical pneumatically agitated reactors where liquid mixing is random (i.e., bubble column), the specific design of airlift reactors (ALRs) causes the liquid to circulate between two interconnected zones known as the riser and the downcomer. The riser and the downcomer are connected by a specific reactor base allowing for liquid circulation and by a gas–liquid separator at the top. Under typical operation conditions, air is injected below the riser section and the removal of gas in the separator generates a mean density gradient between the riser and downcomer zones that causes the liquid broth to circulate. The function of the gas separator is to support efficient gas–liquid disengagement. The fraction of gas introduced in the downcomer section depends on design and operational variables. This fraction has a significant effect on fluid dynamics and, consequently, reactor performance. The focalized introduction of energy for mixing in classical bioreactors generates large shear gradients that cause cells to experience mechanical stress in areas of high turbulence and suboptimal solutes concentrations (i.e., O₂, CO₂, H⁺, and toxins etc.) and or temperature conditions in areas of low turbulence. By contrast, liquid circulation between the riser and the downcomer (rather than gas injection) is the main contributor to fluid dynamics in ALRs. Because liquid circulation is caused by the gradient between the average fluid densities in the two reactor sections, there is no focal point of energy dissipation and shear forces are very homogeneous within each section, causing less cellular stress. The ALRs also supposedly support higher mass-transfer rates per energy input than classical systems and transfer efficiency (i.e., the amount of O₂ transferred per power input) is much less affected by power input in ALRs than in classical systems. The two main advantages of ALRs described here explain why these systems are often preferred for the cultivation of shear-

sensitive mammalian and plant cells or during wastewater treatment applications requiring efficient energy use (aeration costs represent roughly 50% of the energy costs during domestic wastewater treatment).

Research and development on ALRs has hitherto focused in demonstrating the potential of this system in new applications or modeling the complex relationships between design and operational parameters and fluid dynamics and mass transfer. Many experimental and mechanistic models that can describe ALR operation and performance are thus available [3]. However, the validity of these models is too often limited to specific applications or reactor configurations. For this reason, only the most relevant, widely accepted, and generic models are presented here in order to illustrate how design and operational parameters influence fluid dynamics and mass-transfer properties.

The design of Airlift Reactors for a given range of operation variables implies the selection of a set of geometrical parameters. Different types of geometric influences have been studied, such as effect of the ratio of the cross-sectional area of a riser to that of a downcomer, the slenderness ratio, the height of the reactor, the design of the gas-separation section at the top of the reactor and the design of the bottom section on the performance of the reactor. (CHISTI, M, *et al.* 1987; SIEGEL M, *et al.* 1986).

All the above stress the importance of geometry in the scale up of Airlif reactors. The principal changes encountered when passing from laboratory to a larger scale are in the fluid dynamics of the system. Therefore, one of the most important factors in the design and scaleup of reactors is the influence of the geometry of the system on the flow of different phases present. (Merchuk, J.C, *et al.* 1994)

One of the most important factors in the design and scale-up of reactors is the influence of the geometric characteristics of the system on the flow of the different phases present. The interconnections between the design variables, the operation variables and the observable hydrodynamic variables in a concentric tube ALR are sketched in Figure 6. The design variables are: the reactor height, the riser-to-

downcomer area ratio, the geometrical design of the gas separator, and the bottom clearance (C_b , the distance between the bottom of the reactor and the lower end of the draft tube, which is proportional to the free area for flow in the bottom, and represents the resistance to flow in this part of the reactor). The main operation variable is the gas input rate, and to a lesser extent the top clearance (C_t , the distance between the upper part of the draft tube and the surface of the non-aerated liquid). These independent variables set the conditions which determine the liquid velocity in the ALR, via the mutual influences of pressure drops and hold-ups shown in Figure 6. The viscosity is not shown as an independent variable because it is a function of the gas hold-up (and liquid velocity in the case of non-Newtonian liquids), and also because in a real process it will change with time due to the changes in the composition of the liquid.

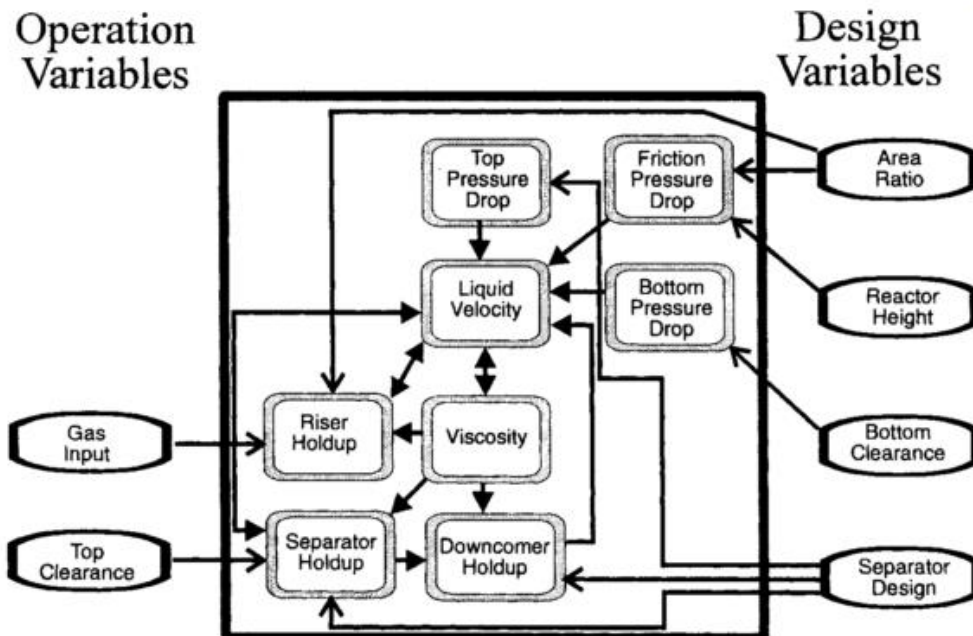


Figure 6 Operation and design variables of ALR
Source: (MERCHUK, J.; *et al.* 1996)

3.2.3 Dry/wet fermentation in two-stage-two-phase systems - hydrolysed production

The total biogas process can be understood as a sequence of at least four consecutive steps: (1) enzymatic decomposition of the polymers ("fermentation"), (2) formation of organic (fatty) acids (acidogenic step), (3) conversion of monomers and higher organic acids into acetic acid (acetogenic step), and (4) methane generation (methanation step). The first two run best under acidic conditions while methanation requires a neutral environment. It is successful to group these steps requiring similar parameters within a particular process stage. Here, step one and two are combined as hydrolysis stage and step three and four as methanation stage. Hence, the two stages are operated under ideal conditions. The hydrolysate as intermediate product connects both stages. For the hydrolysis of solid biomaterial, a percolation system should be preferred in which the solid remains in rest as a fixed bed and the liquid (percolate, hydrolysate) percolates that fixed bed. The hydrolysate is almost solid free. At the end of the process, the remaining solid can be discharged easily and completely (Busch, G. *et al.* 2009). This hydrolysate (of maize silage) was used like substrate in the methanation stage in reactors KG-ASBR and ST-ASBR that will be explain in detail in numeral 6.1 of this research.

4 Process principles

4.1 Stirring systems

In accordance with the various fields of application for agitators, a large number of agitators have been developed over time. However, the various forms can be traced back to a few basic types if they are classified according to the primary flow direction:

4.1.1 Axial stirrers

An axial-flow impeller is one in which the principal locus of flow occurs along the axis of the impeller (parallel to the impeller shaft); include the propeller, often designed on basis of the screw theory, which requires a constant pitch across the face of the blade. This means there is a continuous increase in blade angle from the blade tip to the hub (Figure 1 a and b).

Pitch-to-diameter ratio is equal to the distance, in impeller diameters, that an impeller would advance for each revolution when rotated in a fluid body. For example, if the pitch ratio of a propeller is 1.0, it means that it would generate a path equal in length to its diameter for each propeller revolution. The pitch ratio of most axial-flow impellers is usually between 0.5 and 1.5 times the diameter.

Propellers draw less power than most other impellers of the same diameter, running at the same speed. Therefore, compared with other impellers, propellers must run at much higher speeds to achieve a given horsepower. This results in low torque at a given power level and also results in a very economical series of mixers called portables. Portable mixers are so named because in the smaller sizes they are easily moved about; larger sized, however, require mechanical means to carry them from

one position to another. This kind of mixer is usually available in fractional and integral horsepower ranges, to a maximum of 5 hp (Figure 7 – c and was using in the experimental designs chapter 6.1.4 -ASBR Mechanical stirred).

At higher horsepower, portables give way to fixed-mounted mixers with gearboxes (speed reducers). These usually run at much lower output speeds than portables and at higher horsepower-to-speed ratios (higher torque for a given horsepower). This also means larger axial -flow impellers are required for a given horsepower. Higher torque and larger impellers notwithstanding, these mixers provide high process efficiency and excellent overall mechanical and operating characteristics. (OLDSHUE, J.Y 1983)

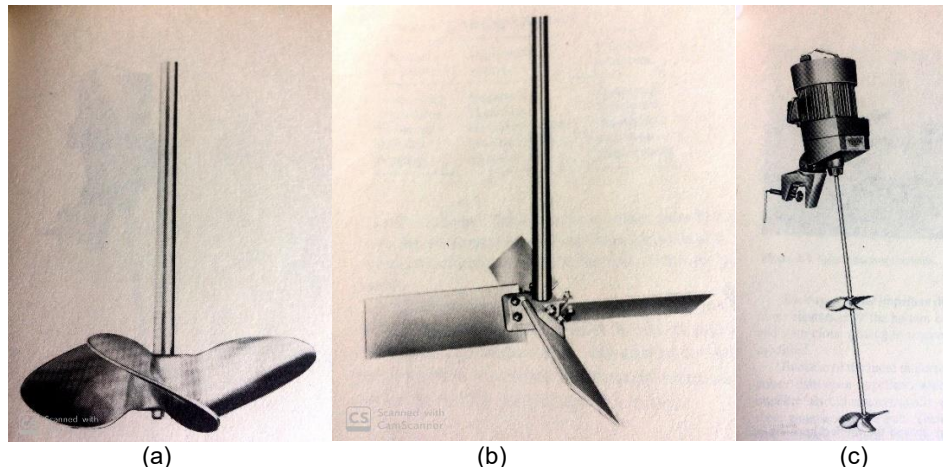


Figure 7 Axial flow impellers. (a) Marine-type impeller; (b) Typical axial-flow turbine; (c) Portable mixer.
Source (OLDSHUE, J.Y 1983)

Axial flow impellers are used for blending, solids suspension, solids incorporation or draw down, gas inducement, and heat transfer. The oldest axial flow impeller design is the marine propeller (Figure 7 - a), which is often used as a side-entering mixer in large tanks and as a top-entering mixer in small tanks. It can be designed with a different pitch to change the combination of pumping rate and thrust. Due to its fabrication by casting, a propeller becomes too heavy when large. It is not generally used as a top-entering impeller for tank sizes larger than 5 ft.

A pitched blade turbine (Figure 8 - a) consists of a hub with an even number of blades bolted and tack-welded on it. It is lighter in weight than a propeller of the same diameter. The blades can be at any angle between 10 and 90° from the horizontal, but the most common blade angle is 45°. The flow discharge from a pitched blade impeller has components of both axial and radial flow velocity in low to medium viscosity liquids and is considered to be a mixed-flow impeller. Most applications require the impeller rotation to direct the flow toward the bottom head or down-pumping. However, in some situations, such as gas dispersion and floating solids mixing, up-pumping may be more effective.

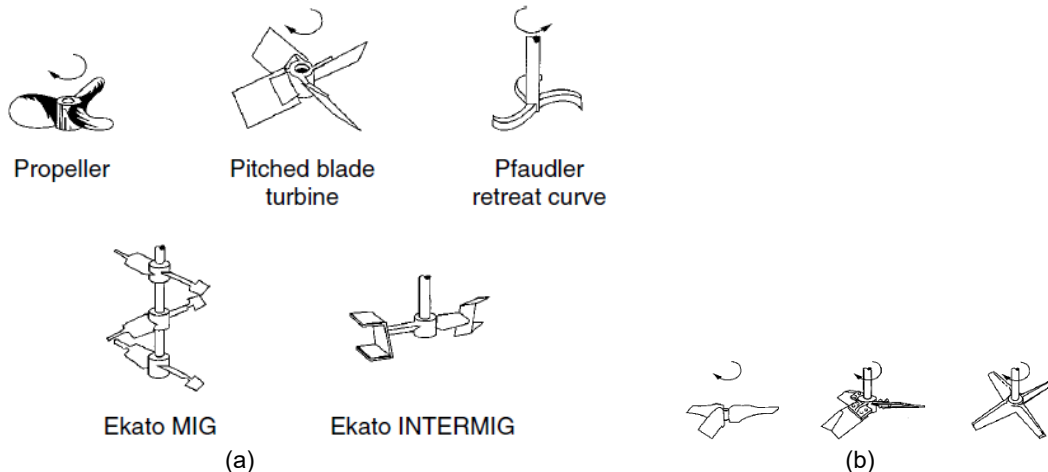


Figure 8 Axial impellers examples (a) including hydrofoil impellers(b)
Source (PAUL, E.D.; *et al.* 2004).

The retreat blade impeller was developed by the Pfaudler Company specifically for glass-lined reactors used for highly corrosive fluids. The Ekato Company developed two two-blade axial flow impellers, the Mig and the Intermig, mainly for high viscosity liquids (Figure 8). However, they can be effective for low to medium viscosity liquids as well. These impellers are designed at high impeller/tank diameter ratio (D/T) and have two sections of blades at opposite angles. If the inner blade pumps down, the outer blade pumps up to enhance the liquid circulation. The outer blade section of Intermig has two staggered sections designed for minimizing local form drag losses,

which results in more distinct axial flow and a lower power number. Three Mig impellers are recommended for a liquid height/tank diameter ratio (H/T) of 1.0, while two Intermig impellers are adequate for the same configuration. Both impellers are sized at $D/T = 0.7$ for turbulent conditions and require wall baffles. For laminar conditions, $D/T > 0.7$ is used without wall baffles. These impellers have been found to be excellent for crystallization operations because they combine low shear with good circulation (PAUL, E.D.; *et al.* 2004).

For applications where axial flow is important and low shear is desired, Hydrofoil impellers were developed. They have three or four tapering twisted blades, which are cambered and sometimes manufactured with rounded leading edges. The blade angle at the tip is shallower than at the hub, which causes a nearly constant pitch across the blade length. This produces a more uniform velocity across the entire discharge area. This blade shape results in a lower power number and higher flow per unit power than with a pitched blade turbine. The flow is more streamlined in the direction of pumping, and the vortex systems of the impeller are not nearly as strong as those of the pitched blade turbine (Figure 8- b).

4.1.2 Radial stirrers

Radial flow impellers may either have a disk (a) or be open (b) and may have either flat or curved blades. Open impeller types (without the disk) do not normally pump in a true radial direction since there is a pressure difference between each side of the impeller. They tend to pump upward or downward while discharging radially (Figure 9). Disk-type radial impellers do tend to pump in more radial direction, although at close clearances at the bottom of the tank or at close proximity to the liquid surface, and with close spacing to adjacent disk impellers, their radial pumping capacities are modified.

Because of the more uniform radial-flow pattern, disk impellers tend to draw more power than open impellers, which affects the economy of their application. The disk impeller also characteristically prevents gas bubbles from passing through the low shear zone around the hub. Therefore, they have been used essentially for gas-liquid-type mixing processes. The use of large-diameter radial flow impellers is typified in the two-blade paddle, which is typical of solid suspension or blending applications where high flow and low shear rates are the requirement (c). These impellers normally operate at low speeds, because that is what the process condition usually requires. Low speed is further necessary because the two-blade impeller is mechanically more unstable than the more common four-to eight-blade impellers. (OLDSHUE, J.Y 1983)

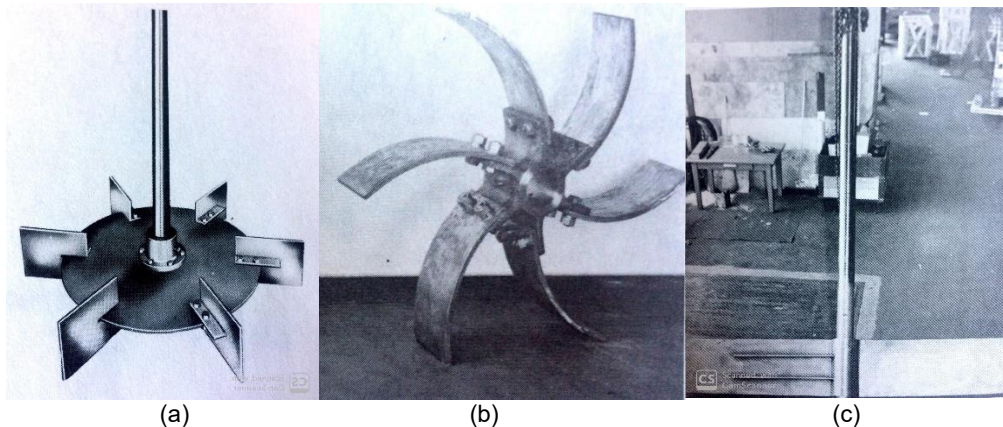


Figure 9 Radial-flow impellers. (a) Flat-blade turbine; (b) Spiral backswept turbines; (c) Paddle impeller.

Source (OLDSHUE, J.Y 1983)

Like axial flow turbine impellers, radial flow impellers are commonly used for low to medium viscosity fluids. Although they can be used for any type of single- and multiple-phase mixing duty, they are most effective for gas-liquid and liquid-liquid dispersion. Compared to axial flow impellers, they provide higher shear and turbulence levels with lower pumping.

Radial flow impellers discharge fluid radially outward to the vessel wall. With suitable baffles these flows are converted to strong top-to-bottom flows both above and below the impeller. Radial flow impellers may either have a disk (Rushton turbine) or be open and may have either flat or curved blades (backswept turbine) (Figure 10). Impellers without the disk do not normally pump in a true radial direction since there is pressure difference between each side of the impeller. This is also true when the impellers are positioned in the tank at different off-bottom clearances. They can pump upward or downward while discharging radially. Radial discharge flow patterns can cause stratification or compartmentalization in the mixing tank. Disk-type radial impellers provide more uniform radial flow pattern and draw more power than open impellers. The disk is a baffle on the impeller, which prevents gas from rising along the mixer shaft. In addition, it allows the addition of a large number of impeller blades. Such blade addition cannot be done easily on a hub. A disk can also be used with a pitched blade turbine for use in gas–liquid mixing.

The Rushton turbine is constructed with six vertical blades on the disk. Standard relative dimensions consist of blade length of $D/4$, blade width of $D/5$, and the disk diameters of $0.66D$ and $0.75D$. The backswept turbine has six curved blades with a power number 20% lower than the Rushton turbine. The backswept nature of the blades prevents material build up on the blades. It is also less susceptible to erosion. Typical applications include general waste and fiber processing in pulp and paper industries.

The developed hollow-blade impellers (Scaba SRGT, Chemineer CD6, and the Smith impeller) provide better gas dispersion and higher gas-holding capacity than the Rushton turbine. The impeller blades are semicircular or parabolic in cross-section. This general shape allows for much higher power levels to be obtained in the process than that obtained by the Rushton turbine during gas dispersion.

The coil or spring impeller was developed for systems where solids frequently settle to the tank bottom. When buried in stiff solids, a spring impeller is able to dig itself out of the solids without breaking an impeller blade (PAUL, E.D.; *et al.* 2004).

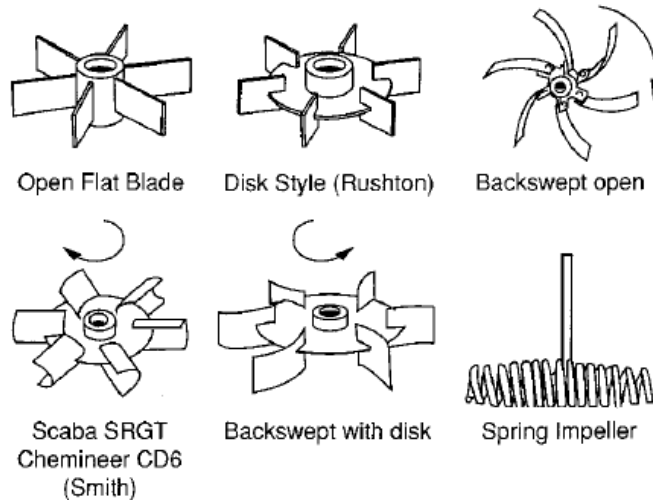


Figure 10 Radial impellers examples
Source (PAUL, E.D.; *et al.* 2004).

4.1.3 Tangential stirrers

Flow is entering in tangential direction with respect to position of blades on the rotor. Tangential stirrers include the bar turbine, the name is because blades are made from square bar stock, it also produces the highest shear rates of basic impellers, are also called high-shear impellers and because of the relatively high speeds, smaller gearboxes are required at a given power level, due to the lower torque (Figure 11). High-shear impellers are operated at high speeds and are used for the addition of a second phase (e.g., gas, liquid, solid, powder) in grinding, dispersing pigments, and making emulsions. These dispersing impellers are low pumping and therefore are often used along with axial flow impellers for providing both high-shear and homogeneous distribution. (PAUL, E.D.; *et al.* 2004).

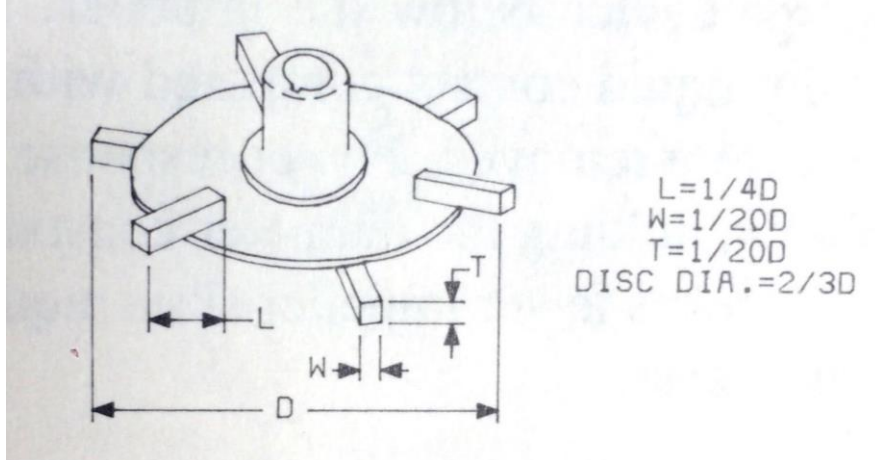


Figure 11 Bar turbine, six blades bolted/welded to top and bottom of support disk.

Source (OLDSHUE, J.Y 1983)

Another typical representative of impellers with tangential flow are the anchor which generally consists of two blades arranged parallel to the shaft, used for higher viscosity applications. These are connected via a cross bar following the contour of the vessel bottom. The anchor impeller has a small wall clearance. Its main task is to reduce the thickness of the highly viscous boundary layer adhering to the vessel wall in order to intensify the heat exchange. Finger or frame impellers have properties similar to anchor impellers.

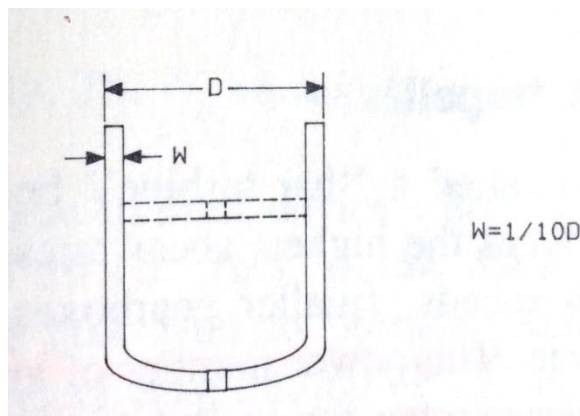


Figure 12 Anchor, two blades with or without cross arm.

Source (OLDSHUE, J.Y 1983)

Mixing processes normally need both flow and various levels of fluid shear rate and turbulence. Thus, the design criterion which maximizes flow at the expense of all other head, shear, or turbulence losses is not applicable in every mixing situation. This is in contrast to the design of pumps, where pumping capacity, system head developed, and hydraulic efficiency are the first criteria. The mixing impeller is not normally confined in a casing or a channel as with a pump.

It is also common, to put axial flow impellers in draft tubes, that is a circular duct usually a vertical, cylindrical tube with diameter slightly larger than the impeller diameter and a height less than the height of the fluid in the tank; this draft tube define a total top-to-bottom circulation pattern in a mixing tank that can be used effectively for many kinds of flow-controlled processes. In this case, there is a defined channel or conduit; so, measurements of impeller pumping efficiency are meaningful and can be used for overall design.

A draft tube is useful in directing liquid flow to and from an impeller where such direction is necessary or desirable. For example, when an impeller must be used in a tank which has a high ratio of tank height to diameter, the draft tube can ensure good top-to-bottom mixing. These devices deliver the highest flow per power of any mixing device available (OLDSHUE, J.Y 1983).

4.2 Stirring performance

The influence of tank geometry and the placement of the mixing system has a great influence on the performance of the reactor. Below are the most common relationships that have been studied for systems with mechanical agitation and vertical cylindrical tanks, as this type of geometry was used in the reactors studied in this research.

4.2.1 Effect of the tank geometry

A conventional stirred tank consists of a vessel equipped with a rotating mixer. The vessel is generally a vertical cylindrical tank. The rotating mixer has several components: an impeller, shaft, shaft seal, gearbox, and a motor drive. Wall baffles are generally installed for transitional and turbulent mixing to prevent solid body rotation and cause axial mixing between the top and bottom of the tank. In tall tanks, the mixer may be installed from the bottom to reduce the shaft length and provide mechanical stability. The mixers can be side entering for large product storage and blending tanks or inserted from the top at an angle for nonbaffled small tanks. The flows generated with side entering and angled mixers are asymmetric, and therefore wall baffles are no longer needed. A vertical, cylindrical tank with a liquid-height-to-tank-diameter ratio (Z/D) equal to 1 is often used as a base point for describing and effect of geometry. For blending and solid suspension, the optimum liquid-depth-to-tank diameter ratio Z/D for minimum power is usually about 0.6 to 0.7. While this may be the ratio for minimum power consumption, it may not represent the minimum Z/D for equipment cost or tank cost. Other factors may enter into the choice of tank shape and batch geometry. The placement of an impeller is more often governed by the requirements for mixing during draw-off (emptying the vessel) than by optimum process conditions. For example, for blending, the optimum impeller position for $Z/D=1$ would be at the midpoint of the liquid depth. However, this is seldom practical since tanks must usually be mixed during draw off. However, the midpoint position should be considered for a continuous flow process tank (OLDSHUE, J.Y. 1983; PAUL, E.D.; *et. al.* 2004).

There are many forms of tank bottoms such as spherical or cone-shaped, however, the commonly used are horizontal cylindrical tank, there is not reason why horizontal cylindrical tanks bottoms cannot be used for adequate mixing. There are, however, some special considerations for solid suspension since some kinds of flow patterns

tend to increase the likelihood of suspended solids settling out in remote corners of the tank.

Regarding to top and bottom clearance regions in GLR, bottom clearance (C_b) refers to the ungasged vertical height of liquid above and below the draft tube, respectively. It is within these distances that the moving liquid makes a 180° turn in direction. Therefore, the shorter these distances become, the greater is the impedance to the liquid's momentum caused by increased loss of kinetic energy. The position of the draft tube in regard to top and bottom clearance or spacing has been reported to be an important parameter. Liquid circulation flow rate becomes higher as the distance between the upper end of the draft tube and the liquid surface lengthens, and this effect continues until the space is double the column diameter, thereafter liquid circulation velocity does not change. Bando, Hayakawa, and Nishimura (1998) found that mixing time increased with: increasing column diameter; increasing column aspect ratio (height to diameter); lower surface tension and viscosity; and top and bottom clearance. They found that mixing time decreased as the bottom clearance increased, but when the bottom clearance gets too large, part of the gas from the sparger can get directly into the annulus which reduces the driving force and liquid velocity. This may be dependent on the placement of the distributor.

In general, the rheological properties of the liquid have much less impact when the bottom clearance is larger. The bottom clearance exerts an influence in all three areas, such that by increasing bottom clearance, riser gas hold-up decreases, as the liquid circulation velocity increases due to less flow restriction. Increasing bottom clearance, increased the downcomer gas hold-up because the increase in liquid circulation velocity increased carryover of entrained bubbles to the downcomer from the riser. Top clearance moderately influenced riser and total gas hold-ups, while it had no effect on downcomer gas hold-up. Increasing top clearance reduces gas hold-up by increasing residence time in the gas-liquid Separator section (MERCHUK, J. *et al.* 1994).

Generally, there is a more pronounced dependency of air flow rate on circulation time at low airflow ranges. This is because higher airflow rates enhance gas entrainment into the downcomer, reducing density differences and liquid circulation velocity. Freitas and Teixeira (1998) found that the density of the solid had a significant influence on circulation time when either the riser superficial velocities are low, or when solids loading is high, at which time circulation time increased by increasing the solids density.

4.2.2 Reynolds number

A number of dimensionless parameters have been developed for the study of fluid dynamics that are used to categorize different flow regimes. These parameters, or numbers, are used to classify fluids as well as flow characteristics (PAUL, E.D *et al.* 2004). One of the most common of these is the Reynolds number, the existence of the two types of flow, namely, laminar and turbulent, was first established by Osborne Reynolds in 1883. Also, it was indicated by Reynolds that at low velocities of flow, even for the fluids having very small viscosity, the viscous forces become predominant and, therefore, the flow is largely viscous in character. However, at higher velocities of the flow the inertia forces have predominance over the viscous forces. Reynolds related the inertia to viscous forces and arrived at a dimensionless parameter as follows (SAHU, G.K. 2008):

$$Re = \frac{\text{Inertia Force, } F_i}{\text{Viscous Force, } F_v}$$

Re number is defined as the ratio of inertial forces, or those that give rise to motion of the fluid, to frictional forces, or those that tend to slow the fluid down. In geometrically similar domains, two fluids with the same Reynolds number should behave in the same manner. For simple pipe flow, the Reynolds number is defined as:

$$Re = \frac{\rho U D}{\mu}$$

where ρ is the fluid density, U the axial velocity in the pipe, D the pipe diameter, and μ the molecular or dynamic viscosity of the fluid. For mixing tanks, a modified definition is used:

$$Re = \frac{ND^2\rho}{\mu}$$

where N is the impeller speed, in rev/s, and D is the impeller diameter. Based on the value of the Reynolds number, flows fall into either the laminar regime, with small Reynolds numbers, or the turbulent regime, with high Reynolds numbers. The transition between laminar and turbulent regimes occurs throughout a range of Reynolds numbers rather than at a single value. For pipe flow, transition occurs in the vicinity of $Re = 2000$ to 4000 , while in mixing tanks, it usually occurs somewhere between $Re = 50$ and 5000 , depending on the power number of the impeller. (PAUL, E.D *et al.* 2004).

Due to the geometry of the reactors used in this research and the hydrodynamic studies in the ALRs and GLRs, flow characterization by Reynolds number determination were performed on pipe flows.

The Reynolds number characterizes turbulence in any given pipeline flow or mixing device. It is instructive to consider first the empty or unpacked pipe and look at the classic experiment by Osborne Reynolds (1883). His demonstration consisted of flowing water through a clear glass tube with capability to vary the water flow rate to achieve a broad range of fluid velocity. At the centre of the tube a fine jet of water-soluble dye is introduced through a capillary tube so that a thin filament of dye injected coaxially into the stream of water has a velocity equal to that of the water at

the point of introduction. Figure 13 (a) shows that at low water velocity the dye filament retains its identity in the water stream, tending to widen very slightly during the downstream passage because of molecular diffusion of the dye into the water. At a slightly higher mean velocity as shown in Figure 13 (b), the dye filament breaks up into finite large eddies. Further downstream the eddies break up further, and the dye that has been introduced tends to become homogeneously dispersed or mixed with the water. At much higher mean velocity, Figure 13 (c) the eddy activity becomes extremely violent, and the region of homogeneous dye colour approaches the point of dye entry. From visual observation it is evident that the eddies in normal pipe flow were on the order of one-tenth the pipe diameter and move in completely random patterns. Subsequent experiments showed further that eddy formation was influenced by system factors such as pipe wall finish, vibration, dissolved gases, and other factors. Abnormal or metastable flow aside, it was shown that an upper limit of viscous flow and a lower limit of turbulent flow seemed to exist and that the limits were separated by a transition region.

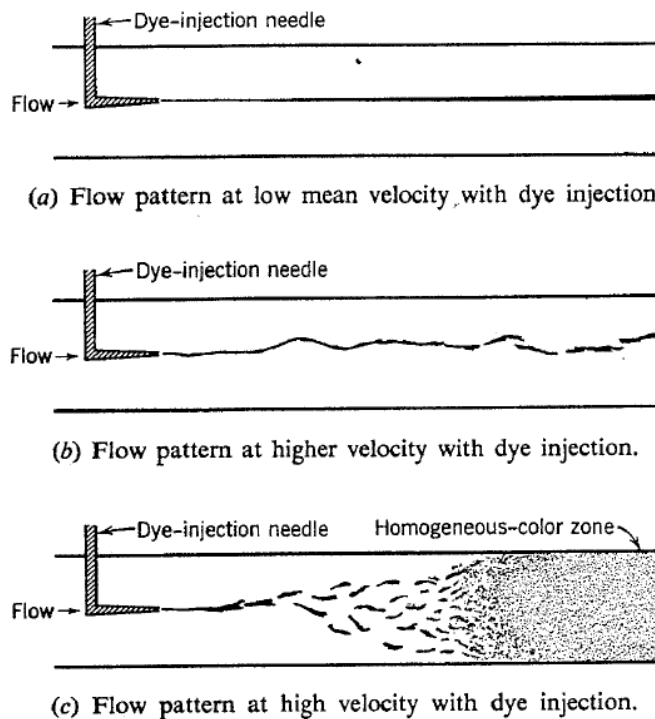


Figure 13 Reynolds experiments

Source: (PAUL, E.D *et al.* 2004)

In the turbulent range (very high Reynolds numbers), power number is essentially constant; so, viscosity has no effect on power draw in that range of Reynolds numbers. In passing through the transitional range to the laminar range the effect of viscosity on power consumption becomes increasingly significant. At very low Reynolds numbers (the laminar range), power number varies inversely with Reynolds numbers (or directly with viscosity, everything else remaining constant). (OLDSHUE, J.Y. 1983).

4.3 Mixing times and homogenization

The mixing time is a useful quantity for measurement of the blending of a phase. However, it is difficult to compare the mixing times obtained by different researchers because they are strongly dependent on the definition and method of measurement of the system non-homogeneities, the probe type, the device used to introduce the tracer, its location, among others. It is important to distinguish between methods which require the presence of a chemical reaction, i.e. chemical methods like decolorization method, pH metric method, and those in which a reaction is absent, i.e. physical methods like thermic method, conductimetric method. In physical methods, the tracer is injected into the system. One or more probes in the reactor measure a quantity which is proportional to the concentration of the tracer; in this case the mixing time is the time interval from the introduction of the tracer to a fixed deviation from homogeneity. (Manna, L. 1997).

Determining the mixing time by the physical method and using the Potassium Chloride (KCL) as a tracer, the experimental tests of this research were done. Additional test was performed with a fluorescent tracer (Uranine without LIF), that is, an optical and colorimetric method that sought to know the flow patterns inside the

reactor. In the numeral 6.1.3.1, it is shown the experimental configuration that was carried out at laboratory level. The optical and colorimetric methods are based on the fluorescence of a dye that emits light of a certain wavelength when excited by a laser beam. In fact, highly accurate results can be obtained in this way, but the high cost and effort involved Laser Induced Fluorescence, (LIF) and the optical accessibility of the reactors are often the obstacles in using this method in day-to-day practice (Manna, L. 1997 and MEUSEL, W *et al.*, 2016).

4.3.1 KCL tracer test

Exist four different methods of introducing the tracer into the system – pulse input, step input, periodic input and random input (Figure 14). Data obtained from pulse and step input are easier to interpret than from periodic or random input. Injecting the tracer as a step input requires a constant concentration of the tracer substance in the feed stream until the same tracer concentration can be detected in the effluent. (LEVENSPIEL 2012 and DIERCKS, K. 2017). Therefore, in this investigation the addition of the tracer in the ALR reactor was done by the pulse input method, besides injecting it just below the draft tube, because as it happens with the process of feeding the reactors, some authors as PAUL, E.D.; *et al.* 2004, argue that should be located in a highly turbulent region for processes requiring quick dispersion of the feed, the inlet nozzle should be sized to prevent back mixing of the tank contents into the inlet pipe, where lack of mixing may cause poor process results.

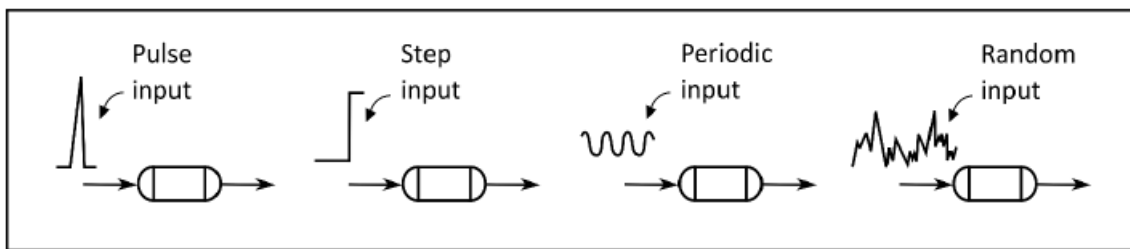


Figure 14 Injection methods for tracer

Source: (LEVENSPIEL 2012)

According to (MERCHUK, J.; *et al.* 1996) recommendations, tracers should be injected with pressure to minimize the injection time. Some gas was also injected to 'wash' the line and avoid tailing, but in such small amounts that it did not disturb the flow in the system.

In order to define a mixing time, is necessary to specify exactly the deviation from system homogeneity. Several definitions of non-homogeneity are possible corresponding to different mixing times. The following definition is considered work for physical methods (Manna, L. 1997):

$$d_s(\mathfrak{R}_s; t) \equiv \max\left(\frac{|C_{Ts}(\mathfrak{R}_s; t) - C_{T\infty}|}{C_{T\infty}}\right)$$

Where:

δ : Fixed value of deviation from homogeneity

\mathfrak{R}_s : Region of scrutiny

C_T : Concentration of tracer, mol/m³

By fixing the deviation from homogeneity as δ , the mixing time t_{δ} is defined as the longest period of time from injection of the tracer to when the deviation $d_s(\mathfrak{R}_s; t)$ reaches δ . This Means:

$$t_{\delta s} \equiv \max(t) \text{ so that } d_s(\mathfrak{R}_s; t) = \delta \rightarrow t_{\delta s} = f(\mathfrak{R}_s, \delta)$$

Definition $d_s(\mathfrak{R}_s; t)$ does not consider the non-homogeneity inside the region of scrutiny \mathfrak{R}_s . Therefore, when the measurement volume of the region of scrutiny \mathfrak{R}_s is increased, the non-homogeneity is neglected for a greater volume, implying a decrease in the mixing time.

By defining $t_{\delta s}^*$ as the maximum time at which $C_{ts}(\mathfrak{R}_s, t) = 0$, we obtain

$t^*_{\delta_s} \equiv \max(t)$ so that $C_{ts}(\mathcal{R}_s, t) = 0$

$$\delta = \frac{C_{T\infty} - C_{Ts}(\mathcal{R}_s; t)}{C_{T\infty}}$$

In the physical case, $t^*_{\delta_s}$ corresponds to the mixing time obtained by considering $d_s(\mathcal{R}_s; t)$ without the absolute value in the numerator as the definition of deviation from homogeneity (Manna, 1997).

In this research, the conductivity data collected by the conductivity probe technique were normalized to eliminate the effect of different probe gains. The data were normalized between an initial zero value measured before the addition of tracer, and a final stable value measured after the test was complete (MEUSEL, W *et al.*, 2016, and CHOMCHARN, N. 2009). The normalized data was obtained by:

$$C'_i = \frac{C_i - C_0}{C_\infty - C_0}$$

C'_i : Normalized conductivity probe output (recorder data)

C_i : Conductivity at time i

C_∞ : Final conductivity (equilibrium)

C_0 : Initial conductivity

The mixing time was defined as the time required for the normalized probe output to reach, and then always remain, within $\pm 5\%$ of the final equilibrium value. This time was defined as the 95% mixing time. According to C'_i , the 95% mixing time was determined at the time when the normalized conductivity output first reached the value of 1 ± 0.05 and then always remained within this interval. To minimize this error,

each experiment was conducted in triplicate and the resulting values were averaged (CHOMCHARN, N. (2009)).

4.3.2 Colorimetric measurements - Fluorescent tracers

From a practical standpoint, colorimetry is by far the most common technique employed for measuring mixing times in stirred vessels (KRAUME, *et al.* 2001). It is a non-intrusive technique extensively reported in the literature, which is used not only to determine the time required to achieve the desired degree of homogenization, but also to visualize qualitatively flow patterns and to reveal the presence of secondary flows generated under steady stirring such as well-mixed regions (caverns), islands and other segregated regions like stagnant or dead flow zones. The technique basically consists of injecting a liquid tracer and observing how it is dispersed in the fluid contained in stirred vessels (ASCANIO, G. 2015).

A Colorimetric measurement, using a fluorescent tracer called Uranine was also performed in this research. Uranine is the most intensely fluorescing tracer dye and easily visible to the naked eye, which is why it is often used for marking waters. Greatly diluted, the highly water-soluble Uranine powder is toxicologically harmless and ideally suited for all leak detections and tightness tests requiring the dyed water to penetrate capillaries. Therefore, the leak becomes apparent with a clear time lag to the dye addition. Even tiny leaks can be rendered visible using a UV lamp. Uranine is a reddishbrown powder that turns vivid yellow-green in water, it is photochemically unstable and loses fluorescence in water with pH less than 5.5 (BUZÁDY, *et al.* 2006). The pure Uranine powder do not fluoresce. When further diluted, however, the uranine will dye the water in a yellow-green to green fluorescent colour.

4.4 Rheology

Fluids may be described as Newtonian or non-Newtonian depending on whether their rheology (flow) characteristics obey Newton's law of viscous flow. Viscosity is the physical property that characterizes the flow resistance of simple fluids. Newton's law of viscosity defines the relationship between the shear stress and shear rate of a fluid subjected to a mechanical stress. The ratio of shear stress to shear rate is a constant, for a given temperature and pressure, and is defined as the viscosity or coefficient of viscosity. Newtonian fluids obey Newton's law of viscosity. The viscosity is independent of the shear rate. Non-Newtonian fluids do not follow Newton's law and, thus, their viscosity (ratio of shear stress to shear rate) is not constant and is dependent on the shear rate (MENDOZA, A.M.; *et al.* 2013)

Newtonian vs. Non-Newtonian in Gas lift reactors

The GLR, with its homogeneous shear effect, is also known for its ability to reduce viscosity in non-Newtonian shear thinning fluids and is often chosen for application, in processes that involve such fluids to reduce the viscosity effect. Often Carboxy Methyl Cellulose, CMC, is used to simulate the rheological behaviour of microbiological cultures in fermentation broths, compound that will also be used in this research to simulate non-Newtonian fluids (PETERSEN E.; *et al.* 2001).

Small vessels, with large wall surface area to volume ratios, and frequent bends lead to frictional effects, and thus liquid circulation patterns not found in larger vessels. More work is needed in the areas of mixing and mass transfer in large-scale industrial bioreactors to include the complex physiochemical properties of actual fermentation media. Foaming, viscosity, rheological properties, elasticity, among others (PETERSEN E.; *et al.* 2001).

That is why in this research a laboratory test in an ALR is carried out in a reactor with a nominal volume of 1200 L, volume that is much higher than the reactors registered in the scientific articles referenced in this research. Also, a test with methyl cellulose (MC) was performed to test the innovative air lift system with a non-Newtonian fluid as far as the mixing process is concerned. To analyse the behaviour viscosity test was also performed.

5 Methodical approach

To follow up the comparison of reactors with innovative mixing system and traditional mixing system, the following analytical parameters were calculated to compare the operation of the reactors in terms of factors influencing the process. The experimental determination of the parameters is explained in detail below.

5.1 Analytical parameters

5.1.1 μ Viscosity

The dynamic viscosity η is regarded as the "measure of the displaceability of the fluid particles against each other". It is also commonly understood as the 'viscosity' of a medium. The more viscous a medium is, the more viscous it is. The effect of the cohesion of these fluid particles is caused by Van-der-Waals forces and Brownian molecular motion, which counteract a displacement of the infinitesimally thin fluid layers against each other when force is applied (Martens, 2016).

Viscosity dependent on temperature and ambient pressure. Its scientific specification is given in $[\eta] = \text{Pa}\cdot\text{s}$. The former unit 'poise' is no longer used (Sigloch, 2008).

$$\eta = \frac{\tau}{D}$$

η : Dynamic viscosity ($\text{Pa}\cdot\text{s}$)

τ : Shear stress (Pa)

D : Shear rate (s^{-1})

The dynamic viscosity is the most important comparative parameter for rheological fluid considerations, which will be used in this research to evaluate the hydrodynamic behaviour of the ALR reactor, which has an innovative mixing system explained in detail in section 6.1.3.1. Likewise, to compare the rheology of sludge of methanization reactors that will be explained further in numeral 6.3.1.

For the determination of the rheological parameters torque (M), shear rate (D) and shear stress (τ) the rotational viscometer Rheomat 140 of the company proRheo was used. It consists of a fixed measuring cup and an immersed measuring body rotating at a constant speed (n) (Searle measuring principle). From the measured torque, the set shear rate and the measuring system used, the Rheomat 140 also calculates the viscosity (η) of the sample. All the samples used were brought to a constant temperature of 26 °C (average room temperature) in the preliminary run, as the viscosity of a fluid depends on the temperature and can only be compared if this physical variable is approximately constant.

The dynamic viscosity was determined for one and the same sample in two test runs, firstly with the anchor stirrer system 71 at intervals of approx. 75 to 325 revolutions per minute and then with the slightly smaller anchor stirrer system 72 for the speed range of approx. 300 to 600 revolutions per minute. For the series of measurements with the 71 system, an average of 10 min was applied per pass, for the series of measurements with the 72 system approx. 15 min per pass. In each case approx. one minute was waited until approximately constant values were read. Between the runs, the samples were brought back to the constant temperature in a thermostat at 26 °C for at least one hour. The temperature was checked manually with a small hand thermometer before and after the test runs. (MARTENS, C. 2016 and UNKRIG, L. 2018).

5.1.2 TS and OTS

The dry substance TS of a sample consists of all non-volatile compounds which are still present after 24 hours drying (approx. 105 °C) until the weight is constant (VDI 4630, 2006). It contains both organic and inorganic anhydrous solids. By determining the loss on ignition GV of the sample, the organic dry substance oTS of the sample can be concluded. The GV results from the mass remaining from the same sample after the determination of the dry matter and after 3 hours of asing (approx. 550 °C). The difference between the weighed dry matter and the GV forms the oTS. It indicates how much biomass, from simple organic molecules to whole microorganisms, is present in the sample. (BTU, 2006)

5.1.3 COD (Chemical Oxygen Demand)

The COD expresses the amount of oxygen originating in 1 litre of water under the working conditions of the specified procedure.

1 mol $K_2Cr_2O_7$ is equivalent to 1.5 mol O_2

Results are expressed as mg/l COD (=mg/l O_2)

Measurement of the content of compounds prone to oxidation by an oxidizing agent. It is a measure of electrons available in an anaerobic organic compound, expressed in terms of the amount of O_2 required to accept them when the compound is completely oxidized to CO_2 and H_2O (ANAYA, 2017). It can be determined following the DIN ISO 15705 using the sealed tube method and is expressed in [mg/l COD].

5.1.4 PH

Abrupt changes in pH values of the biomass might indicate inhibitions of the system such as acidification, high concentrations of ammonia; volatile fatty acids accumulation, among others. These lead to the decrease of methane yield and therefore it is an important operational parameter to be controlled. The optimal pH range results to be between 6.6 and 7.8 with possible failures if such values are lower/higher. Ph values were measured daily with a pH-meter WTW series Ph/Cond 720 was used to do the measurements by stirring gently the electrode throughout the sample just after being taken to avoid changes in temperature and gas composition. (Rios, 2015, Anaya, 2017)

5.1.5 T°C

All the test was run in the mesophilic temperature range (25-35°C) since it provides to methanogens an ideal environment to grow. Acidogenesis might be enhanced by increasing the temperature, however this may affect the ability of acetogenic and methanogenic bacteria to convert the volatile solids into methane and carbon dioxide. It was intended to keep the temperature within 37°C ±1 range by daily monitoring of the temperature of the reactors.

5.2 Operational variables

5.2.1 OLR

The organic load rate is defined as the ratio of the organic daily load to the ASBR, expressed in unit mass of COD per volume of the fermenter per day → $[Kg_{COD}/(m^3 * d)]$. For the case of liquid substrates COD is applicable, otherwise the OLR can also be expressed in $[Kg_{oTS}/(m^3 * d)]$.

To assess the biogas yield and degradation behavior, suggests running the reactor at different OLR's. The first load is about 0,5 $[Kg_{COD}/(m^3 * d)]$ until daily methane

production gets stable, at least for four days. Then the OLR can be increase stepwise by 0,5 units according to VDI 4630. The OLR may be increased until the methane productivity no longer increases or even starts to decrease.

5.2.2 Hydraulic retention time (HRT)

The parameter HRT is used to determine the average retention time (in days) of substrates in biogas plant digesters

$$HRT = \frac{V_{Digester}}{Q_{substrate}}$$

where $V_{Digester}$ [m^3] represents an active digester volume and $Q_{Substrate}$ [m^3/d] an average daily substrate input flow. . (Kamarád, L.; *et al.* 2013).

5.2.3 Productivity (MBR CH_4) and Methane Yield (Y_{CH_4})

A_{CH_4} Methane gas (Nm^3/t_{COD})

\dot{m}_{COD} Added organic dry matter (t/d)

The specific methane Y_{CH_4} , refers to the COD quantity converted in the reactor and is also a statement parameter for the performance of the system. It is related to the initial substrate.

y_{CH_4} Methane formation rate (Methane Yield) ($m^3/(kg_{COD} \cdot d)$)

$m_{CSB,zu}$ Inlet mass (kg_{COD})

$m_{CSB,ab}$ Outlet mass (kg_{COD})

The equivalent, to the specific methane formation rate is the productivity P of the entire system. It indicates how much methane is produced by the biomass in a given period of time in relation to the total size of the reaction chamber.

$$P_{CH_4} : \frac{\dot{V}_{CH_4}}{V_R}$$

P : MBR_{CH_4} : Methane Productivity ($m^3/(m^3 \cdot d)$)

5.3 Mathematical models in ARL/GLR reactors hydrodynamics

Air-lift reactors (ALR) have great potential for industrial bioprocesses, because of the low level and homogeneous distribution of hydrodynamic shear. Some of the ALR have been widely used in bioprocesses like the Airlift column reactors. They have advantages such as higher liquid circulation and higher intensity of turbulence. Moreover, they can be characterized as reactors with good gas dispersion, simple construction and low costs (Vunjak-Novakovic, G.; *et al.* 2005; MUSIAŁ, M.; *et al.* 2014).). The characterization of the ALRs not only column reactors but also their different configuration can be done using computer models that allow the analysis of the hydrodynamic behavior. One of the difficulties in developing a model for the ALR is describing gas holdup and its relationship to gas and liquid velocities. In the ALR, these velocities are not independent. The gas flow rate determines the liquid flow rate and the gas holdup. Also, because of the different direction and velocity of the liquid flow in the various sections of the ALR, it is necessary to distinguish each section when writing the momentum balances for these reactors. (Siegel, M.; *et al.* 1986).

The design, scale-up, and performance evaluation of such reactors all require extensive and accurate information about the gas–liquid flow dynamics, particularly as computational fluid dynamics (CFD) has become more popular in the last decade. However, due to the limitation of most conventional techniques for gas–liquid flow dynamics measurement, only global hydrodynamic parameters (e.g., cross-sectionally averaged liquid circulation velocity, overall gas holdup, and overall mass transfer rate) have been studied. The local flow characteristics (e.g., the macro-mixing and the turbulence intensity) remain unclear (MUTHANNA H.AL-D. *et al.*

2008; MERCHUK, J.; *et al.* 1996). The results also suggest that the top and bottom clearances have significant effects on the flow structures, which may have substantial effects on the bioreactor performance. (MUTHANNA H.AL-D. *et al.* 2008).

In the case of Gaslift bioreactor (GLR) many complex phenomena are occurring at the same time, thus it would be impossible to mathematically describe the mass transfer or gas hold-up process without the approach of specifying a "regime". By specifying a "regime" it enables us to find a solution or model through simplification. This means that by doing so researchers are assuming that most of the phenomena taking place have negligible effects, while a few of them are the only relevant ones. Modeling of liquid circulation velocity and hydrodynamics has been reported (PETERSEN E.; *et al.* 2001; VUNJAK-NOVAKOVIC, G.; *et al.* 2005); A hydrodynamic model is dependent on the flow regime, and thus the amount of recirculation. One problem lies in trying to predict the effect of gas recirculation on the gas hold-up, and another is phase interaction. The difference in gas hold-up between the riser and downcomer regions creates a driving force for liquid circulation. For recirculation calculations, most researchers equate the driving force for liquid circulation to the head losses occurring in the recirculation flow path. (PETERSEN E.; *et al.* 2001)

Numerals 6.3.4 and 7.3.4 include the theoretical mathematical concepts that were used in this investigation, as well as the results of a simulation of the hydrodynamics of the reactor flows that allowed to characterize the fluid inside the ALR reactor; as some authors report (PETERSEN E.; *et al.* 2001 and HWANG, S-J.; *et al.* 1997), the model analyses riser and downcomer sections only. The model did not take into consideration interactions between phases.

6 Experimental design

This chapter describes the experimental design carried out during the laboratory phase of this research, their analytical determination, data processing, the description of materials and equipment used.

All laboratory level testing was performed at the Waste Management Chair -BTU facilities. Which were divided in two:

- Experimental tests carried out with reactors
- The analytical tests required for the operation of these reactors

The experimental tests in the reactors were carried out in the Laboratory Hall 4C where all the reactors of this research were built and operated, which are described in numeral 6.1, these are:

First phase: traditional **ASBR** mechanically mixed was tested in the liquid single stage fermentation of organic food waste.

Second phase: compared the methanation of the hydrolysate maize silage (obtained in a double-stage solid–liquid process) in three reactors: the traditional stirred design of an **ASBR**, the second reactor is the same design with addition of packaging material (expanded clay/ Blähton) **ASBR+B** and the third reactor with the traditional design, but operated as a Continuous Stirred-Tank Reactor **CSTR**.

Third phase: compared the methanation of the hydrolysate maize silage (also obtained in a double-stage solid–liquid process) in two reactors operated simultaneously, the first reactor mixed with mechanical agitation (traditional stirred **ST-ASBR**) and the second reactor mixed with innovative pneumatic agitation with a concentric draught tube (internal loop configuration) and using the same biogas produced in a Gas Lift Reactor (**KG-ASBR**). Finally, a hydrodynamic analysis of the pneumatically mixing was performed in a new Air-Lift Reactor **-ALR**, on a larger

scale but with the same innovative design of KG-ASBR, to analyse the operation of the system and rheological behaviour.

Additionally, the determination of physical, chemical and rheological parameters was performed in the analytical determination laboratory equipped with all the apparatus required to carry out this research and which are mentioned.

An explanation and description of the conduct of laboratory testing is provided below.

6.1 Experimental configuration

Several types of experiments were designed to analyse the operation of the ASBR reactor. Relative comparisons were made of the performance of an innovative ASBR reactor design using a new mixing system and food waste and maize silage as substrate.

6.1.1 Traditional stirred ASBR - single-stage processes

In the first phase of research, an ASBR system for the fermentation of food waste was operated, using like a substrate a simulation of the composition of municipal market waste (organic fraction) of Medellín, Colombia. The anaerobic digestion occurred at the single-stage processes.

Organic waste, as a main constituent of municipal solid waste, has as well as solid biomass a high potential for biogas generation. Despite the importance of biogas generation from these materials, the availability of large-scale biogas processes lacks behind the demand (Fei-Baffoe B 2006; Busch, G. *et al.* 2009).

In this phase of the research, the goal was to know the effectiveness of this type of reactors for the treatment of organic waste, since, in Latin America, and in the

specific case of Colombia, there is a high potential for the development of renewable energies (large-scale biogas plants), because the typical composition of municipal solid waste can contain between 50 and 60% of organic waste.

The ASBR from this experiment has a nominal volume of 30 l and is shown below in Figure 15; the numbers of the following description refer to the numbers in said figure. The materials used allowed the maintenance of temperature in the mesophilic range. The prepared feed went into the reactor (2) through the overture with a diameter of 8.5 cm. There were two locations for extraction, (10) and (3), but only (3) was used in order to withdraw the effluent. The cycle schedule was set with a manually programmed timer (4) that regulated the duration as well as the start of mixing with the motor mechanical stirrer (11) which produced axial stirring movements. The cumulative gas production measurement was recorded with a gas meter Ritter drum/type (5) and gas composition monitoring was made with a gas analyzer ansyco (6), yielding values for volume percentage of methane, carbon dioxide, and oxygen.

The gas was stored in the impermeable bag (7), which was emptied daily using a pump (8) to avoid condensation and errors in measurement or alterations in the experiment's environment. The gas concentration percentages were measured at points (12). Additionally, the overture cylindrical tube was elongated to 16 cm (b) to prevent air (oxygen) contact, in order to guarantee anaerobic conditions. Finally, the height of the reactor (a) was of 0.5 m and the reactor's diameter (c) was of 0.3 m, while the surrounding cylinder (d) is an isolated chamber that guarantees mesophilic conditions with a diameter of 0.4 m. The thermometer (9) indicated temperature values inside the reactor. (RIOS, A. 2015, Liebscher, S 2015)

The arrangement of the reactor can be observed in Figure 15:

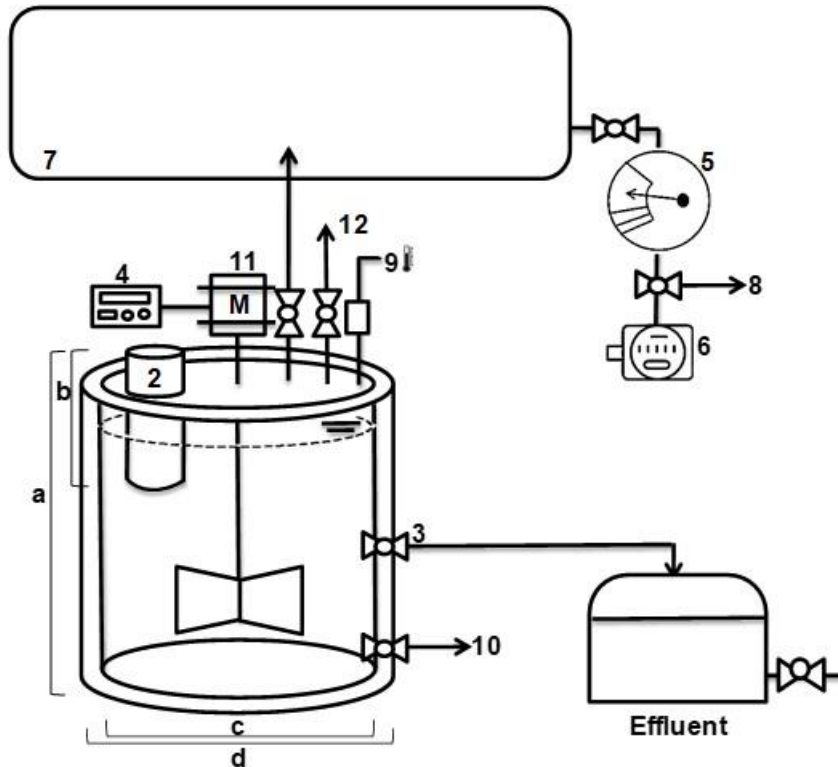


Figure 15: Overview of the experimental setup of traditional ASBR.
 Source (own elaboration, based on RIOS, A. 2015)

6.1.2 ASBR, ASBR+B and CSTR

The experimental setup consists in the operation of three reactors, all reactors with the same volume and feeding with the same substrate (hydrolysate of maize and grass silage): the first reactor was a classical ASBR, the second an ASBR+B (Blähton with addition of expanded clay) and the third a continuous stirred tank reactor – CSTR. The design of the three reactors was identical and could therefore be compared well with each other throughout all research. In the following Figure 16 the basic experimental setup is graphically illustrated.

The three reactors are cylindrical in shape and are largely made of polyethylene (PE) and have a double wall for mesophilic temperature regulation. This regulation was implemented by means of a hot water circuit with continuous temperature

measurement using sensors (1). Inclined blade stirrers (30 rpm) (2) were used to mix the reactor contents, continuously in CSTR and periodically in ASBR and ASBR+B. According to the stirring technique, the flow direction could be assumed to be mainly axial. An analog timer was used to implement sequential mixing, which regulated a six-hour rhythm and reactors nominal volumes of 30 l each one. (BUHLE, 2016)

During the test, all three reactors were supplied with hydrolysate via a common storage tank (3) of 50 l capacity to determine the limit ORL. Analyses were performed at the methanation stage of the maize silage hydrolysate obtained in a double-stage solid–liquid process described in numeral 3.2.3. To definite the residence time, however, each required a separate output storage tank (4) with also a volume of 50 l each in order to be able to convert the correspondingly high daily volume flows during the withdrawal.

The hydrolysate storage tank was continuously mixed by a motor (2), which is connected to the inclined blade stirrer.

The substrate was transported into the respective methane reactor by means of a peristaltic pumping device (feeding pump) of the Heidolph design Pumpdrive 5206 and 5201 (5). These pumps are variable adjustable in speed, quantity and frequency of pumping operations. The introduced material can then be converted into methane by the microorganisms (reaction). The resulting biogas flows out of the reactor during the entire period and passes through a drum-type gas meter (6) of the type TG05 from Ritter, which displays the produced gas volume. A gas analyzer from Geotech (7) was used for the gas analysis composition, which was carried out via connections on the respective experimental reactor. As shown in above, an overflow (8) has been installed to separate the clear phase or old substrate and transfer it to a effluent container.

The structure of the test stand shown in Figure 16 applies to the ASBR and CSTR. The second ASBR+B was filled with carrier material. Instead of conventional fillers, expanded clay was used, which proved to be suitable after a test run. The particle

size of the expanded clay used was 10-16 mm and was fed into the reactor once with a volume of 5 litres.

The following illustration provide an all-encompassing insight into the entire experimental setup.

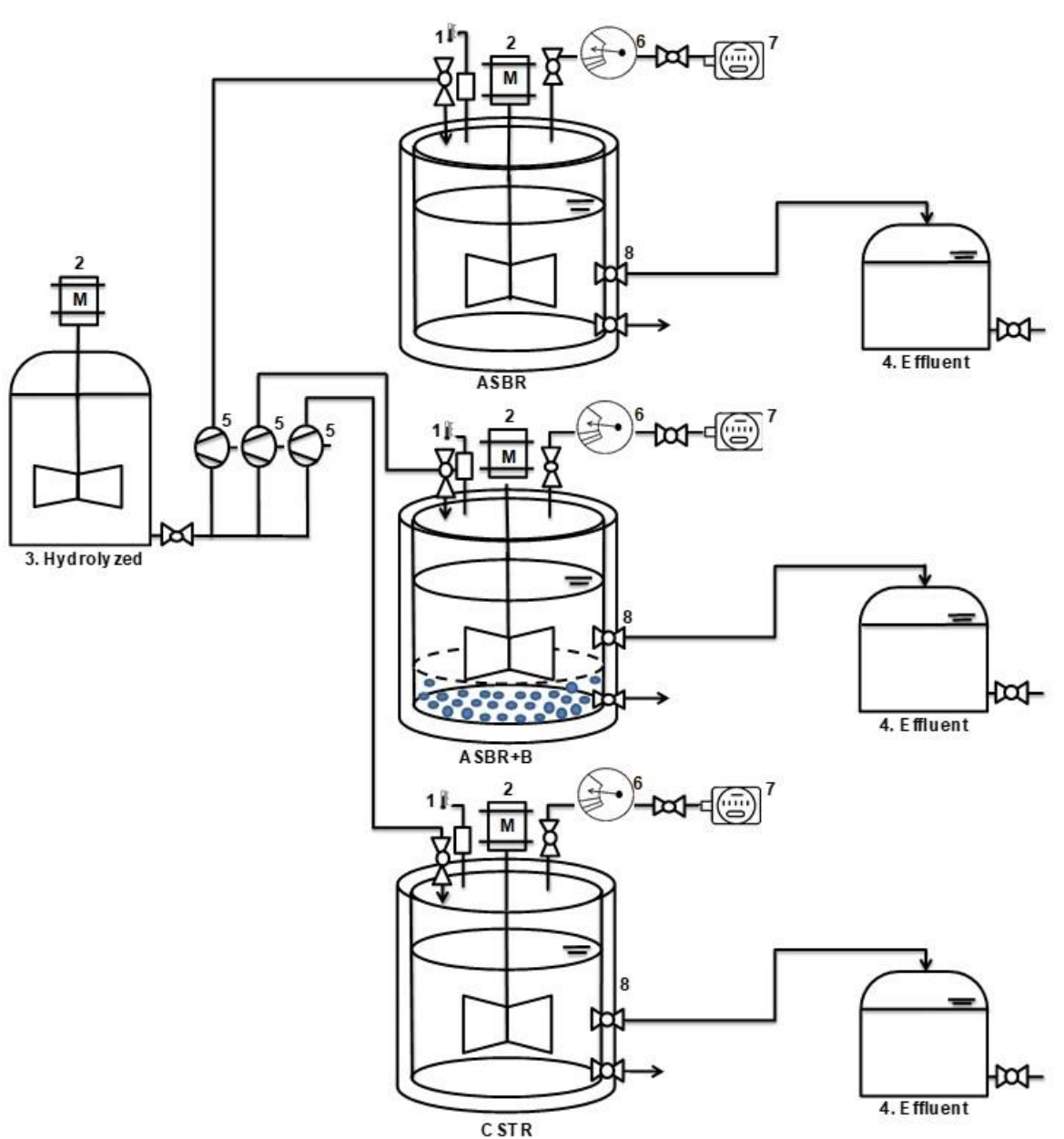


Figure 16. Overview of the experimental setup (ASBR, ASBR+B, CSTR)

Source: (own elaboration, based on BUHLE, 2016)

The purpose of this phase of the investigation was compare the different reactors to define the operation limits, residence time behaviour and the influence in the plan to build and operate the following systems (air/gas lift reactors) defined in the numeral 6.1.3, and also to have a productivity and methane yield reference values in the biogas to be produced in the tests explained in numeral 6.1.5 corresponding to the comparison of ASBR systems with mechanical mixture (ST-ASBR) and with pneumatic mixture respectively (KG-ASBR).

6.1.3 Air/ Gas lift reactors

To evaluate the innovative mixing technology, two Air/Gas lift reactors were built, both with the same geometric design and pneumatic mixing system but with different volumes.

The first one ALR worked in a water- air lift system, with a nominal volume of 1200 liters and was built to study the hydrodynamic behaviour of the reactor. For this purpose, a flow meter and a rotameter were installed, which allowed to know the real values of liquid and gas that were transported through the reactors internal draft tube. Three conductivity probes were also installed at the top, middle and bottom of the reactor to evaluate mixing time and internal homogenisation using Potassium Chloride (KCl) like a tracer test.

The ALR reactor, built as an airlift system to analyse the hydrodynamic conditions. In the Airlift system, the homogenisation achieved by the innovative mixing system was evaluated by means of tracers and physical methods for the estimation of mixing times, as well as the evaluation of rheological parameters that allowed to conclude about Newtonian and non-Newtonian liquid mixture, this last one, for simulated the behaviour of the process sludge in the methanation stage of GLR (or KG-ASBR reactor).

The second GLR (or KG-ASBR) with a nominal volume of 200 L operated under anaerobic conditions in the phase of a methanation in two-stage fermentation process, which was operated with the actual 4 cycles of an ASBR anaerobic reactor. It was a real system for biogas production in two-stage fermentation, ASBR was operated in the methanization phase and maize silage hydrolysate was used as substrate.

Likewise, to optimize the operating regime in the classical ASBR with regard to the cycle times and the intensity of the mixing (rotational speed), a third reactor ST - ASBR (mixing by mechanical stirring) was also commissioned as a methanation reactor. Both anaerobic reactors (mechanical agitation ST-ASBR and gaslift mixing KG-ASBR) are compared in terms of productivity and methane yield. The design of each one is detailed below.

6.1.3.1 Water- Air lift reactor

In this research the strategy agitation is carried out by use of an air-lift system with the aim to evaluate the liquid circulation velocity and the homogenization in the reactor. The Air Lift has been investigated as a potential reactor for a wide variety of biological and chemical process. Most of the work on these reactors has involved the study of their hydrodynamic.

The Airlift reactor are also pneumatic, consist of a liquid pool divided into two distinct zones. The part of the reactor containing the gas-liquid upflow is the raiser (R) and the region containing the downflowing fluid is known as the downcomer (D). The overall behaviour of the airlift is determined by the sum of the riser, downcomer and gas-liquid separator. In this study the type of air lift system used is an internal loop airlift may have a concentric draught tube (Dt) configuration, which enables the gas or air may be sparged by four orifices of 4 millimetres each (Gs).

The ALR reactor (see Figure 17) consists on a cylindrical tank with 1200 l of nominal volume, but an effective volume of 1120 l. On the lateral, five ball valves are located along the tank to ease the output sampling at different level: T=Top, Mt=Middle top, M=Middle, Mb=Middle Bottom, B=Bottom. The lateral has three conductivity probes (Mettler Toledo InPro 7100i/12/120/4435) were also installed at the top, middle and bottom with a sensor technology of 4-pol contacting and measuring range between 0,02-500 mS/cm.

The conductivity data were transmitted by Meter Toledo M300 for the sensors InPro 7100 VP and the data logging was done every second using a Data logger ProfiLab (1 second) from Delphin Technology AG, all measuring signals for the data logger were transmitted in the form of 4-20 mA. Finally processed in a software called Profisignal, also from Delphin Technology AG and installed on a computer that allowed processing the data presented in numeral 7.3.2.

Inside the reactor the concentric draft tube is screwed to the upper cup and have a length of 810 mm and 100 mm of diameter, with a top clearance (Ct) of 210 mm and a bottom clearance (Cb) of 100 mm that was fixed once the calibration of the flow and the influence of the variations of the clearance regions (Ct y Cb) were determined (numeral 7.3.1). An ABB magnetic - inductive flow meter (Fm) reference FEP 500/FEH521/FET521) was installed in the middle of the draft tube, which is highly accurate, and the flow measurement is independent of density, temperature and pressure of the medium.

The air was recirculated through a KNF compressor (C) reference PM-17992-0150/1457283 which uses a maximum pressure of 2 bar and whose air flow was measured and regulated at an average flow rate of 32 l/min by means of an Analyzer Rotameter (R).

The physical tracer method was used to perform the mixing time measurement tests, which also allowed the evaluation of the homogenization of the reactor: The reactor was coupled with a system that enabled the injection of the conductivity tracer (KCL) at the same level as the air injection in the lower part of the tube. The system

consisted of a tube containing the dilution to be injected (1 liter – 1 molar solution) with a manual timer and a valve that opened at the exactly end of the injection in order to release excess pressure (the pressure used was 3 bar), thus ensuring 100% solution injection (KCL) and washing the tube. With this system the loss of solution was eliminated, and the injection tube is washed to avoid slow introduction of the injected solution tracer into the reactor. The water-air lift was also switched on before the tracer was injected to ensure turbulent flow in the raiser. According to the recommendation described in 4.3.1 (Manna, L. 1997 and MEUSEL, W *et al.*, 2016)

Several liters of 1-mole KCL solution were injected into the reactor containing tap water (it was not necessary to use demineralised water because of the probe sensitivity range and the KCL calibration curve Annex 01). Specific graphs of conductivity vs. time and homogenization vs. time were obtained. Mixing times that were averaged were also calculated by checking a normal distribution of errors (measurements of each experiment were taken under the same experimental conditions).

Finally, experiments were conducted using methylcellulose (Swing Decor Vliestapeten-Kleister: methyl cellulose, starch ether, polyvinyl acetate powder, additives) in order to simulate non-Newtonian fluids more similar to the process sludge of the methanization phase, increasing the viscosity of the fluid and analyzing output samples at the same points where conductivity was analysed, at the Top (T), Middle (M) and Bottom (B) of the reactor; for this purpose the dynamic viscosity of the fluid was determined using a rotational viscometer ProRheo 140 with anchorage structures 71 and 72. The density and pH in the output samples was also measured in order to analyse possible fluid stratification.

The results of these tests, homogenization and viscosity are presented in chapter 7, numeral 7.3.2.

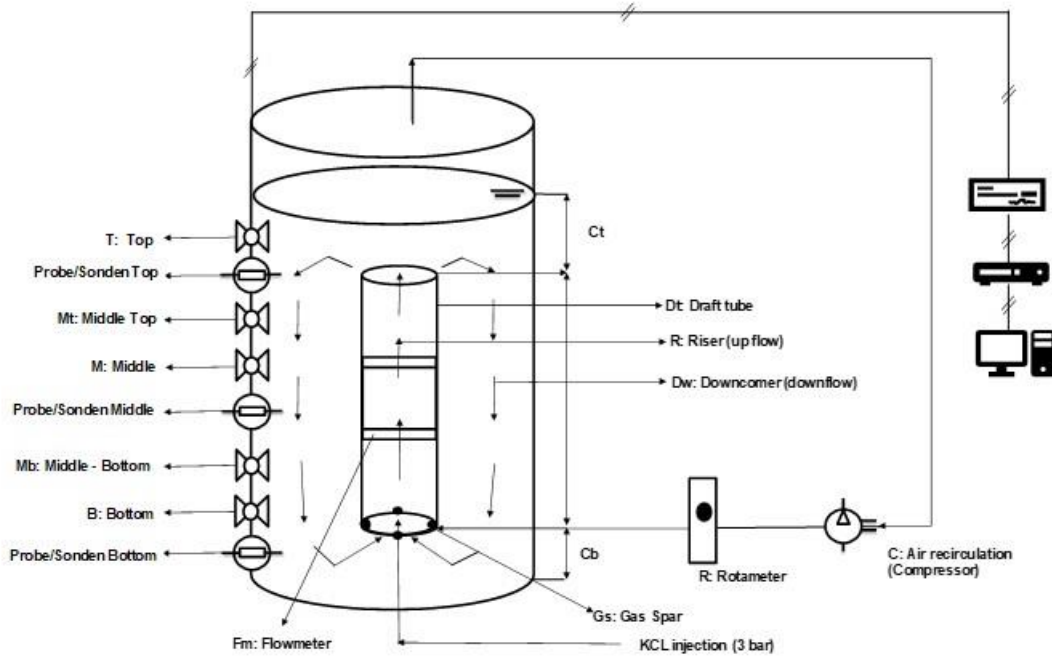


Figure 17. Experimental set up of ALR reactor used for the homogenization test.
 Source: (own elaboration)

6.1.3.2 Gas lift reactor (KG- ASBR)

In order to test the innovative air-lift mixing system in anaerobic conditions (in a real biogas production system) and test the behaviour of the productivity and methane yield in the methanation stage of the gas lift, the second “Kleiner Gas-Reaktor” KG-ASBR was built in a laboratory scale and also feeding with hydrolysate of maize silage obtained in the same double-stage solid–liquid process described in numeral 3.2.3.

The KG-ASBR reactor consists on a cylindrical tank with 200 l of nominal volume, but an effective volume of 160 l. A temperature sensor was fixed on the reactor cover (1) linked to the digital screen. The reactor was covered by a thermal jacket allowing to keep the inner temperature within the mesophilic range for the methanation process (37°C). On the lateral, sample valves were located along the tank to ease

the substrate sampling at different levels (T: top, M: middle, B: bottom), thus the physical and chemical conditions of the substrate were observed.

Inside the reactor the concentric draft-tube (2) was screwed to the upper cover, which was 504 mm long and 100 mm in diameter. The upper volume between the maximal liquid level and the top of the tank was left for the storage and recirculation of biogas. The biogas was sucked from the upper area (biogas out) and re-injected in the bottom of the riser (biogas in) by means of the gas sparger that has 4 holes with 4 mm diameter, where the gas is scattered into the draft-tube causing the gas upward-flow and therefore the circulation of the fluid throughout the downcomer (circular mix see Figure 18). The diaphragm vacuum pump (3) model ME 2S was programmed by an analog timer to implement a sequential mixing at 1.9 m³/h, which regulated a mixing cycle every six hours, taking care of the recirculation of the biogas produced and therefore the mixing of the substrate. The condenser (4) was allocated to capture some water residues of the biogas-pumping process.

The tests were carried out with two independent recirculation times that lasted 20/40 minutes respectively and began simultaneously with the feeding stage, so it occurred every 360 minutes. Afterwards the settling stages were (5h:20min/40min) and the effluent removal was done by an overflow or output pipe-elbow (5) installed to separate the clear phase or old substrate, the main idea of this pipe-elbow system was to keep the liquid level of the reactor right at the elbow height and transfer it to an effluent container (6).

In the start-up of the KG-ASBR reactor, the feeding process was made using a Heidolph peristaltic pump system 5201 (7), the pump enables the feeding every 360 minutes according to the predetermined input volume and flow rate. The input volume was programmed according with the chemical oxygen demand (COD [mg/l]) of the substrate (hydrolysate of maize silage) and the required organic loading rate per unit reactor volume (OLR [$\frac{Kg_{COD}}{m^3*d}$]), which was increased along the study-period step by step in a weekly basis as suggested by VDI 4360 and achieve the KG-ASBR cycle. The input volume was transported from the input tank (8) that contains the

hydrolysed of maize silage which was continuously mixed to avoid settling by means of a mechanical stirrer. When the hydrolysed was consumed, the container was filled up again manually. (ANAYA, L. 2017)

Finally, the cumulative biogas production was measured by the gas meter Ritter ref. TG05/6 (9) and a gas analyser from Geotech was used for the gas analysis composition, which was carried out via connections on the respective experimental reactor (10).

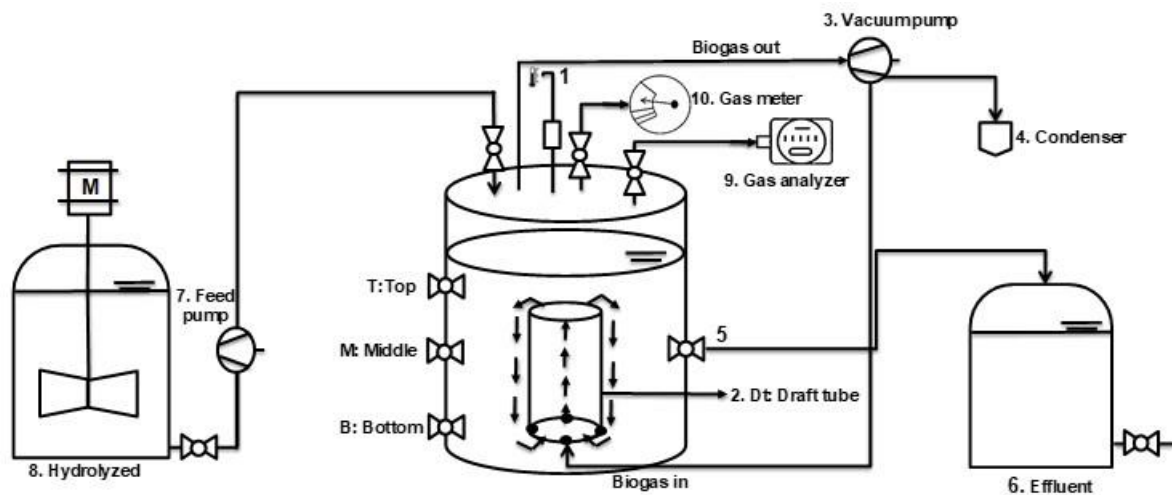


Figure 18 KG-ASBR gas-lift setup and distribution in the laboratory.
Source: (own elaboration)

6.1.4 Mechanical stirring ST-ASBR

A “Stirred Tank” reactor ST-ASBR with an effective volume of 109 l was operated to compare the performance of KG-ASBR system with the traditional mechanical mixing method (axial mixing). In the start-up of the ST-ASBR the reactor was fed from the input tank that contains the hydrolysed of maize silage which was continuously mixed to avoid settling by means of a mechanical stirrer (1). Once the

reactor was stabilized, it began to operate simultaneously with the KG-ASBR (process described in numeral 6.1.5).

The main reactor was also equipped with six ball valves at different heights and a side opening for sampling (T: Top, Mt: Middle top, M: Middle, Mb: Middle bottom and B: Bottom). On the reactor cover was fixed an electric inclined blade agitator - axial mixing (2) and the connection for valves to analyse the cumulative gas production in the gas meter model: Ritter TG 05-PVC (3) and the gas analysis composition using al Geotech analyser (4); both above the reactor and in the form of a three-way valve in the gas pipe.

The middle valve (5) was converted to an overflow that would allow the discharge at the level of the formed clear phase in the effluent container (6). The reactor was also heated at 37°C around the exterior of the tube and insulated against the environment with a foam rubber mat for maintain a mesophilic condition during the test.

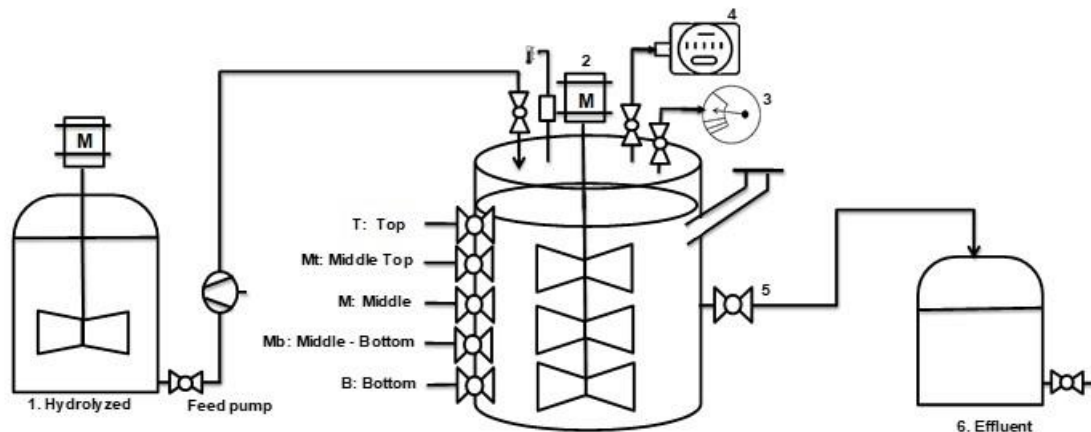


Figure 19 ST-ASBR stirred traditional reactor set up in the laboratory

Source: (own elaboration, based on MARTENS, C. 2016)

6.1.5 Comparison between KG-ASBR and ST-ASBR

Although both reactors were already inoculated and previously operating at low OLR, for purposes of the scientific comparison test a hydrolysate feed tank with capacity

of 60 l was installed that simultaneously fed both reactors (1) with the maize silage hydrolysate produced at the BTU facilities.

Likewise, were installed the peristaltic feed pumps (2) Heidolph Hei-FLOW Pumpdrive 5201 connected between the feed tank and the reactor to enable exact dosing of the hydrolysate),

The comparison phase of both reactors began with the gradual increase of the OLR as suggested by the VDI 4630 for the evaluation of the degradation behaviour and gas yield in the fermentation tests, starting with a low OLR of $0.5 \text{ kg}_{\text{COD}}/\text{m}^3\text{d}$ and increasing them in units of 0.5 as soon as the daily methane production is constant over at least four days (empirical value).

The mixing frequencies and feeding cycles were the same in both reactors with respect to the total test time which was 14 weeks. Four daily cycles of feeding, reaction, sedimentation and effluent withdrawal were programmed every 6 hours as described in 6.3.1, with the intention of identifying if there was any variability in terms of substrate sedimentation, mixing effectiveness and evolution of substrate rheology. In order to determine this, the percentages of OTS and TS in 3 side outlet valves of each one of the reactors were analysed.

Both reactors were equipped with temperature sensors that guaranteed mesophilic (37°C) conditions throughout the test. The innovative gas-lift mixing system of the KG-ASBR reactor kept the gas injection rate at 31.6 l/min which was the pump capacity (3). The mixing system of the ST-ASBR reactor was carried out by means of traditional axial mixing agitators whose motor was kept at a speed of 20 -30 rpm (4).

The composition of the gas was determined manually with a portable biogas analyzer from Geotech by connecting the instrument to the valves fixed on the reactor cover (5). The values read corresponded to the content of methane, carbon dioxide and oxygen. The measurement was performed once a day between 12 - 13:00 hours after the mixing stage was completed. A device measuring the temperature and ambient pressure in the test room allowed the subsequent

conversion of the gas volumes on different days into the corresponding volumes under standard conditions.

The daily gas production of both reactors was also recorded in a Ritter TG 05-PVC drum (6). Finally, an overflow has been installed to separate the clear phase or old substrate and transfer it to an effluent container for each of the two reactors with capacity of 60 l (7).

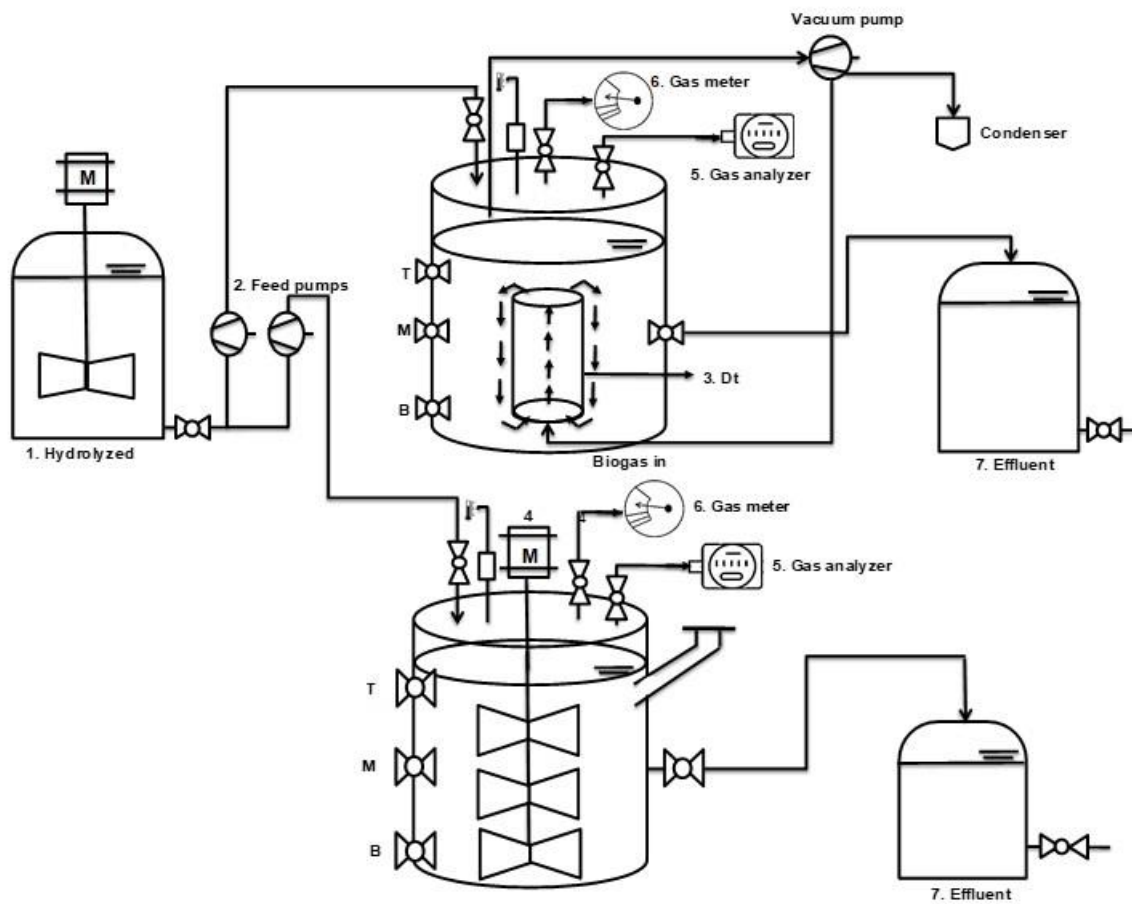


Figure 20 Overview of the experimental setup comparison KG-ASBR and ST-ASBR

Source: (own elaboration)

6.2 Substrate Characterization

The following describes the characterization of the substrate used in each of the three phases of the investigation. The first one is the characterization of the organic waste in a simulated composition of the city of Medellin Colombia; the second one is the characterization of the hydrolysed corn that was produced in the BTU facilities according to number 3.2.3 that was sometimes mixed with grass silage, and the third one is the hydrolysed obtained in the same way with maize silage.

6.2.1 Substrate characterization – Organic food waste.

The substrate itself was a prepared combination of fruits and vegetables simulating the average composition of those at La Mayorista municipal market food. The feed proportions included sweet fruits (28.1%), citrus (11.1%), vegetables with hard skin (19.3%), and vegetables with soft skin (41.5%). The contents of each main group are shown in Table 1 (RIOS, A. 2015):

Table 1: Fruit and vegetable content of the four main groups of feed

Group	Percentage (%)	Components
Sweet fruits	28.1	Apple, banana, coconut, mango, melon, tangerine, papaya [*] , pear.
Citrus fruits	11.1	Lemon, lime, maracuya [*] , orange
Vegetables with soft skin	41.5	Broccoli, cauliflower, celery, coriander, lettuce, onions, paprika, tomatoes
Vegetables with hard skin	19.3	Avocado, carrot, cassava [*] , maize, cucumber, physalis [*] , potatoes, zucchini, banana.

* Minimum percentage found in the supermarket, but included because it is a typical product in Colombia

These proportions were respected for each feed preparation and the fruits and vegetables employed were kept at 4°C in a refrigerator, in order to avoid their decomposition. Their provenance was German food market retailer Selgros.

Each vegetable or fruit was sliced into cubes of no more than 0.5 cm in length. This size pre-condition is necessary to ensure a high amount of surface readily available for microorganisms to settle and thus enhance degradation per volume unit, as shown by experiments using unsorted municipal solid waste and market waste, which were treated with a double stage dry-wet fermentation (Fei-Baffoe B, 2006 and G. Busch, et al. 2009). The feed for each week was prepared one week in advance in order to ensure a steady supply and fresh. To make sure each of these portions (6 in total) had a similar composition, they were mixed until a relatively homogenous mix was obtained. Once prepared, the feed was kept in a refrigerator at 4 °C. Furthermore, the substrate characteristics are shown in the following Table 2:

Table 2: Substrate characteristics of organic waste

Parameter (average)	Units	Value
COD	(mg/L)	154745
oTS _{FM}	(%)	9.91
N	(mg/L)	1580
TOC	(mg/L)	42870

The OLR was increased gradually, until 3,32 (Kg OTS/m³*d) according to recommendations of Guideline VDI 4630. It was possible to analyze the behavior of the substrate in terms yield and methane productivity, until the day 245 when acidification occurred in the system and was necessary for reactor operation.

6.2.2 Substrate characterization - Hydrolysate of maize and grass silage produced at the GICON biogas plant.

The substrate used in the experiment is hydrolysate of maize and grass silage. This means that only the phase of the methanation, was investigated in the experiments. The hydrolysate was made available by GICON GmbH from Biogas Cottbus Plant during the entire study and was supplied in containers of 30 and 60 l.

Since storage capacities are limited, especially in the refrigeration area at Lab Hall 4C BTU, new substrates were collected from the company as required. In the case of the tests carried out, the COD, showed certain deviations with regard to the different batches. Deviations from canister to canister were also possible, which is why the values given should be interpreted as an average value (see Table 3). The following table lists the essential parameters of the substrates used.

Table 3: Characteristics of the substrates used (hydrolysates)

Substrat	TS [Ma.-%]	oTs [Ma.-%]	COD[g/l]
Hydrolysate 01	5,176	3,912	51,186
Hydrolysate 02	4,947	3,666	52,000
Hydrolysate 03	4,635	3,388	49,863

Source: (Buhle, 2016)

Since it could not be ruled out that the material properties might change during the storage time, a sample had to be taken for characterization after each filling of the hydrolysate storage tank. In this way, it was ensured that up-to-date data is always available for evaluation (e. g. calculation for increasing the OLR).

Standard fermentation tests (according to VDI 4630 in mesophyll condition 37°C)

were carried out with the various hydrolysates to determine the substrate quality and the associated methane gas yield of the substrates. The experimental methane gas yields obtained ranged from 283.9 NI/kg_{COD} to 368 NI/kg_{COD}, while the methane concentrations were between 60.5% and 66.0% (see Table 4).

Table 4 Evaluation of standard fermentation tests according to VDI 4630.

Substrat	Y _{CH₄} [NI/kg _{CSB}]	C _{CH₄} [%]
Hydrolysate 01	283,9	60,5
Hydrolysate 02	368,0	66,0
Hydrolysate 03	328,9	65,6

Source: (Buhle, 2016)

6.2.3 Substrate characterization - Hydrolysate of maize silage produced at the BTU

The substrate used in the experiment is hydrolysate of maize silage (obtained in the process described in numeral 3.2.3). Also, in this experimental setup only the phase of the methanation, was investigated. The Hydrolysate maize silage was produced at the Lab Hall 4C BTU facilities during the entire study and was storage in the refrigeration area and supplied in containers of 30 and 60 l, new substrate were produced in the Laboratory as required. In the case of the tests carried out, the COD, showed certain deviations with regard to the different batches. Deviations from canister to canister were also possible, which is why the values given should be interpreted as an average value (see Table 5). The following table lists the essential parameters of the substrates used.

Table 5 Characteristics of hydrolysate produced in BTU Hall Lab.

Parameter	Units	Value
COD	[g/l]	25,208
oTS, fresh	[%]	1,093

Additionally, to determine the substrate quality and its methane yield potential was carried out a fermentation test according to the standard VDI 4630. Hydrolysates produced in different dates were compared under this test to recognize the overall performance. For instance, Table 6 present the results of substrates produced on Hall LAB, whose fit expected average yields of methane regarding the substrate. It is to be clarified that hydrolysed quality had during the study period similar characteristics. However, as COD values may lightly change, also parameters such as OLR and feeding volume were calculated whenever a new substrate was utilized. Therefore, as it will be shown further, yield and productivity values were also dependent on the substrate quality (ANAYA,L 2017).

Table 6 Fermentation test results according to standard VDI 4630

Substrat	CODg/l	Y_{CH_4} [Nl/kg _{CSB}]	c_{CH_4} [%]
Hydrolized 01	26,40	384,9	79,6
Hydrolized 02	23,55	299,5	80,9

This hydrolysate produced at the same BTU facility was used as a substrate to simultaneously compare the performance of the KG-ASBR reactor with the ST-ASBR in terms of productivity and methane yield.

6.3 Performance of the experimental execution

The cycles that were carried out in each of the experiments using ASBR reactors are described below.

6.3.1 The ASBR – food waste cycle

The ASBR that was used for food waste degradation worked in a single stage, that is, all the phases of biogas production such as hydrolysis, acidogenesis, acetogenesis and methanogenesis were performed in the same container.

A traditional mechanical mixing was programmed using the timer shown in Figure 15:

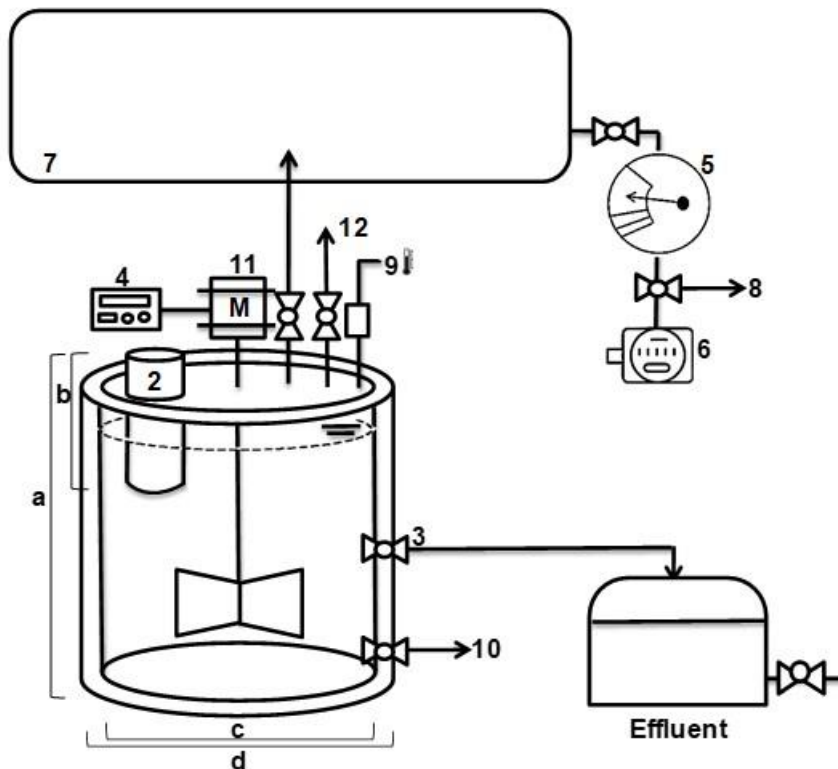


Figure 15 and lasted 60 minutes. There were four one-hour-long mixing periods per day, every six hours. Feeding occurred before the second mixing period of the day, shortly before midday 12:00. Withdrawal and sampling occurred approximately 24 hours after feeding and was always of the same volume as the introduced feed. All samples of the effluent to be analysed were kept in a refrigerator at 4°C, generally less than one week. Table 7 show one cycle of the day (Rios, A 2015.)

Samples were taken for analyses before and after mixing, in order to compare oTS values and their evolution over the weeks.

Table 7. Cycle of a single stage ASBR- substrate organic food waste

Reactor	Feeding/withdrawal	Mixing (Reaction)	Sedimentation
ASBR	5min	60min	295min

6.3.2 The ASBR, ASBR+B and CSTR cycle

The operation of the experimental reactors was carried out by cyclic operation, whereby fresh substrate was pumped into the reactors four times a day at intervals of 6 hours. The reactors then went through their specific process control variants (see Table 8). The set regimes are shown in the following table. The three mechanical agitators that performed the mixing were set at 30 rpm.

Table 8 Cycle of a methanation stage of ASBR, ASBR+B and CSTR

Reactor	Feeding/withdrawal	Mixing (Reaction)	Sedimentation
ASBR	5-15min	60min	255min
ASBR+B	5-15min	60min	255min
CSTR	5-15min	continuesly	-

6.3.3 The KG – ASBR and ST – ASBR cycle

The cycle that was defined to compare the KG-ASBR and ST-ASBR reactors, was planned according to experience obtained in the tests of the three reactors ASBR, ASBR+B and CSTR. Therefore, 4 cycles per day were maintained with feeding and reaction periods every 6 hours. Table 9 shows the cycles for each reactor and Table 10 shows the mixing strategies for each week of sampling. Effluent withdrawal happens simultaneously with feeding.

Table 9 Cycle of a methanation stage of KG-ASBR and ST-ASBR

Reactor	Feeding/withdrawal	Mixing (Reaction)	Sedimentation
KG -ASBR	5-15min	20/40min	320/340min
ST-SBR+B	5-15min	20/40min	320/340min

Table 10 shows the cycles for each reactor. However, in order to know how the reactors were reacting by reducing the mixing periods, they were reduced to two periods of 20 minutes and 40 minutes which were interspersed each week.

Table 10 Shows the mixing strategies for each week of sampling

Week	Mixing Time (min)	Mixing strategy ST-ASBR (rpm)	KG-ASBR Vacuum pump capacity (m ³ /h)
1	40	20	1.9
2	20	30	1.9
3	40	20	1.9
4	20	30	1.9
5	40	20	1.9
	40	30	1.9
7	40	20	1.9
8	20	30	1.9
9	40	20	1.9
10	20	30	1.9
11	40	20	1.9
12	20	30	1.9
13	40	20	1.9
14	20	30	1.9

6.3.4 The ALR hydrodynamic flows characterization

For the hydrodynamic characterisation of the ALR reactor described in 6.1.3.1, different tests were carried out at laboratory level to determine the influence of the air flow supplied by the KNF compressor with a maximum pressure of 2 bar. Also, different water flow rates were analysed and determined by an ABB magnetic - inductive flow meter, which made flow measurements independent of density, temperature and pressure of the medium. The fluid used to make this characterization was tap water from the city of Cottbus⁸.

⁸ Trinkwasserbeschaffenheit für das Versorgungsgebiet des Wasserwerkes Cottbus – Sachsendorf.
<https://docplayer.org/9066381-Cottbuser-umwelt-fakten-und-zahlen-aus-der-arbeit-des-umweltamtes.html>

The following variables that influence the hydrodynamic behaviour of the reactor were characterized:

Gas flow variation: the determination of different gas (air) flow rates was made by measurement of the values in ANALYZER rotameter with a measurement range between 2 l/m and 42 l/m of gas (0.12 m³/h and 2.52 m³/h), whose air was provided by the KNF compressor.

Water flow variation: the determination of different water flow rates was made by the ABB flowmeter located in the central part of the draft tube, in a range of values between 91.3 l/min and 367.3 l/min of water (5.77 m³/h and 22.51 m³/h).

Clearance regions Ct and Cb: variation of the position of the draft tube inside the reactor was possible because draft tube was fixed to the reactor cover by means of a mobile system that allowed modified the value of Ct and Cb. Three position of Ct and Cb was tested. (A) Ct:21 cm and Cb:10 cm; (B) Ct:18 cm and Cb:13 cm; (C) Ct:12 cm and Cb:19 cm.

The results of these three variables are presented in the numeral 7.3.1.

6.4 Description of mathematical model in ALR

Although there is research in which for the first time develop a mathematical model that predicts the effect of gas flow rate, column height, column diameter, and cross-sectional areas on the productivity of a process in an ALR; and report results of models that analyse the effects of the operating variables using a mathematical models that accounts for the effects of ALR geometry and fluid flow (WU, X.; *et al.* 2004 and VUNJAK-NOVAKOVIC, G.; *et al.* 2005); this field has not yet been widely developed, due to the complexity of the modelling each zone. From a

mechanical point of view the ALR bioreactor is beautifully simple, but from a hydrodynamic point of view it is very complex, making modeling difficult (PETERSEN E.; *et al.* 2001).

Therefore, in this research it is presented a theoretical description of the way to understand the hydrodynamics of the reactor based on his geometry, also were used the data obtained in the real laboratory test of the characterization of the flow in the ALR presented in paragraph 7.3.1

The values of the design variables of the ALR reactor are shown in the Figure 21. The determination of the equations and the characterization of the flow using the calculation of the Reynolds number (Re as dimensionless number) is presented below.

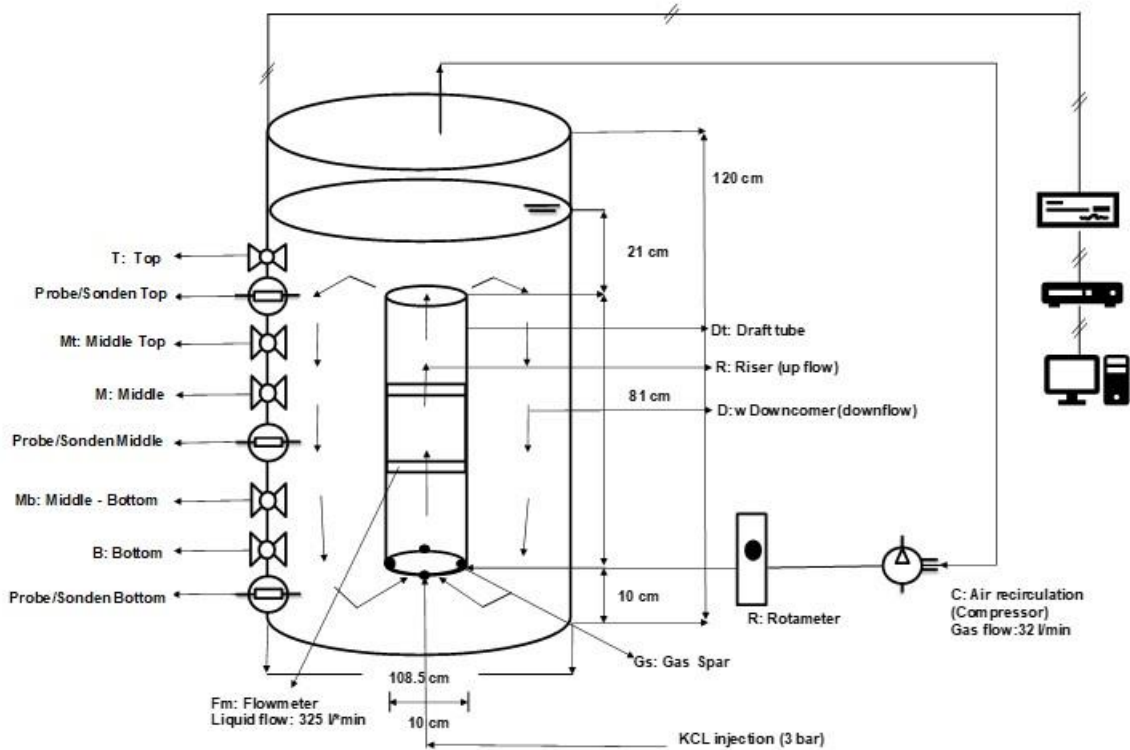


Figure 21 Values of design variables of ALR
 Source (own elaboration)

From the volume of a cylinder, the volume of the draft tube is known.

$$\text{Cylinder volume} = \left(\frac{\pi \cdot D^2}{4} \right) \cdot h$$

Draft tube Diameter D_{Dt} :

$$D_{Dt} = 10\text{cm}$$

Height Draft tube H_{Dt} :

$$H_{Dt} = 81\text{cm}$$

Volume of the draft tube V_{Dt} :

$$V_{Dt} = \left(\frac{\pi \cdot 10^2}{4} \right) \cdot 81$$
$$V_{Dt} = 6361.7\text{cm}^3 \quad \text{or} \quad V_{Dt} = 6.36\text{l}$$

The second step was to determine the time it takes to pass that volume through the draft tube. Assume T_{Dt} (minutes to pass through the cylinder):

$$T_{Dt} = \frac{\text{Volume}}{\text{Velocity}} = \frac{\left(\frac{\pi \cdot D^2}{4} \right) \cdot h}{V_e}$$

The velocity in the draft tube is known by the average reading of the fluid velocity, since it was measured in the flow meter every second, the average was: $19.53 \text{ m}^3/\text{h}$ or $325.49 \text{ l}/\text{min}$. Then T_{Dt} :

$$T_{Dt} = \frac{\left(\frac{\pi \cdot 10^2}{4}\right) \cdot 81}{325490}$$

$$T_{Dt} = 0.020min \quad \text{or} \quad T_{Dt} = 1.17 sec$$

The linear velocity (V_{Dt}) in the draft tube can be determined by knowing the height of the draft tube and the time it takes to pass through it.

$$V_{Dt} = \frac{H_{Dt}}{T_{Dt}}$$

That means the linear velocity (V_{Dt}) in the draft tube is:

$$V_{Dt} = \frac{81}{1.17} = 69.07 \frac{cm}{s}$$

To know the total volume in the ARL to be homogenized is necessary use the total liquid level to calculate the reactor effective volume:

$$Reactor Volume V_R = \left(\frac{\pi \cdot (108.5)^2}{4}\right) \cdot (81 + 21 + 20) = 1035.5 l$$

If it takes 1.17 seconds (T_{Dt}) for it to pass through the internal cylinder 6.36 liters, then for it to pass 1035.5 l will take 190.49 seconds, about 3.17 minutes T_R per complete lap.

The **Reynolds number** can be calculated as a theoretical exercise for the draft tube knowing that the fluid ($KCL + H_2O$) in this reactor has the following characteristics:

$$T^\circ C = Reactor temperature = 25^\circ C$$

$$\rho: Liquid density = 0.9 \frac{g}{cm^3}$$

$$\mu: \text{Dynamic viscosity (measured on a viscometer)} = 0.015 \frac{Kg}{m \cdot s} = 0.15 \frac{g}{cm \cdot s}$$

$$V_{Dt} = \text{Linear velocity} = 69.07 \frac{cm}{s}$$

$$Re_{Dt} = \text{Reynolds in draft tube} = \frac{D_{Dt} \cdot V \cdot \rho}{\mu}$$

$$Re_{Dt} = \frac{10cm \cdot 69.07 \frac{cm}{s} \cdot 0.9 \frac{g}{cm^3}}{0.15 \frac{g}{cm^3}}$$

$$Re_{Dt} = 4144$$

Finally, the same calculation was done for the reactor, theoretical exercise for the external diameter (**reactor diameter**) assuming a negligible wall thickness and an average velocity in the flow of the rest of the reactor took into account a few seconds of loss (2 seconds) in the path that runs between the draft tube and the Top and Bottom Clearances (Cb and Ct / horizontal flow). These two seconds were calculated according to the test carried out with a colorimetric tracer called Uranine described in numeral 4.3.2 and 7.3.2 and whose video is in Annex 2, in which the return flow patterns inside the reactor are visually appreciated in a video taken by immersion of a GoPRO camera inside the ALR reactor, which allowed to determine 2 seconds approximately of transit time in the clearances regions.

$$H_{RTL}: \text{Height total liquid level in ALR} = (81 + 10 + 21) = 112cm$$

$$H_{RAL}: \text{Average height (liquid level) in ARL: } \frac{112 + 81}{2} = 96.5 \text{ cm}$$

$$V_R = \text{Linear velocity in dowcomer} = \frac{H_{RAL}}{T_R - 2s} = \frac{96.5 \text{ cm}}{190.49 \text{ s} - 2 \text{ s}} = 0.512 \frac{cm}{s}$$

$$Re_R = \text{Reynolds in reactor} = \frac{D_R \cdot V_R \cdot \rho}{\mu}$$

$$Re_R = \frac{(108.5 \text{ cm} - 10.0 \text{ cm}) \cdot 0.512 \frac{\text{cm}}{\text{s}} \cdot 0.9 \frac{\text{g}}{\text{cm}^3}}{0.15} = 301.41$$

$$Re_R = 301.41$$

The flow will be laminar if the Reynolds number is less than 2300 and turbulent if it is greater than 4000. Therefore, according to Reynolds number the flow in the draft tube is classified as turbulent and the flow in the reactor (downcomer or annulus) is classified as laminar.

In the draft tube the fluid particles are in an extreme state of disarray, their velocity fluctuations are erratic (turbulent: $Re_{Dt} = 4144$) and they develop rotary movements.

In the downcomer the fluid particles moved in layers with one layer of fluid sliding smoothly over an adjacent layer (laminar flow: $Re_R = 301.41$). (SAHU, G.K. 2008).

7 Results and discussion

7.1 ASBR Performance - single-stage processes

In relation to the gas production and composition shown in Figure 22, the CO₂ gas increased gradually until day 19, after which an abrupt drop in values can be seen from days 20 to 25. After this, the concentration CH₄ remains between 35 and 50 percent until day 136. Furthermore, on day 137 the concentration decreases to values below 40%, but increases again on day 141 to the previous range 35-50%.

Furthermore, the methane gas concentrations decreased during the first 20 days, but dropped suddenly and were nearly zero throughout days 20 to 25, after which the expected values between 40 and 50 percent nearly at all times were reported.

Oxygen concentrations were expected to be smaller than 1% and when higher, a thorough examination of the reactor assemblage and measuring was made, generally successfully identifying and avoiding further air entrance. As it can be seen in Figure 22, the oxygen concentrations were at all times equal to or nearly zero, except for days 20 to 25.

As for gas production and composition, it can be said that the different gases concentrations are acceptable, with the exception of a period of five days on day 20. The reason for the sudden drop of CO₂ and CH₄ throughout days 20 to 25 is a small hole in the reactor, which allowed air intrusion, toxic for methanogens. That is why the oxygen, concentration is similar to that of air, approximately 20 percent, in this period of time. Fortunately, the hole was identified, and the problem fixed. Finally, the productivity values reach in the last days values close to 1, which is a normal outcome, and may indicate a certain degree of stabilization. (Rios. A 2015)

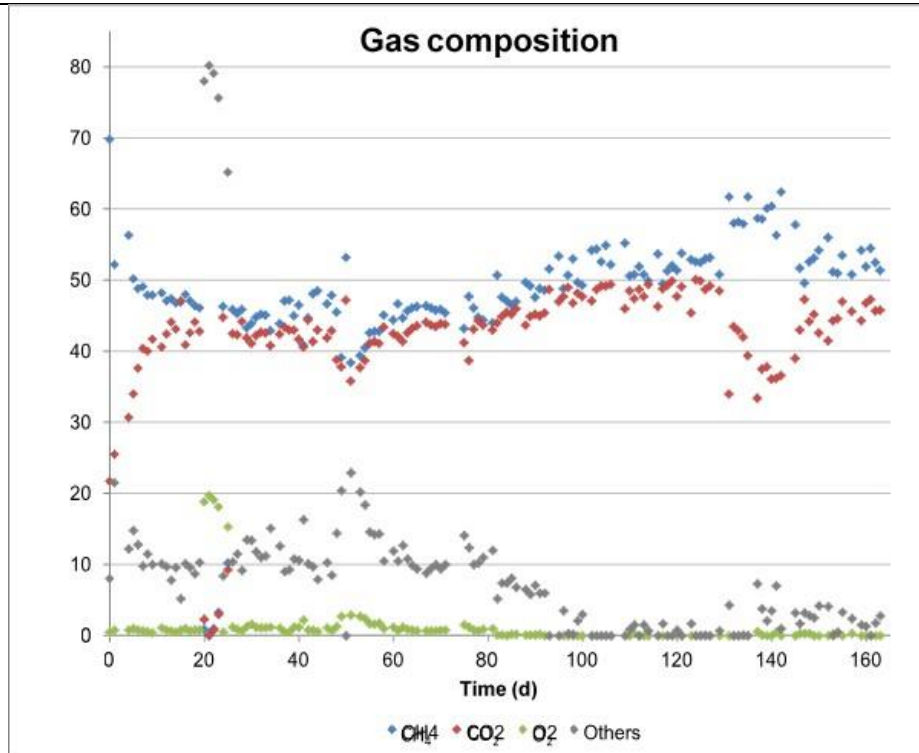


Figure 22 Gas composition in volume percentage over time of the biogas produced

7.2 ASBR, ASBR+B, CSTR Performance – Methanation stage

The purpose of this phase of the investigation was compare the different reactors to have a productivity and methane yield reference values in the biogas to be produced in the tests that compare of ASBR systems with mechanical mixture (ST-ASBR) and with pneumatic mixture respectively (KG-ASBR).

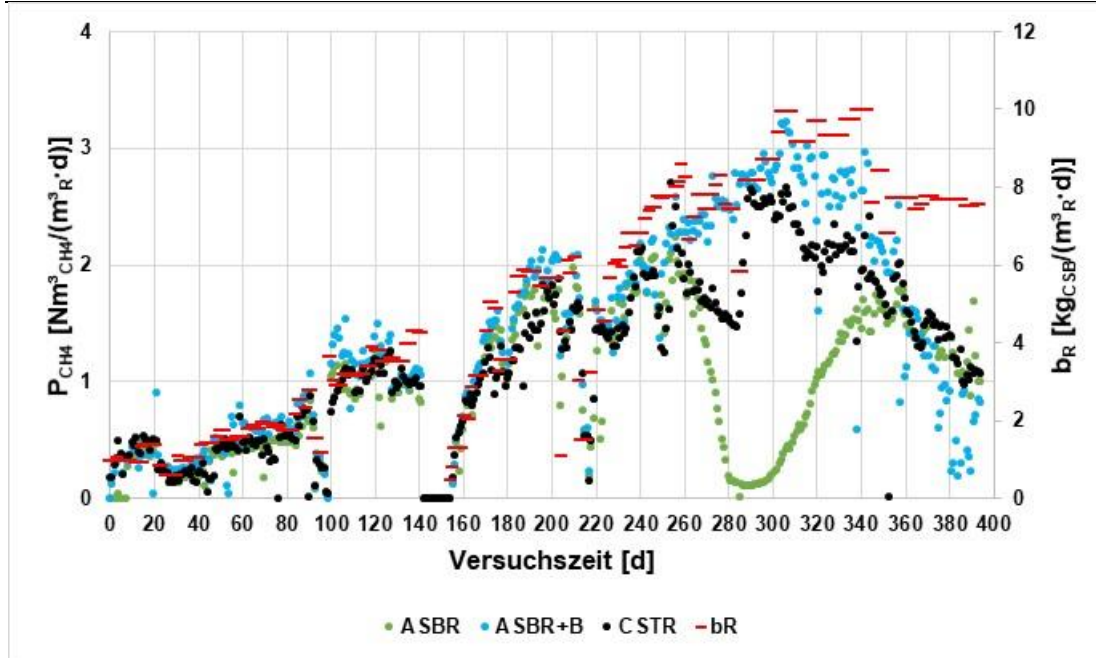


Figure 23 Comparison of P_{CH_4} vs. OLR in the 3 reactors ASBR, ASBR+B and CSTR

Source: (Buhle, D. 2016)

Comparing ASBR and ASBR+B, CSTR experimental reactors (Figure 23), in terms of productivity P_{CH_4} with increasing OLR (b_R), it is noteworthy that continuous increases in OLR in the ASBR + B reactor also have the highest productivity. During a OLR of 9,94 kgCOD/($m^3R \cdot d$) the highest productivity was recorded, which is 3,23 $Nm^3CH_4/(m^3R \cdot d)$ and HRT of minimum 4,5 days. This comparison demonstrates the influence of using support material as it allows bacterial immobilization, which is combined with an appropriate mixing velocity, not disturb the microorganisms formed on the expanded clay and facilitates the sedimentation process. (PULGARIN, I, *et al.* 2017).

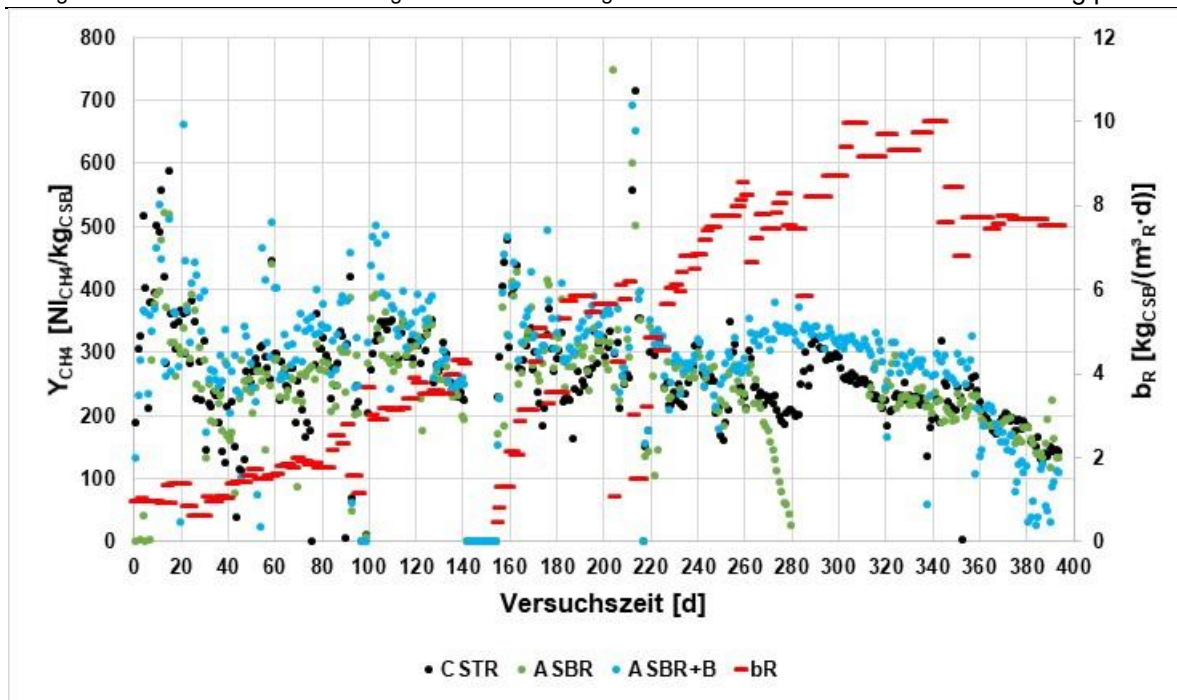


Figure 24 Comparison of Y_{CH₄} vs. OLR in the 3 reactors ASBR, ASBR+B and CSTR

Source: (Buhle, D. 2016)

Comparing ASBR and ASBR+B, CSTR experimental reactors (Figure 24), in terms of Methane Yield Y_{CH₄} with increasing OLR, it is clear that the ASBR+B was almost consistently able to achieve the highest methane yields. Especially with the high OLR (up to 10 kg COD/(m³Rd)) it can be clearly seen that the ASBR+B is the most efficient. It was the only one that was able to achieve the previously calculated methane yield of 320 NI_{CH₄}/kg_{COD} for most of the test time. The two other test reactors (ASBR, CSTR), on the other hand, have a lower methane yield and are very similar in their performance. In the graph shown, the individual measuring points of the two methane reactors are therefore usually located above each other or very close together (BUHLE, D. 2016)

7.3 ALR reactors performance

This section includes the results of the characterization of the ALR reactor, which consists of a cylindrical tank with 1200 l of nominal volume and was describe in numeral 6.1.3.1.

7.3.1 ARL hydrodynamic flows characterization

The initial characterization exercise of the ALR reactor was presented in numeral 6.4 where the theoretical mathematical model showed the first calculation of the linear velocity in the draft tube $V_{Dt} = 69.07 \frac{cm}{s}$. After the performance tests of both the water and air flow inside the reactor have been carried out, it can be compared with the theoretical value obtained.

In order to make this comparison, a rotameter was used to characterize the gas flow between 0,12 and 2,42 m³/h and a magnetic-inductive flow meter characterized the flow of liquid between 5,77 and 22,51 m³/h. This made the flow measurement independent of the density, temperature and pressure of the medium inside the reactor. The measuring range was limited by the non-detection of very low flow rates (<2 l/min air supply) as well as the occurrence of highly turbulent flows (> 40 l/min air supply) (see graphic Annex 4). The air was supplied to the bottom of the draft tube, with a flow liquid velocity of 0.204 - 0.796 m/s (20.4-79.6 cm/s). (PULGARIN, I. *et al.* 2017)

As the experimental tests reported in numeral 7.3.2 were carried out by keeping the gas (air) inlet flow to the ALR reactor constant at 32 l/min, the velocity value in the draft tube specifically for that air flow is presented below. Similarly, the velocity values obtained in both the theoretical mathematical model (numeral 6.4) and the

system dynamics simulation model (to be presented in number 7.3.4) are shown in

Table 11 Velocities in the draft tube obtained in different scenarios Table 11.

Table 11 Velocities in the draft tube obtained in different scenarios

Flow air (m ³ /h)	Flow air (l/mi)	V _{Dt} [cm/s] Experimental test	VDt [cm/s] Tehorical Value	VDt [cm/s] lthink simulation
1.92	32	69.42	69.07	68.97

All the velocity values in the draft tube are similar and therefore it is a mathematical validation of the results made at laboratory level. Similar values in hydrodynamic studies were obtained by Milivojević *et al.* 2010 on an air-lift reactor, as well as Glennon *et al.* 1993 on an air-lift loop reactor.

With respect to the variations in the clearance zones (CT and C_b), no significant differences were observed in the flow behavior curves. The three variations on the clearance reagios Ct and C_b that were tested maintained the same flow behavior ranges in both water and gas. However, the draft tube was set at Ct=21 cm and Cp=10 cm to developed the laboratory test of KCL traces since the curve design was better dispersion. The graphs are presented in Annex 5.

7.3.2 Homogenization and mixing time

The results of the homogenisation tests, which were previously described in sections 4.3 and 6.1.3.1, are presented below. The results of the fluorescent tracer (Uranine) and a statistical analysis and error analysis of the tests carried out at laboratory level are also presented.

Determination of the mixing time and homogenization by physical methods **(tracer test with KCL)**

In order to carry out the tracer test, a KCL calibration curve was first drawn up to determine the range of values in which the same 1000 L of water contained in the ALR reactor could be used without the need to replace the water due to KCl saturation and without using demineralised water (BTU, H &W, 2006). In this way it was ensured that no water exchange was necessary at each KCl injection and a sensor technology of 4-pol contacting of the 3 electrodes of the Top, Middle and Bottom probes fixed in the ALR reactor were in the design measuring range detailed in 6.1.3.1. The curve is presented in Annex A and has a maximum measuring range of up to 5 mS/cm.

The results obtained by the software Profisignal coupled to the ALR reactor, whose data recording was done every second, were presented in the digital file in Annex 5. Using these data, it was possible to calculate the homogenization in each second using the C'_i : Normalized conductivity probe, described in the concepts explained in numeral 4.3. With these data, the different graphs were obtained, which were determined for a total of 9 KCl injections, in order to have the result in triplicate, as suggested MEUSEL, W.; *et al.* 2016. The Table 12 shows the mixing times for each injection and the position of the 3 probes in the ALR reactor.

Table 12 Time to reach the homogenization

Time to reach 95% of homogenization			
Injection number	Top	Middle	Bottom
1	00:02:37	00:03:29	00:02:59
2	00:02:55	00:03:10	00:03:09
3	00:03:54	00:04:02	00:04:23
4	00:03:01	00:03:22	00:03:26
5	00:02:59	00:03:31	00:04:00
6	00:03:25	00:03:49	00:03:29
7	00:03:05	00:03:13	00:03:05
8	00:04:11	00:03:13	00:03:54
9	00:02:30	00:02:38	00:03:02

Mean (1-9)	00:03:11	00:03:23	00:03:30
Min	00:02:30	00:02:38	00:02:59
Max	00:04:11	00:04:02	00:04:23
Total mean value			00:03:21

Using the KNF compressor with a constant air injection rate of 32 l/min, an experimental average of time to reach the homogenisation was determinate: 3.11 minutes are needed at the top of the ALR, 3.23 minutes in middle y 3.30 minutes in bottom. The maximum time required to achieve homogenisation in the ALR reactor was recorded at the bottom probe, with a value of 4.23 minutes, with differences from the average maximum values of the middle probe (4:02 minutes) and the Top probe (4.11 minutes),: however, in most cases the pattern found shows longer homogenisation times at the bottom of the ALR.. This could be a reason associated with the normal distribution of the cyclic flow within the reactor, which requires more time to complete a lap or closed cycle.

The Conductivity vs. Time and Homogenization vs. Time graphs are included in Annex 5. From these, it can be concluded that from the experimental point of view, the measured mixing times were averaged assuming a normal distribution of errors are a time of 3.21 minutes are required for complete homogenization of the solution.

Statistical analysis – Homogenization and error analysis

To make the statistical analysis, the program R Core Team (2019)⁹ was used, which is a free software environment for statistical computing and graphics. An experimental set up was carried out to measure the homogenization time in a 1000 L airlift reactor -ALR, (described in numeral 6.1.3.1). This test was performed 9 times according to the recommendations for process engineering characterisation of single-use bioreactors and mixing systems by using experimental methods (MEUSEL, W.; *et al.* 2016). The reactor had conductivity sensors in three positions (bottom, middle and top). The entire system for measuring conductivity and making second by second data transmission was also described in the same numeral. Below are the homogenization graphs with the results obtained in each of the sensors located in the three Top, Middle and Bottom positions of the reactor are presented below. In each position, the 9 injections of the tracer are presented (Figure 25).

⁹ R: A language and environment for statistical computing. R Foundation for Statistical Computing, Vienna, Austria. URL. <https://www.R-project.org/>

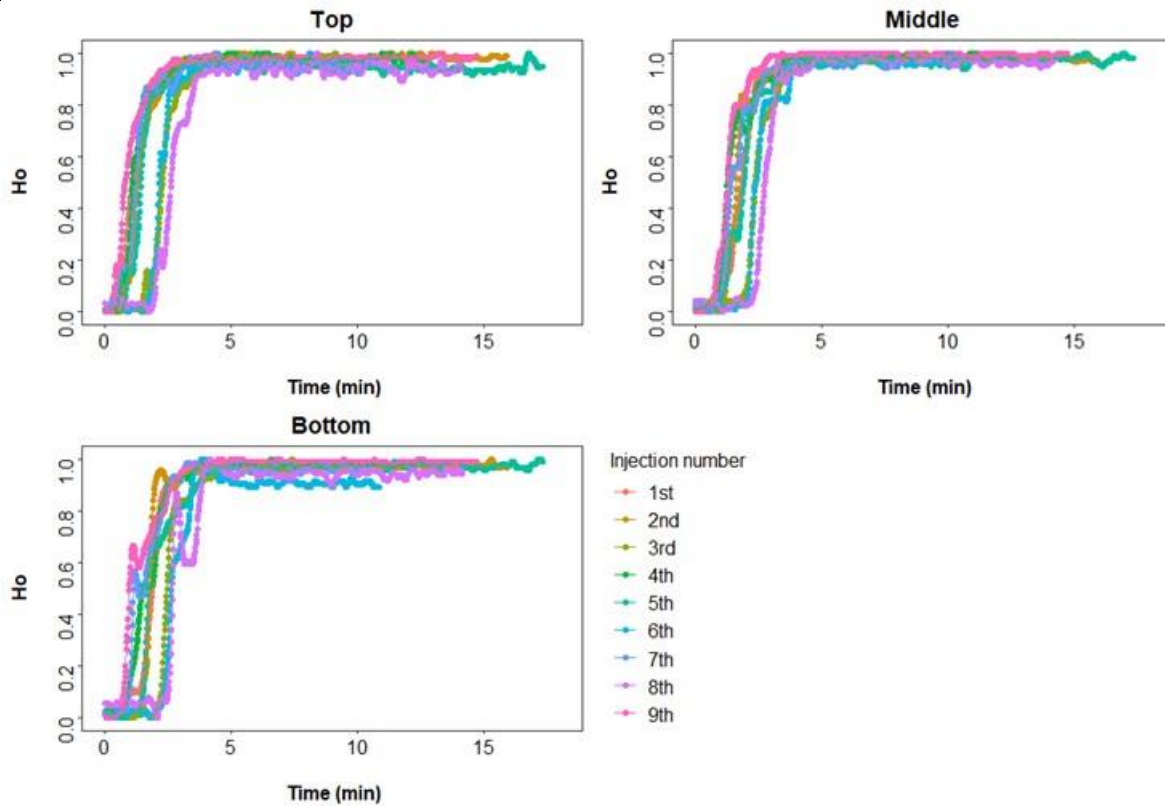


Figure 25 Results of homogenisation vs. mixing time at the three sensors of ALR.

In the Table 13 the mean and median time (in minutes) show that the homogenization took longer to be observed at the sensor located at the bottom, and the shortest homogenization time observed corresponds to the top. However, the boxplot shows that no statistical difference was observed between the homogenisation times (see Figure 26). The standard deviation is the most common measure of dispersion, which in this case indicates how dispersed the data are from the mean. As the standard deviation is smaller, the less dispersion or variability there is in this case.

Table 13 Mean, Median and Standard Deviation of the homogenisation times

Position	Statistic		
	Mean	Standard Deviation	Median
Bottom	3.494	0.604	3.433
Middle	3.383	0.404	3.367
Top	3.180	0.497	3.017

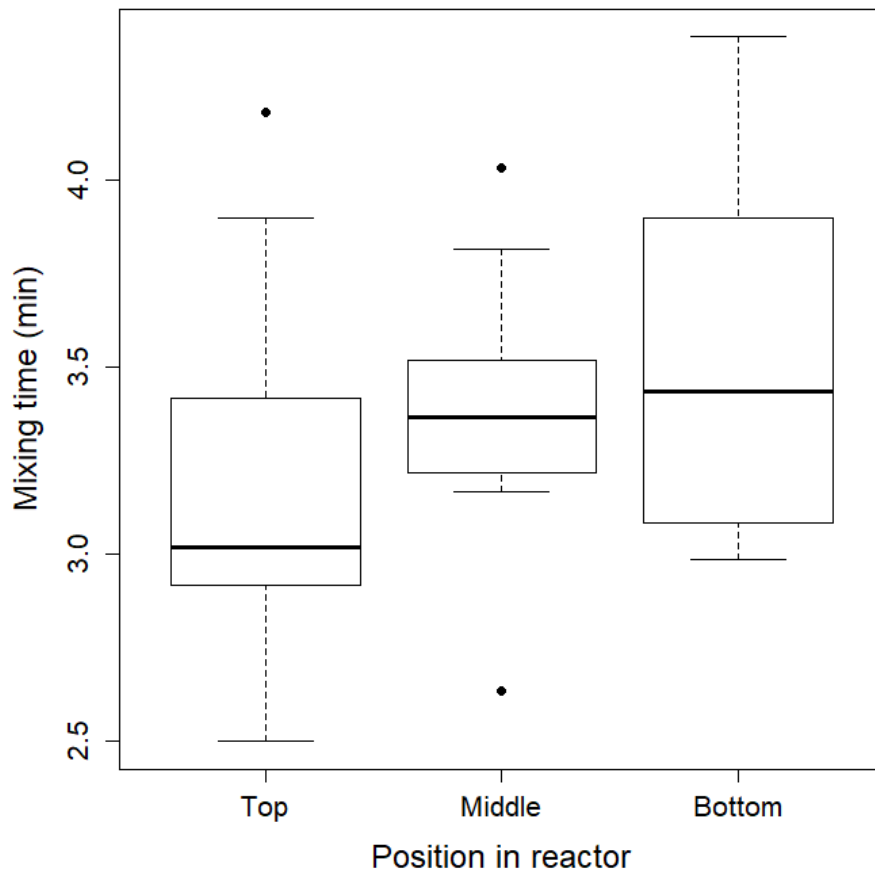


Figure 26 Boxplot of the homogenization time in the positions of the ALR

Let T, M, B be letters to designate the top, middle and bottom positions within the reactor. According to what was observed in the descriptive statistics regarding the results of the experiment, the following hypothesis is proposed:

$$H_0: \mu_T = \mu_M = \mu_B$$

$$H_1: \mu_i \neq \mu_j,$$

for some $i \neq j$, with $i = \{T, M, B\}$ and $j = \{T, M, B\}$, where μ_i is the average homogenization time for the sensor located in position i . To verify the hypothesis formulated, an ANOVA test was performed (see Table 14).

Table 14 Results of ANOVA test

ANOVA Test					
	DF*	Sum Sq.	Mean Sq.	F value	p-value
Position	2	0.459	0.229	0.952	0.400
Residuals	27	5.784	0.241		
Total	29	6.243	0.470		

*Degrees of freedom

According to the ANOVA test, there are no statistically significant differences between the homogenization times observed at the three reactor positions with a 95% confidence level ($p\text{-value} = 0.400 > 0.05$). The assumption of constant variance, which is fundamental to validating the ANOVA test result, is tested by testing the following hypothesis:

$$H_0: \sigma_T^2 = \sigma_M^2 = \sigma_B^2$$

$$H_1: \sigma_i^2 \neq \sigma_j^2,$$

for some $i \neq j$. To verify it, the Levene test is performed, under which the null hypothesis is not rejected ($p\text{-value} = 0.741 > 0.05$) with 95% confidence, as shown in the Table 15:

Table 15 Results of Levene Test

Levene Test		
F value	DF*	p-value
0.304	2	0.741

*Degrees of freedom

Homogenization time

From the previous analysis, it was established that the homogenization time is not significantly different in the three measurement positions. To estimate the homogenization time of the reactor, a non-linear logistic model was adjusted:

$$Ho(t) = \frac{Ho_{max}}{1 + \exp[-k(t - t_0)]}$$

where:

- Ho_{max} is the maximum homogenisation value reached.
- k is the growth rate.
- t_0 is the time corresponding to the midpoint of the sigmoid.
- t is the time elapsed since the start of the experiment (injection procedure).

The setting is illustrated in the Figure 27 and Table 16, where a solid black curve corresponds to the adjusted model.

Table 16 Results of a non-linear logistic model

Parameter	Estimate	Std. Error	t value	p value
Ho_{max}	0.970	0.001	1078.2	<0.001
k	2.005	0.018	110.8	<0.001
t_0	1.703	0.005	336.3	<0.001

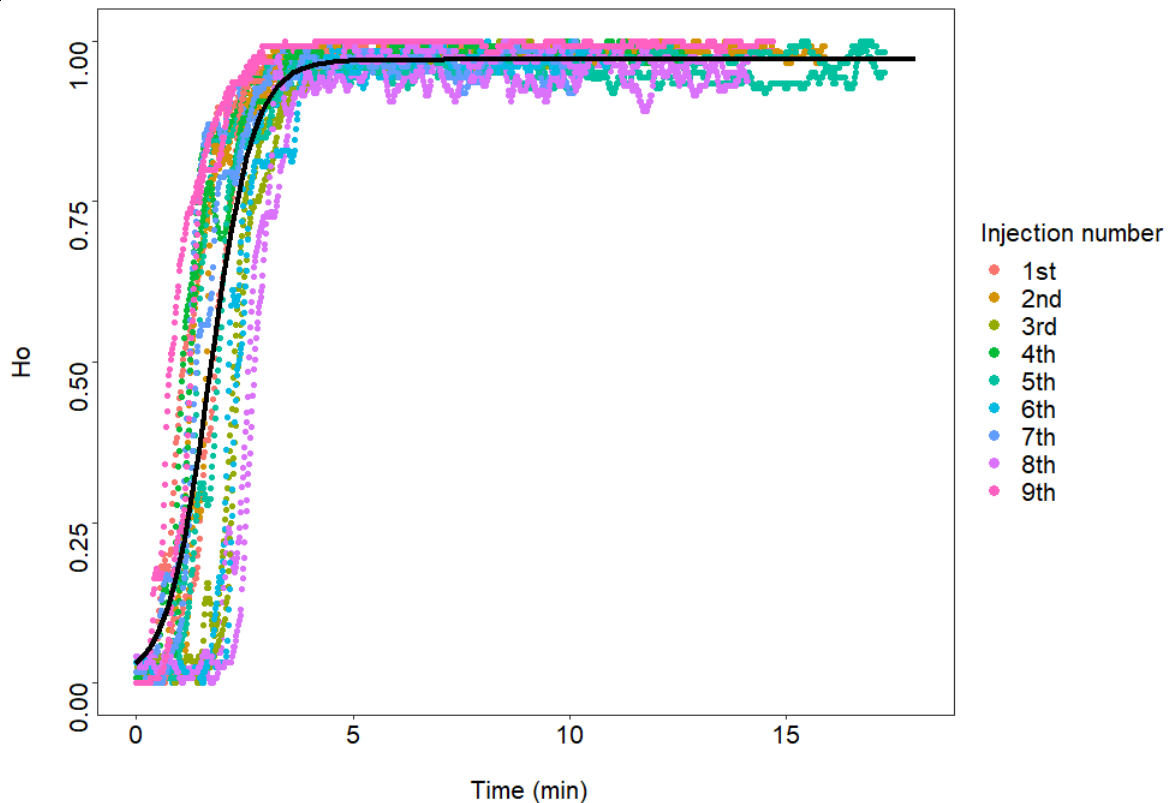


Figure 27 Non-linear logistic adjusted model using each injection

According to the estimated values, after 1.703 minutes half the rise has taken place (parameter t_0) and the rise rate is 2.005 units per minute. To estimate the homogenization time, the establishment time (t_s) is calculated, which corresponds to the time value for which a 5% change is observed with respect to the maximum homogenization (Ho_{max}). This situation occurs when the slope becomes very small, and can be expressed as follows:

$$\frac{Ho_{max} - Ho(t_s)}{Ho_{max}} = 0.05.$$

Replacing the adjusted model, the following expression is obtained:

$$Ho_{max} - \frac{Ho_{max}}{1 + \exp[-k(t_s - t_0)]} = 0.05Ho_{max}$$

Clearing the establishment time, it must be:

$$t_s = -\frac{1}{k} \log\left(\frac{0.05}{0.95}\right) + t_0,$$

where $\log(\cdot)$ is the natural logarithm. Replacing the adjusted values of the parameters, it is obtained that $t_s = 3.172 \text{ min}$.

Uranine Test

A laboratory test was performed using Uranine as a fluorescent tracer, which was injected into the ALR with the same system used in the KCL tracer tests. The ALR was turned on and a GoPro underwater camera was installed inside the reactor. In the video of Uranine it is appreciated the mouth of injection of the tracer to the draft tube, exactly under the gas injection made by the 4 orifices located in the ring of the tube.

After 2:30 minutes from the ignition, the injection of one litre of drinking tap water, in which pure Uranine powder had been previously diluted, was carried out for a final concentration of 20 mg/l in the injection. The entire injection system and the interior of the reactor can be seen in the video of the Annex 2 with a total duration of 8:49 minutes, that is, more than 6 minutes of mixing were guaranteed so that the complete lap and homogenization of the tracer was achieved (>3.21 min) and also the maximum value (4.23 min).

Finally, a second video was taken where the entire water column is shown completely mixed and the presence of the colorimetric tracer can be seen both in the water column and in the samples taken at the outlet of the sampling valves located on the side of the ALR reactor.

The most important result of this test was the possibility of calculating at least 2 seconds of inefficiency or delay in movement of the horizontal flow of the clearances zones of the reactor (C_t and C_b) that were used in the calculation of the theoretical mathematical model presented in numeral 6.4.

7.3.3 Rheology performance in ALR

Newtonian fluids

The rheological behaviour of the ALR reactor for Newtonian fluids could be carried out in a satisfactory manner, due to the characterization of the fluid by the Reynold number equation, whose mathematical basis was described in numeral 6.4. The flow regimes were turbulent in the draft tube and laminar in the downcomer. The viscosity tests performed for the water and KCl solution gave an average value for the samples taken at Top, Middle and Bottom of 0.015 Pa*s (UNKRIG, L. 2018), values that were used for the calculation of the Reynolds number described above.

Non-newton (using methylcellulose)

In order to analyse the behaviour of non-Newtonian fluids in the ALR, 2 kg of methyl cellulose (MC: comercial Vliestapeten-Kleister) was dissolved in the reactor water, which was then turned on to make the mixing system work previously and to ensure that the addition of the MC was done in a completely mixed medium.

However, the results of the test showed that the recirculation system of the mixture from the downcomer to the draft tube is insufficient for fluids that do not have a Newtonian behaviour. It was evident that the precipitation of the added MC was

contained in the region of the bottom clearance without being able to be raised again to the riser by the draft tube.

The viscosity values determined at laboratory Top: 0.015 Pa*s, Middle: 0.015 Pa*s and Bottom: 0.015 Pa*s (UNKRIG, L. (2018) showed that there were no differences with the viscosities determined for the KCl solution, which confirms that the material was not suspended again, precipitating to the bottom of the reactor.

7.3.4 Performance mathematical simulation model

To create a model of the hydrodynamic behavior of the ALR, previously described in numeral 6.1.3.1 , a software called ITHINK or STELLA (Systems Thinking, Experimental Learning Laboratory with Animation) V.9.0.2 was used, which allows the modeling of system dynamics. It was introduced by Barry Marshall Richmond in 1985, who created a company called isee systems (formerly High Performance Systems)¹⁰, the software was commercially developed and allows users to run models created as graphical representations of a system using fundamental building blocks. STELLA has been used in academia as a teaching tool and has been utilized in a variety of research and business applications.

The software registration number used in this research corresponds to No. 90047722182, version used by students of the university “Escuela de Ingeniería de Antioquia -EIA” in Medellin, Colombia and belonging to the professor (Pulgarin, B. 2019) expert in simulation who provided advice on the handling of this tool. The following is a description of the analysis performed and the variables included in the model. In addition, in Annex 3 a tutorial is presented to run the model performed for the ALR (with IThink software).

The basis for creating the model was based on Figure 28 also described presented in numeral 3.2.2 (Figure28), which shows the operating and design variables of gas-lift bioreactors and their influence on hydrodynamic properties. Based on this, the

¹⁰ <https://www.iseesystems.com/resources/tutorials/> Find tutorials for Dynamic Modelling.

variables that were studied in this research were prioritized, such as viscosity, liquid velocity, flow in the riser, and, the geometric variables as Top and Bottom Clearances (Ct, C), Reactor Height and separator design.

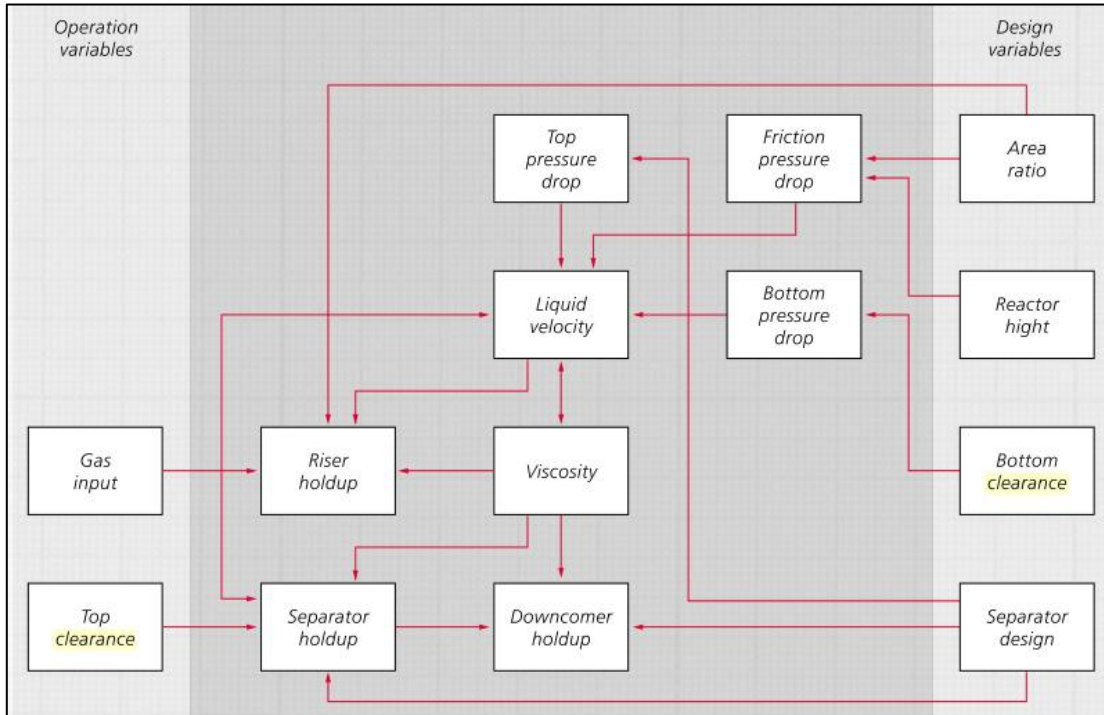


Figure 28 Operating and design variables

Source: (SCHWEINFURTH, K.; et al. 2013)

The model assumes that there are no changes in the liquid level in the reactor (as was the case during the ALR laboratory tests), therefore there is no possibility of flow losses. The variables and values used are described below, the dimensions of the reactor and data included in the model were previously explained in numeral 6.4 in the description of mathematical model, including the Figure 21 from which the values in centimeters, grams and seconds are taken.

$$C_t = \text{Top clearance} = 21$$

$$C_b = \text{Bottom clearance} = 10$$

$$\text{Cycle} = \text{Time_in_Dt} + \text{Time_in_Ct} + \text{Time_in_Dw} + \text{Time_in_Cb}$$

$$Dt = \text{Draft tube diameter} = 10$$

$$D = \text{Reactor_diameter} = 108.5$$

$$\text{Flow} = \frac{\text{VelRiser}}{60} * 1000$$

$$HDt = \text{Height in Draft tube} = 81$$

$$\text{Linear Velocity in Dt} = \frac{HDt}{\text{Time_in_Dt}}$$

$$\text{Linear Velocity in Dw} = \frac{HDt}{\text{Time_in_Dw}}$$

$$\text{Time_in_Ct} = \frac{\text{VolCt}}{\text{Flow}}$$

$$\text{Time_in_Cb} = \frac{\text{VolCb}}{\text{Flow}}$$

$$\text{Time_in_Dt} = \frac{\text{VolDt}}{\text{Flow}}$$

$$\text{Time_in_Dw} = \frac{\text{VolDw}}{\text{Flow}}$$

$$VDt = \text{Draft tube volume} = \frac{\pi Dt^2}{4} * HDt$$

$$VDw = \text{Downcomer volume} = \left(\frac{\pi D^2}{4} \right) * HDt - VDt$$

$$\text{VolCb} = \text{Bottom clearance} = \frac{\pi D^2}{4} * Cb$$

$$\text{VolCL} = \text{Clearances volume} = \frac{\pi D^2}{4} * (Ct + Cb)$$

$$\text{VolCt} = \text{Top clearance} = \text{VolCL} - \text{VolCb}$$

$$\text{VolTot} = \text{Total Volume} = VDt + VDw + \text{VolCL}$$

$$\rho = \text{Fluid density} = 0.997$$

$$\mu = \text{Dynamic viscosity} = 0.15$$

The model is a tool that allows to simulate or model any system that changes over time. All the circles are similar to the Excel systems, formed by columns and rows, where the columns are the names of the circles or in the Excel systems the equivalent to column A, B, C, and each row is equivalent to a time differential, then there would be as many columns as time differentials exist; in this software the circles are called signal converter that could give different results as time goes by. The software also has level variables, which are called stoke (tanks); the tank is a level variable that with time can change and therefore the level variables makes the system dynamic.

The object of the model was to analyse the hydrodynamics of the ARL reactor, which was done taking into account the geometric variables of the reactor, the determinations of the linear velocities in the riser and in the downcomer, the definition of volumes (cylindrical) and the calculation of the Reynolds number for both the riser and the downcomer (in this case similar to the characterization of the flow in pipes).

To explain the cycle that was modelled in this software, the 4 stages that were selected for analysis within the reactor are presented. The first one refers to the analysis of the flow from the draft tube to the top clearance (No. 01 in Figure 29); the second one is the flow from the top clearance to the dowcomer (No. 02 in Figure 29), the third one is the flow from the downcomer to the bottom clearance (No. 03 in Figure 29) and the fourth one is the flow from the bottom clearance to the draft tube (No. 04 in Figure 29); in this way the cycle is closed and the complete turn in the flow is assured, which in the theoretical mathematical analysis took 190.49 seconds (3.17min - numeral 6.4) and in the experimental test of mixing time to reach homogenization 3.21 min. seconds (numeral 7.3.2).

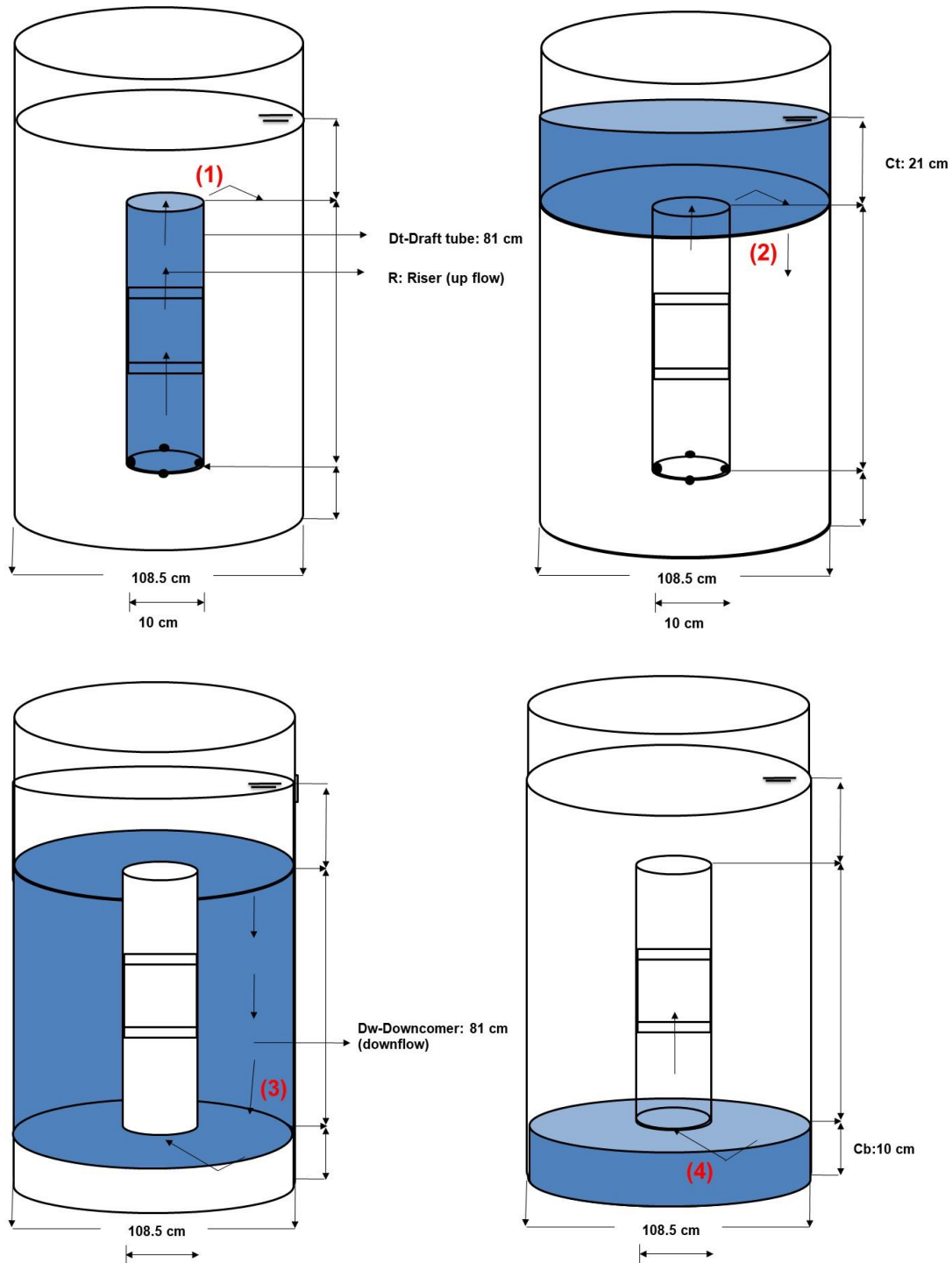


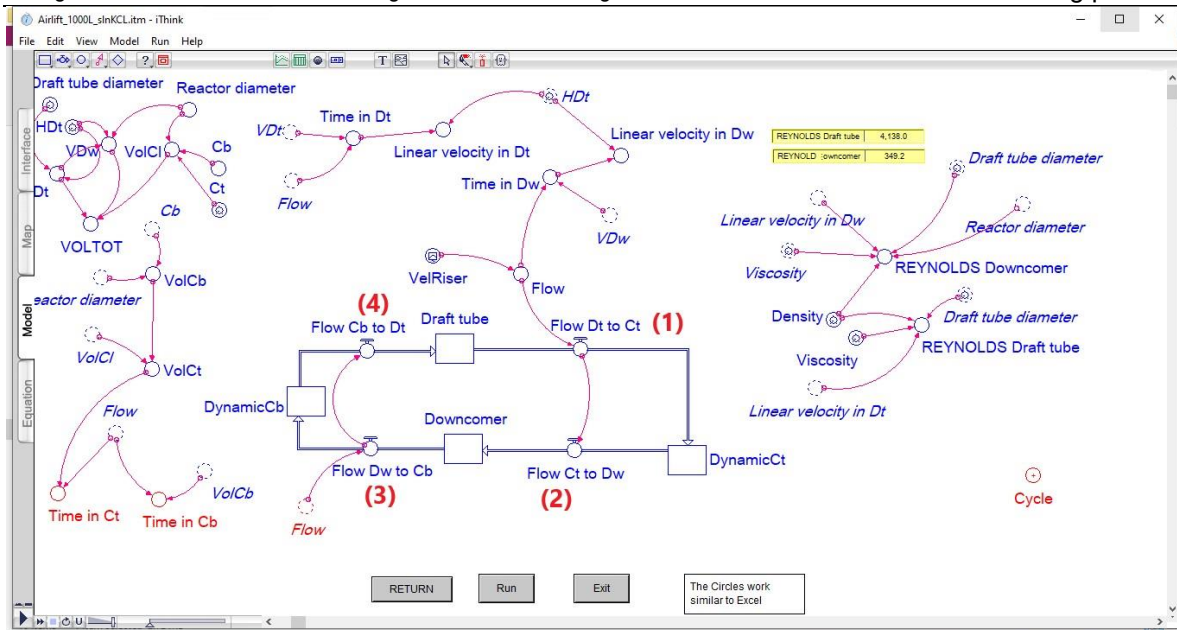
Figure 29 Complete flow cycle in ALR

Source (Own elaboration)

It should be noted that unlike the assumptions of the theoretical mathematical model presented in paragraph 6.4 (where the time of the horizontal flow of the clearances is assumed as two seconds determined in the video of the tracer with uranine) for flow modelling effects in the down comer, the same height of the draft tube was taken for the down comer.

Below is the screenshot with the level variables (or stock) that correspond to the tanks that connect with the flows described in Figure 29. These tanks are the ones that can change in time, that is, the volumes of C_t and C_b can change according to the position of the draft tube, the operational conditions established when the reactor starts operating or to the geometric variables to be modified in the design. This image is known as a causal loop diagram or Forrester diagram, which receives that name from Professor Jay Forrester who is one of the creators of systems dynamics (his first publication on systems dynamics was in 1961), a causal loop diagram is a simple map of a system with all its constituent components and their interactions. These diagrams can be used in different systems dynamics software, it is not exclusively for use in IThink and no license is required for it.

Forrester Diagram



With this simulation it was sought that in addition to the graphic demonstration of the homogenization reached with KCL tracer test and statistical analysis presented in numeral 7.3.2, the model would permit to analyze the geometric variables that can influence the design of the reactor ALR, also allow hydrodynamically characterize the flow in which the Reynolds number theoretically determined in the draft tube (numeral 6.4) gave a value of $Re_{Dt} = 4144$ and the number of Reynolds determined in the systemic simulation model gave a number of $Re_{Dt} = 4138$; these values corroborate that the hydrodynamic behavior of the draft tube in the ALR reactor is classified as turbulent. Likewise, the hydrodynamic characteristics in the reactor are checked, which for the case the theoretical mathematical model gave a Reynolds number of $Re_R = 301.41$ classifying the flow as laminar, but which in the simulation model was mathematically more precise due to the fact that the geometric tube structure (pipe) can only be used in the area corresponding to the downcomer giving a reynolds value of $Re_{Dw} = 349.2$. The small difference between the two values is due to the fact that in the theoretical model an inefficiency or loss of time was assumed in the horizontal areas of Ct and CB, which were discounted by 2 seconds according to the tests carried out with the Uranine fluorescent tracer.

Finally, it is verified that the mixing time for the flow to be completely mixed and homogenized must be greater than 191.2 seconds (3.19 min); that is, the mixing periods programmed for future anaerobic digestion and biogas production tests in both the KG-ASBR and ALR reactors must be greater than 3.2 minutes.

7.4 Comparison ST-ASBR and KG-ASBR reactors

With the results obtained in the methanization phase of the ASBR, ASBR+B and CSTR reactors, it was possible to establish the operational parameters that would allow to operate the KG-ASBR and ST-ASBR reactors in a stable way and thus make the comparison in terms of reference values of Y_{CH_4} and MBR .

7.4.1 Performance of operational and evaluation parameters

Methane Yield (Y_{CH_4}) and OLR

The Figure 30 and Figure 31 show the behaviour of the KG and ST -ASBR reactors respectively in terms of Y_{CH_4} vs OLR.

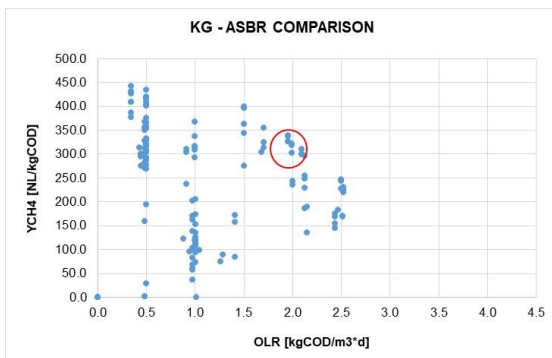


Figure 30 Y_{CH_4} in KG ASBR

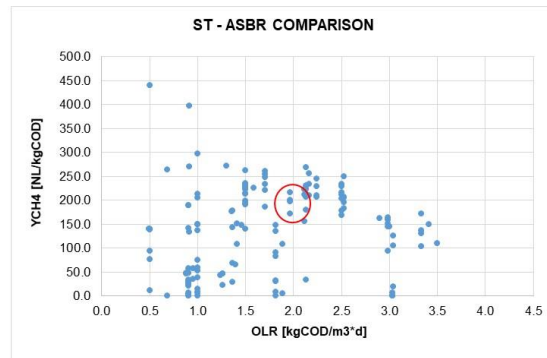


Figure 31 Y_{CH_4} in ST -ASBR

From Figure 30 and Figure 31 it can be seen that the reactor with the innovative mixing system KG-ASBR, reaches higher methane yields Y_{CH_4} :300-350 NL/kg_{COD} (presents better data dispersion) at low organic loads of operation (OLR \approx 2

$\text{kg}_{\text{COD}}/\text{m}^3\cdot\text{d}$) compared to the ST-ASBR reactor (150-250 NL/ kg_{COD}), being within the normal ranges reported for this type of substrate (FNR)¹¹. Furthermore, if this result is compared with those reported by Buhle,2016, where yield values between (200-300 NL/ kg_{COD}) were obtained at the same OLR, it can be deduced that the reactor KG-ASBR has a good performance of the new mixing system compared to the ST-ASBR system.

Productivity (MBR CH₄) and OLR

The Figure 32 and Figure 33 show the behaviour of the KG and ST -ASBR reactors respectively in terms of MBRCH₄ vs OLR.

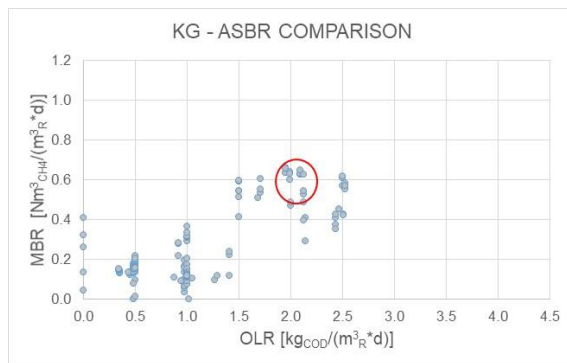


Figure 32 MBRCH₄ in KG ASBR ASBR

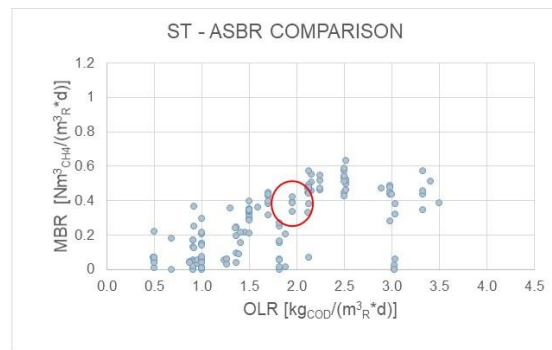


Figure 33 MBR CH₄ in ST - ASBR

As it happened with the methane yield at the same OLR, the productivity behaves better in the KG-ASBR reactor (MBRCH₄: 0.5-0.7 Nm³/m³·d) than in the ST-ASBR (MBRCH₄: 0.3-0.4 Nm³/m³·d). Likewise, if it is compared with the results reported by Buhle, 2016, MBRCH₄ values between 0.5-0.6 Nm³/m³·d at the same OLR are observed, then a good performance in both systems can be appreciated.

¹¹ Average biogas yield of maize silage 340 NL/ kg_{COD} . Rohstoffe, F. N. Guide to biogas. From production to use Fachagentur Nachwachsende Rohstoffe, 2010, 5th edition.

YCH₄ and MBRCH₄ vs HRT

Due to the fact that the substrate or hydrolysate preparations were made in the same laboratory, it was not possible to maintain constant COD loads values during the feeding of both reactors (OLR_{COD}). This fact can affect HRT results and lead to an error. However, it is known from research conducted with the three ASBR reactors that the optimum hydraulic retention times found for this substrate in mechanically mixed ASBR was HRT: 4.5 - 5 days. From the above, it can be deduced that a good result is obtained for both reactors in terms of yield and methane productivity behaviour (range in both reactors YCH₄: 100-200 NI/Kg_{COD} and MBR CH₄: 0.4-0.6 Nm³/m³*d) at 5 days of HRT, see Figures 34 and Figure 35.

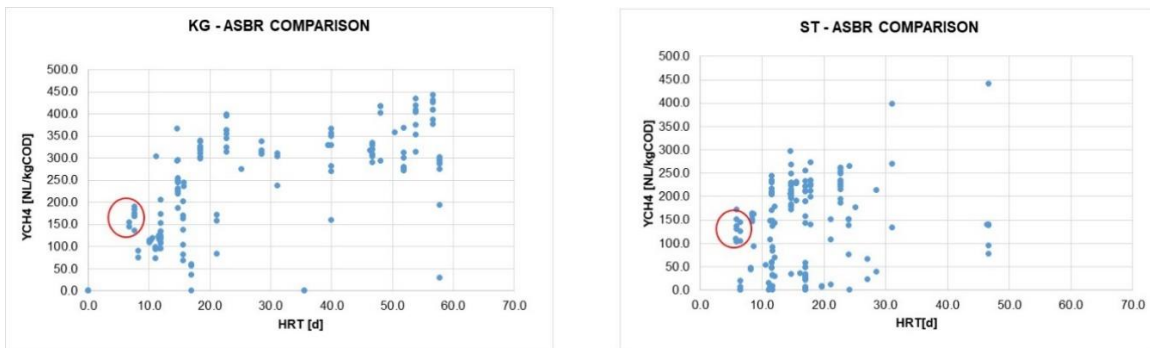


Figure 34 YCH₄ vs HRT in both reactors (KG-ASBR and ST-ASBR)

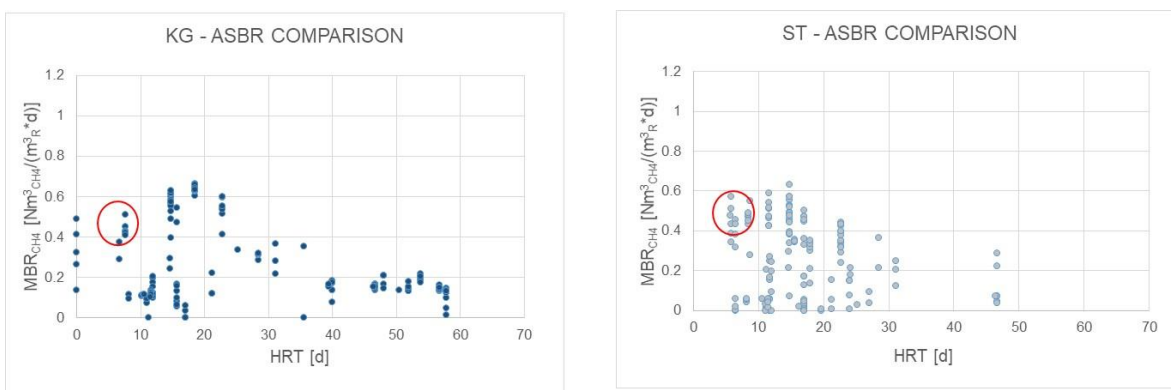


Figure 35 MBRCH₄ vs HRT in both reactors (KG-ASBR and ST ASBR)

For measuring date reference see Annex 6.1 and 6.2.

7.4.2 Comparison Mixing strategy

Dynamic viscosity and mixing strategy

Viscosity values in 14 weeks of sampling are presented in Figure 36, Figure 37, Figure 38 and Figure 39; a graph for each type of anchor stirrer system 71 and 72 and each three sampling valves of each reactor (Top, Middle and Bottom).

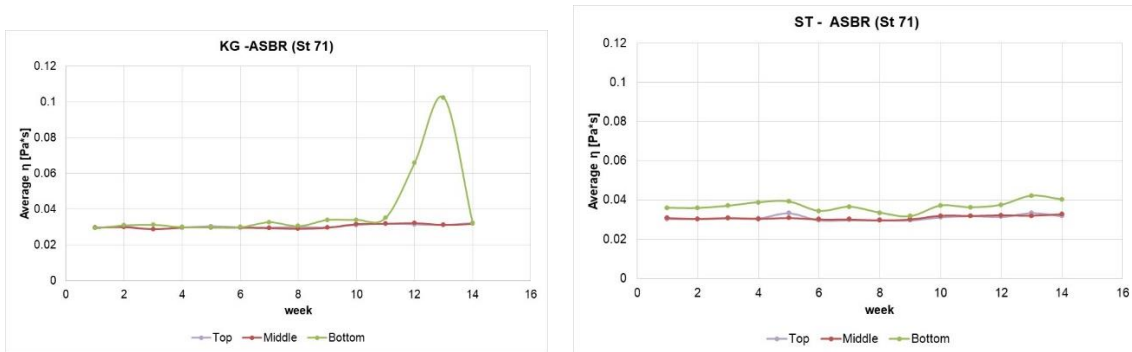


Figure 36 Dynamic viscosity in KG ASBR (Anchor 71) and Figure 37 Dynamic viscosity in ST ASBR (Anchor 71)

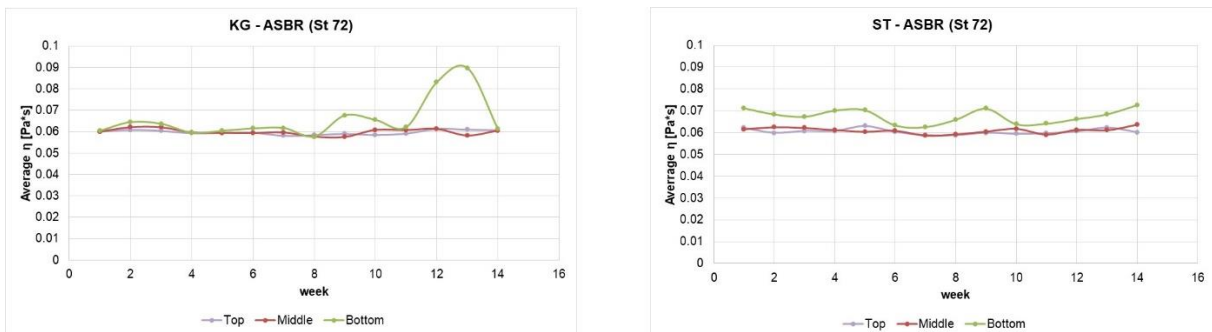


Figure 38 Dynamic viscosity in KG ASBR (Anchor 72) and Figure 39 Dynamic viscosity in ST ASBR (Anchor 72)

In week 13, there was an error in the sampling of the laboratory and therefore this point is not analysed. There are also no differences in the rheological analysis of the two reactors. Since the dynamic viscosity values were within the same range, with average values between 0.06 and 0.07 Pa*s. These values are similar to those presented by Martens, 2016, who determined the rheological characteristics of the ST - ASBR reactor in its start-up phase, the values she reports are also in the range (0.06-0.08 Pa*s), using the same anchor system.

For measuring date reference see Annex 7.

OTS before and after mixing

TS and OTS values in 14 weeks of sampling are presented in Figure 40, Figure 41, Figure 42 and Figure 43; the samples correspond to three sampling valves in each reactor (Top, Middle and Bottom) and two samples per week, one before the mixing process and one after the mixing process.

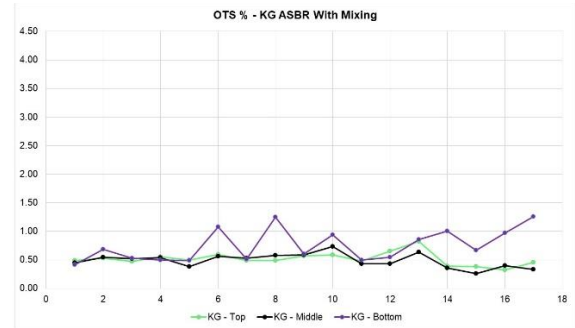


Figure 40 OTS% in KG ASBR without mixing and Figure 41 OTS% in KG ASBR with mixing

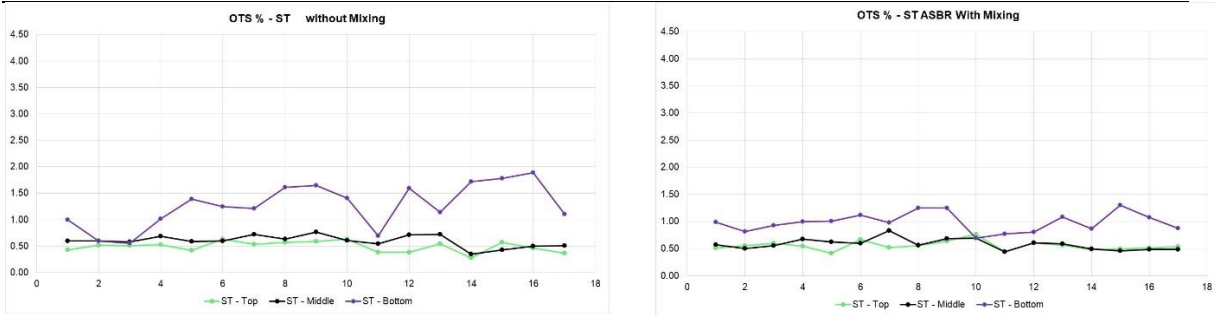


Figure 42 OTS% in ST ASBR without mixing and Figure 43 OTS% in ST ASBR with mixing

There was only a slight improvement in mixing homogeneity associated with the OTS values determined in sampling before and after the mixing cycle. In general, both mixing systems show that there is effective resuspension of biomass required for the reaction cycle of the ASBR reactor. But at the same time, it is also visualized that there is a possible increase of sludge accumulation in the bottom clearance of the KG ASBR reactor, which could have a negative influence in the performance if the viscosity of the fluid increases and beginning a stratification process.

For measuring date reference see Annex 8.

8 Conclusions and recommendations

Although the Methane Yield values of the KG-ASBR reactor are higher than those of ST-ASBR, both values determined at laboratory level are within the expected values for maize silage substrate. The operation cycles programmed for the KG ASBR and ST ASBR reactors worked adequately, demonstrating that there are no significant differences in terms of Methane Productivity with respect to the sampling time. It is concluded that there is no difference between the agitation speed selected for the ST mixture (20-30 rpm), as well as in the mixing times of 20min and 40min, making energy expenditure unnecessary in longer periods of mixing time or self-consumption energy requirements that are not required.

It was possible to determine the hydrodynamic characterisation of the flows of the ALR reactor, which began with a theoretical mathematical model allowing the calculation of the linear velocity in the draft tube (0.6907 m/s) and the measurement range of values for the liquid and gas flows respectively (0.12 and 2.42 m³/h: water and 5.77 and 22.51 m³/h air). Likewise, the range of linear velocity of the liquid that can be measured in the draft tube was determined through the series of experiments carried out with the transmission of data from the flow meter, which at a fixed air supply value of 1.92 m³/h gives a value very similar to that found in the theoretical mathematical model (0.6942 m/s). In this way, the mathematical, graphical and statistical validation of the results obtained in the laboratory is given, allowing these data to be used in possible scale-up studies at a semi-industrial level with companies such as GICON GmbH.

The mathematical model developed in IThink also validates the results obtained in the experimental test (V_{dt} and rheological behavior with respect to viscosity and Reynolds number equation), thus simplifying the analysis of scale-up scenarios at an industrial level since it allows the modification and optimizing of geometric variables and the hydrodynamic analysis of the flows in each section of the reactor.

It is concluded that the selection of the air supply chosen to reach the homogenization (1.92 m³/h) allowed to obtain linear velocities that guaranteed the good operation of the reactor with gas/air lift systems such as the ALR and the KG-ASBR, as long as the fluids are classified as non-Newtonian and have low solids content, as in the case of methanization of hydrolysed substrates obtained in two-stage-two-phase system for the fermentation process (substrates with high solids content that are suitable for the first phase of percolation) and subsequent methanization in a gas lift reactor such as the KG-ASBR.

For the KG-ASBR reactor, it was possible to verify that the flow of the selected air flow of 1.9 m³/h did not generate disturbances in the methanogenic microorganisms due to good yields and productivity of methane. As a recommendation, it is suggested to perform a laboratory level test of anaerobic digestion with municipal organic waste substrates such as those from the city of Medellin, Colombia, in a two-stage process where percolation of the substrate provided the hydrolysed and the methanization phase is carried out in a gas lift system reactor (like KG-ASBR), if possible under “tropicalization” conditions in Colombia.

Regarding the rheological characterization of the flow by the equation of Reynolds number and dynamic viscosity measured in the laboratory, it is concluded that the reactor has a turbulent flow in the raiser and laminar in the downcomer that allows obtaining the homogenization of the mixture after a maximum time of 4.23 minutes and an average time of 3.21 minutes. Although the flow is laminar in the down comer, for fluids that are Newtonian there will be no influence of the geometry of the reactor to reach the homogenization. However, when non-Newtonian fluids or higher dry matter content are involved, new designs should be explored to prevent substrate precipitation at the bottom of the reactor with undesirable stratification.

The values of time required to reach the homogenization analysed in the theoretical mathematical model (3.17 min) and those determined in the experimental test at laboratory level (3.21 min), such as the values of the statistical analysis of data (3.172 min) and the homogenization values given by the simulation program (3.19

min) prove that it is possible to minimize mixing times during the 4 cycles programmed per day for the ASBR reactors in this investigation, significantly reducing the total mixing time to less than 20 minutes per day and therefore achieving process optimization in terms of savings in mixing times, that as mentioned in this document, at industrial level required high OPEX costs because in an industrial biogas plant about 40% of energy is consumed in the mixture of anaerobic digesters according to studies reported by Kamarád, L. et al. 2013

It is also shown that based on the comparison of the OTS and TS values, and viscosity of the KG-ASBR and ST ASBR reactors, there are no major differences in the mixing periods of 20 and 40 minutes, therefore it is concluded that it is possible to reduce the reaction periods in the 4 daily cycles set for the operation of the ASBR reactors in the methanization phase.

Finally, regarding the effect of the geometric design on the performance of the reactor, it is recommended to continue exploring the use of the system dynamics model and developing new models that allow future analyses of the influence of geometric variables and determination of a weighted average of the Reynolds number for the clearance zones in Top and Bottom (highlighted in red in the Forrester diagram of the model in IThink), so that at the end 4 Reynolds numbers will be known instead of the 2 that were determined in the scope of this research (to explore a hydrodynamic curvature of the shape of the upper diameter of the draft tube); as well as exploring new and more complex simulation models to be applied for example to the modelling of the behaviour of multi-phase gas-lift bioreactor according to the developments made by MACDONALD, J, M.; *et al.* 2011.

9 Summary

The Anaerobic Sequencing Batch Reactor (ASBR) operates by sequential batches, has been studied as an alternative treatment for different systems because of their versatility. The ASBR is applicable for the conversion of a wide variety of organic wastewaters to methane and carbon dioxide (biogas). The main factors affecting the overall performance of the ASBR are: agitation, Substrate/Biomass ratio, geometric configuration of the reactor and the feeding strategy. In this research the strategy agitation was carried out by used of a gaslift system coupled to an ASBR. The aim of the research was the creation of bases for the design and process control of an Anaerobic Sequencing Batch Gaslift Reactor on a laboratory scale in order to find the optimal operating regime and optimize the process. The type of gaslift system to be used is an internal loop with a concentric draught tube configuration, which enables the gas may be sparged either the draught tube or the annulus. The simple design of a gas lift reactor permits less expensive operation, requires less maintenance, low investment costs, low interference and low power consumption. Scientific and technical objectives of the research include the analysis of macro geometric dimensions of the reactor, developing innovative solutions for optimization of mixing process (gaslift mixing), analysis of the hydrodynamics and the homogenization inside of the reactor.

This study also includes the flow determination in the riser, the evaluation of the liquid circulation velocity in the downcomer and the influence of the vertical draft tube and the effect of top and bottom clearance. Also, the goal was to find an adequate mixture to not destroy microorganisms but to allow the sedimented biomass and undigested solids may rise quickly and mixed with the feed substrate.

REFERENCES

ANAYA, L. (2017). Determination of behaviour of Organic Load Rate in the Start-up and operation of Gas-Lift Anaerobic Sequence Batch Reactor. Study Project. Cottbus. P. 1-39.

ASCANIO, G. (2015). Mixing time in stirred vessels: A review of experimental techniques. Chinese Journal of Chemical Engineering 23. 1065–1076

BANDO, Y., HAYAKAWA, H., AND NISHIMURA, M. (1998). Effects of equipment dimensions on liquid mixing time of bubble column with draft tube, J. Chem. Eng. Japan., 31 (5), 765

BTU - Brandenburgische Technische Universität. LS für Hydrologie und Wasserwirtschaft (1997 aktualisiert Juli 2006). Skript: Konzeption und Durchführung eines Tracerversuches in einem kleinen Fließgewässer. Cottbus. P. 1-17.

BTU - Brandenburgische Technische Universität. Chair of Waste Management. (2006). Practical Exercise on Waste Analysis. P. 1-65.

BUHLE, D. (2016). Die Methanisierung von Hydrolysaten im CSTR und ASBR – Ermittlung der Leistungsfähigkeit und der Betriebsgrenzen. Masterarbeit. Cottbus. P. 1-60.

BUSCH, G.; GROSSMANN, J.; SIEBER, M.; BURKHARDT, M. (2009). A New and Sound Technology for Biogas from Solid Waste and Biomass. Water Air Soil Pollution : Focus 9 (1):89-97.

BUSCHMANN, J. (2015). Erhöhung der Leistungsfähigkeit von Feststoffvergärungen in zweistufigen-zweiphasigen Systemen. Dissertation. Cottbus. S. 1-138

BUZÁDY, A.; EROSTYÁK, J.; PAÁL, G. (2006). Determination of uranine tracer dye from underground water of Mecsek Hill, Hungary. J. Biochem. Biophys. Methods 69. P. 207 – 214.

CHISTI, M.Y; MOO-YOUNG, M. (1987). Airlift Reactors: Characteristics, Applications and Design Considerations. Journal Chemical Engineering Communications, Volume 60, Issue 1-6. P.195-242.

CHOMCHARN, N. (2009). Experimental investigation of mixing time in a stirred, torispherical-bottomed tank equipped with a retreat-blade impeller. Thesis Submitted to the Faculty of New Jersey Institute of Technology. Department of Chemical, Biological and Pharmaceutical Engineering. P 1-42.

DAGUE, R (1993) Anaerobic Sequencing Batch Reactor. Patent Number: 5,185,079, USA.

DEUBLEIN, D; STEINHAUSER, A. (2014). Biogas from waste and renewable resources. An Introduction Second, Revised and Expanded Edition. Wiley-VCH Verlag GmbH & Co. KGaA. Weinheim, Germany.

DIERCKS, K. (2017). Optimization of anaerobic digestion of sewage sludge by cascade design: Determining retention time by full-scale tests and Ecological Assessment. Master Thesis. P1-75.

FARINA, R.; CELLAMARE C, M.; STANTE, L. and GIORDANO, A. (2004). Pilot scale anaerobic sequencing batch reactor for distillery wastewater treatment in 10th World Congress of anaerobic digestion. Vol 30, Montreal, Canada. ENEA, Agency for New technologies, Energy and Environment, PROT-IDR. Bologna, Italy

FEI-BAFFOE B. (2006). Double stage dry-wet fermentation of unsorted municipal solid waste. Ph.D. thesis at BTU Cottbus.

FREITAS C, TEIXEIRA J.A. (1998). Hydrodynamic studies in an airlift reactor with an enlarged degassing zone. Bioprocess Engineering. 1998; 18:267-79

GLENNON, B. & AI-MASRY, W. & MacLOUGHLIN, P. & MALONE, D.. (1993). Hydrodynamic Modeling in an Airlift Loop Reactor. Chemical Engineering Communications - CHEM ENG COMMUN. 121. 181-192.

HWANG, S-J.; CHENG, Y-L. (1997) Gas holdup and liquid velocity in three-phase internal-loop airlift reactors. *Chemical Engineering Science*. Volume 52, Issues 21–22, P. 3949-3960.

KAMARÁD, L.; POHN, S.; BOCHMANN, G.; HARASEK, M. (2013). Determination of mixing quality in biogas plant digesters using tracer tests and computational fluid dynamics. *Acta Universitatis Agriculturae et Silviculturae Mendelianae Brunensis*, LXI, No. 5, P. 1269–1278.

KOWALCZYK, A.; HARNISCH, E.; SCHWEDE, S.; GERBER, M.; SPAN, R. (2013): Different mixing modes for biogas plants using energy crops. *Applied Energy* 112. P. 465–472.

KRAUME, M.; ZEHNER, P. (2001). Experience with Experimental Standards for Measurements of Various Parameters in Stirred Tanks: A Comparative Test. *Chemical Engineering Research and Design* Volume 79, Issue 8, P. 811-818.

LE FRANCOIS, L. MARILLER, L. G., AND MEJANE, J. V. (1955). Effectionnements aux procedes de cultures forgiques et de fermentations industrielles / Improvements to fungal cultures and industrial fermentation processes. French Patent No. 1 102 200 /A.

LEVENSPIEL, O. (2012). *Tracer Technology Modeling the Flow of Fluids*. Springer. P. 1-135.

LIEBSCHER, S (2015). Determination of the stabilization of the organic loading rate, productivity and yield of biogas production in the operation of an Anaerobic Sequence Batch Reactor –ASBR– fed with organic food waste. Diplomarbeit. Cottbus, P. 1-46.

MACDONALD, J, M.; TIKUNOV, A, P. (2011). Multi-Phase, Gas-Lift Bioreactor for Generation of Biogas or Biofuel From Organic Material. Patent International Publication Number WO 2011/017420 A3.

MANJUSHA, Ca., SAJEENA, Bb. (2016). Mathematical Modelling and Simulation of Anaerobic Digestion of Solid Waste. *Procedia Technology* 24. P. 654 – 660.

MANNA, L. (1997). Comparison between physical and chemical methods for the measurement of mixing times. Chemical Engineering Journal 67. P.167-173

MERCHUK, J.C; Siegel, M.H. (1988). Air-Lift Reactors in Chemical and Biological Technology. J. Chem. Tech. Biotechnol. Vol 41, P. 105-120.

MERCHUK, J.C; Ladwa, N.; Cameron, A.; Bulmer, M. and Pickett, A. (1994): Concentric-Tube Airlift Reactors: Effects of Geometrical Design on Performance. AIChE Journal. Vol. 40, No. 7. P 1105-1117.

MERCHUK, J.; LADWA, N.; CAMERON, A.; BULMER, M.; BERZINB, I.; PICKETT, A. (1996). Liquid Flow and Mixing in Concentric Tube Air- Lift Reactors. J. Chem. Tech. Biotechnol. UK. Vol, 66, P.174-182.

MERCHUK, J.C.; GLUZ, M. (1999). Bioreactors, air-lift reactors. John Wiley & Sons, Inc. P. 320-394. Published Online: October 2002.

MARTENS, C. (2016). Analyse der Schlammentwicklung in einem ASBR - Methanisierungsreaktor während der Einfahrphase. Bachelorarbeit. Cottbus. P. 1-82.

MENDOZA, A.M.; ESCAMILLA, E.M.(2013). Airlift Bioreactors: Hydrodynamics and Rheology Application to Secondary Metabolites Production. Journal Mass Transfer - Advances in Sustainable Energy and Environment Oriented Numerical Modeling. P. 387-429

MEUSEL, W.; LÖFFELHOLZ, C.; HUSEMANN, U.; DREHER, T.; GRELLER, G.; KAULING, J.; EIBL, D.; KLEEBANK, S.; BAUER, I.; GLÖCKLER, R.; HUBER, P.; KUHLMANN, W.; JOHN, G. T.; WERNER, S.; KAISER, S.C.; PÖRTNER, R.; KRAUME, M. (2016): Recommendations for process engineering characterisation of single-use bioreactors and mixing systems by using experimental methods. DECHEMA Gesellschaft für Chemische Technik und Biotechnologie. Frankfurt am Main P. 4-22, 32-38.

MILIVOJEVIĆ, M.;DANIJELA, A.; BRANKO, B. (2010). Effects of air-lift reactor dimensions on its hydrodynamic characteristics/ Uticaj Geometrije Pneumatskog Reaktor. University of Belgrad JOUR. Hem. ind. 64 (1). P. 35–46.

MUTHANNA H.AL-D; HU-Ping. L. (2008). Local characteristics of hydrodynamics in draft tube airlift bioreactor. Chemical Engineering Science. Volume 63, Issue 11. USA. P. 3057-3068.

MUSIAŁ, M.; BITENC, M; KARCZ, J. (2014). Mixing characteristics for gas-liquid system in an external-loop air-lift column. Technical Transactions Chemistry. Department of chemical engineering, West Pomeranian University of Technology, Szczecin. P. 105-114.

OLDSHUE, J.Y. (1983). Fluid mixing Technology. Chemicak Engineering, McGraw-Hill Publications Co. New York. USA.

PAUL, E.D.; ATIEMO-OBENG, V.A.; KRESTA, S. M. (2004). Handbook of industrial mixing: science and practice. John Wiley & Sons, Inc., Hoboken, New Jersey. Published simultaneously in Canada.

PETERSEN E.; MARGARITIS, A. (2001). Hydrodynamic and Mas Transfer Characteristics of Three-Phase Gaslift Bioreactor Systems. Critical Reviews in Biotechnology. Canada. Vol 21:4,P. 233-294.

PULGARIN, B. (2019). Professor em. of System Dynamics, expert in simulation and Theory of Constrains. EIA, Escuela de Ingenieria de Antioquia, Medellín Colombia and Universidad Nacional de Colombia, Campus Medellín.

PULGARIN, I.; BUSCHMANN, J. (2017). Fundamentals of process design and control of anaerobic sequencing batch gas-lift reactor. Progress in Biogas IV - science meets practice: abstracts booklet of the international conference 8th-11th. University of Hohenheim, Stuttgart, Germany. S. 36 - 37.

RENEWABLES 2019 GLOBAL STATUS REPORT https://www.ren21.net/gsr-2019/chapters/chapter_03/chapter_03/ (accessed 25/06/19)

RIFFAT, R (2013). Fundamentals of Wastewater Treatment and Engineering. First edition. CRC Press. USA.

RIOS, A. (2015). Sedimentation rate and biodegradability during the start-up of an Anaerobic Sequence Batch Reactor –ASBR– using a simulate composition of the organic waste of food from Medellin – Colombia. Bachelor Thesis. BTU-Cottbus. P. 1-47

R Core Team (2019). R: A language and environment for statistical computing. R Foundation for Statistical Computing, Vienna, Austria. URL. <https://www.R-project.org/>

SAHU, G.K. (2008). Handbook of Piping Design. New Age International Publishers Pvt. Ltd. New Delhi.P.1-490. Reprint (2017)

SCHÖNFETER, R *et al* (2007) Best Biogas practice https://nachhaltigwirtschaften.at/resources/edz_pdf/0745_best_biogas_practise.pdf (accessed 27/06/19).

SCHWEINFURTH, K.; SCHULZE, R.; FUCHS, O.; MEURER, G; NAUMER, C. (2013). Konstruktion und Implementierung reaktors zur Kultivierung thermophiler Mikroorganismen / Construction and operation of a gas-lift bioreactor for cultivating thermophilic microorganisms. Blickwinkel • konstruktion. RWTH Aachen University and BRAIN AG. Germany.

SIEGEL, M.H; MERCHUK, J.C.; SCHUGERL, K. (1986). Air lift reactor analysis: Interrelationships between riser, downcomer, and gas-liquid separation behavior, including gas recirculation effects. AIChE -American institute of chemical engineers- Journal. Vol. 32. No. 10. P 1585-1596. P. 7-19.

SPYRIDON, A.: GERRIT, JWE. (2016). Theoretical analysis of biogas potential prediction from agricultural waste. Resource Efficient Technology 2, P.143-147.

UNKRIG, L. (2018). Verhalten von Tracern in einem aeroben diskontinuierlichen Biogasreaktor. Bachelorarbeit. BTU Cottbus, Germany. P.1.-47.

VDI 4630. (2016). Vergärung organischer Stoffe Substratcharakterisierung, Probenahme, Stoffdatenerhebung, Gärversuche/ Fermentation of organic materials Characterisation of the substrate, sampling, collection of material data, fermentation test. Verein Deutscher Ingenieure.

VUNJAK-NOVAKOVIC, G.; KIM, Y.; WU, X.; BERZIN, I.; MERCHUK, J. (2005). Air-Lift Bioreactors for Algal Growth on Flue Gas: Mathematical Modeling and Pilot-Plant Studies. American Chemical Society. Ind. Eng. Chem. 44, P. 6154-6163.

WOOD, L. A.; THOMPSON, P.W. (1987). Applications of the Air Lift Fermenter. Applied Biochemistry and Biotechnology. Vol 15. P. 131.

WU, X; MERCHUK, J. (2004). Simulation of algae growth in a bench scale internal loop airlift reactor. Chemical Engineering Science; Volume 59, Issue 14. P.2899-2912.

List of figures

Figure 1 Representation of the fermentation process..... 20

Figure 2 Biochemical steps in an anaerobic digester 21

Figure 3 The four steps of an ASBR: feeding, intermittent mixing, settling time, and withdrawal. 27

Figure 4 ALR configuration 30

Figure 5 Different types of ALR..... 31

Figure 6 Operation and design variables of ALR 34

Figure 7 Axial flow impellers. (a) Marine-type impeller; (b) Typical axial-flow turbine; (c) Portable mixer. 37

Figure 8 Axial impellers examples (a) including hydrofoil impellers(b)..... 38

Figure 9 Radial-flow impellers. (a) Flat-blade turbine; (b) Spiral backswept turbines; (c) Paddle impeller. 40

Figure 10 Radial impellers examples..... 42

Figure 11 Bar turbine, six blades bolted/welded to top and bottom of support disk. 43

Figure 12 Anchor, two blades with or without cross arm..... 43

Figure 13 Reynolds experiments..... 49

Figure 14 Injection methods for tracer 51

Figure 15: Overview of the experimental setup of traditional ASBR..... 67

Figure 16. Overview of the experimental setup (ASBR, ASBR+B, CSTR) 69

Figure 17. Experimental set up of ALR reactor used for the homogenization test. 74

Figure 18 KG-ASBR gas-lift setup and distribution in the laboratory. 76

Figure 19 ST-ASBR stirred traditional reactor set up in the laboratory 77

Figure 20 Overview of the experimental setup comparison KG-ASBR and ST-ASBR 79

Figure 21 Values of design variables of ALR..... 90

Figure 22 Gas composition in volume percentage over time of the biogas produced 96

Figure 23 Comparison of PCH ₄ vs. OLR in the 3 reactors ASBR, ASBR+B and CSTR	97
Figure 24 Comparison of YCH ₄ vs. OLR in the 3 reactors ASBR, ASBR+B and CSTR	98
Figure 25 Results of homogenisation vs. mixing time at the three sensors of ALR.	104
Figure 26 Boxplot of the homogenization time in the positions of the ALR.....	105
Figure 27 Non-linear logistic adjusted model using each injection	108
Figure 28 Operating and design variables	112
Figure 29 Complete flow cycle in ALR	115
Figure 30 YCH ₄ in KG ASBR Figure 31 Y CH ₄ in ST -ASBR.....	119
Figure 32 MBRCH ₄ in KG ASBR Figure 33 MBR CH ₄ in ST -ASBR.....	120
Figure 34 YCH ₄ vs HRT in both reactors (KG-ASBR and ST-ASBR)	121
Figure 35 MBRCH ₄ vs HRT in both reactors (KG-ASBR and ST ASBR).....	122
Figure 36 Dynamic viscosity in KG ASBR (Anchor 71) and Figure 37 Dynamic viscosity in ST ASBR (Anchor 71).....	122
Figure 38 Dynamic viscosity in KG ASBR (Anchor 72) and Figure 39 Dynamic viscosity in ST ASBR (Anchor 72).....	122
Figure 40 OTS% in KG ASBR without mixing and Figure 41 OTS% in KG ASBR with mixing.....	123
Figure 42 OTS% in ST ASBR without mixing and Figure 43 OTS% in ST ASBR with mixing.....	124

List of tables

Table 1: Fruit and vegetable content of the four main groups of feed 80

Table 2: Substrate characteristics of organic waste 81

Table 3: Characteristics of the substrates used (hydrolysates) 82

Table 4 Evaluation of standard fermentation tests according to VDI 4630. 83

Table 5 Characteristics of hydrolysate produced in BTU Hall Lab..... 84

Table 6 Fermentation test results according to standard VDI 4630 84

Table 7. Cycle of a single stage ASBR- substrate organic food waste 86

Table 8 Cycle of a methanation stage of ASBR, ASBR+B and CSTR 86

Table 9 Cycle of a methanation stage of KG-ASBR and ST-ASBR 87

Table 10 Shows the mixing strategies for each week of sampling 88

Table 11 Velocities in the draft tube obtained in different scenarios 100

Table 12 Time to reach the homogenization 102

Table 13 Mean, Median and Standard Deviation of the homogenisation times... 105

Table 14 Results of ANOVA test 106

Table 15 Results of Levene Test..... 106

Table 16 Results of a non-linear logistic model 107

Annexes

Annex 1 KCl calibration curve

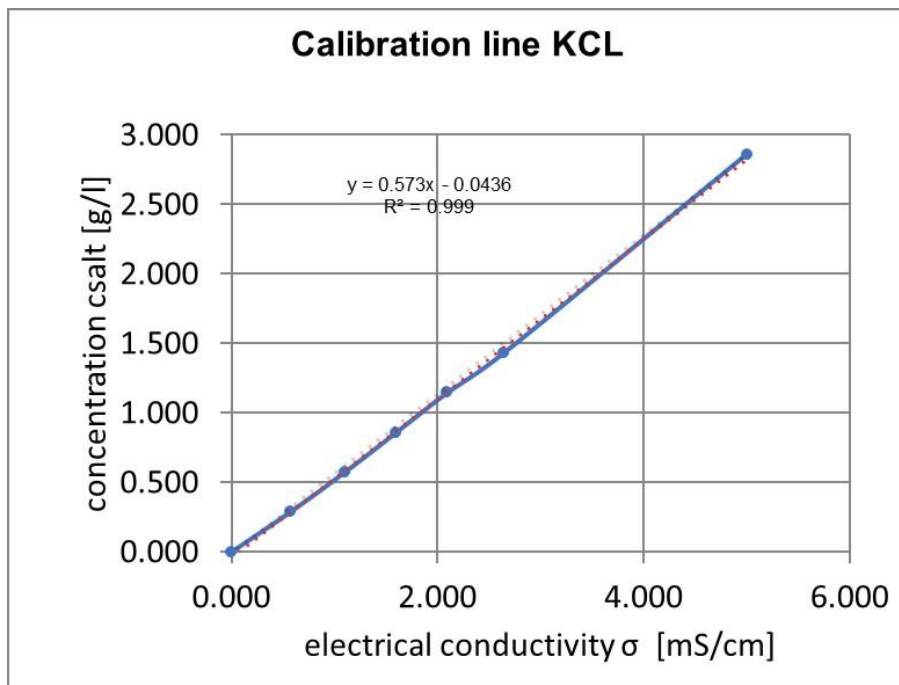
The electrical conductivity of the water is measured at certain intervals. Without a calibration line an evaluation of the electrical conductivity measurements is not possible. Using the calibration line, the corresponding KCl concentration [g/l] can be read off for any electrical conductivity [mS/cm].

Seven litres of water are poured into a bucket and portions of KCl are gradually added. After each individual addition, the KCl-water mixture is whisked with a stirrer to bring all the salt into solution. When all salt is dissolved, the electrical conductivity is measured.

At the beginning the electrical conductivity increases proportionally with the amount of salt. From a certain amount of salt saturation occurs, i.e. the existing amount of water is no longer able to dissolve the salt. The linear range is left, and the electrical conductivity no longer increases proportionally to the quantity of salt added. This completes the calibration. The salt solution thus prepared is used further on in the following as a tracer for the experiment.

The following measured values were recorded during calibration:

		Water volume [l]	7.0		
		Base line elec. conductivity σ_0 [mS/cm]	0.0072		
single amount salt KCl [g]	total amount salt [g]	concentration c_{salt} [g/l]	electrical conductivity σ [mS/cm]	$\sigma - \sigma_0$ [mS/cm]	
0	0	0.000	0	0.000	
2	2	0.286	0.575	0.568	
2	4	0.571	1.105	1.098	
2	6	0.857	1.603	1.596	
2	8	1.143	2.1	2.093	
2	10	1.429	2.65	2.643	
10	20	2.857	5.01	5.003	



Source: Own elaboration

Up to about 5 mS/cm there is a linear relationship between electrical conductivity and salt concentration. To create the calibration line, therefore, only those measured values that lie within this range are selected.

Annex 2 Uranine Video. For references please contact the author

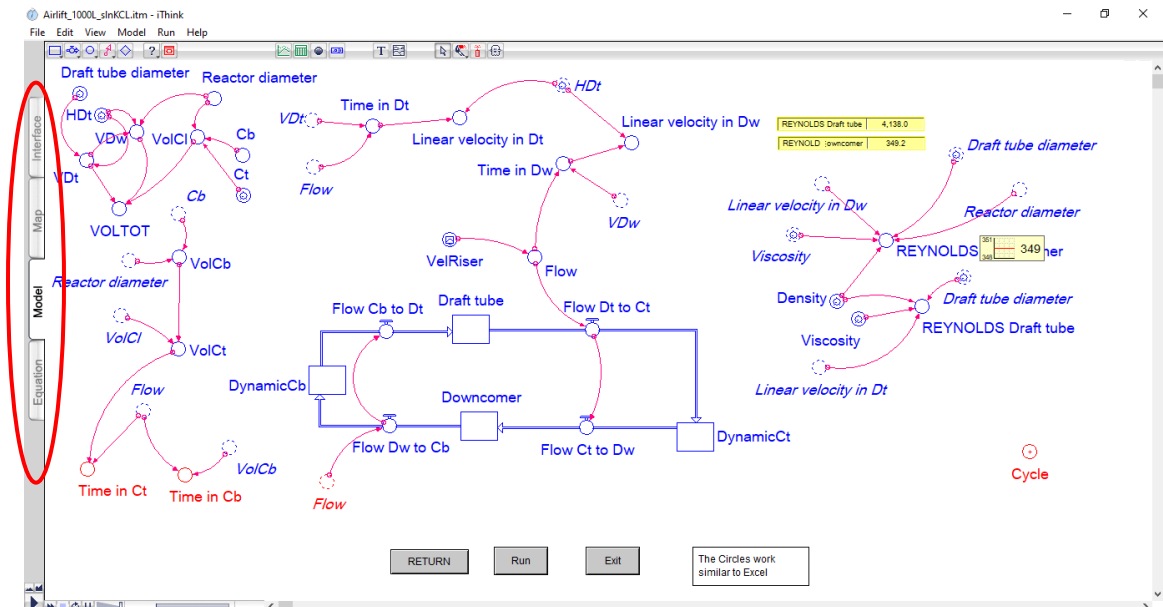
Annex 3 Mathematical model

Tutorial: Model simulation in IThink

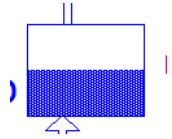
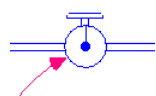

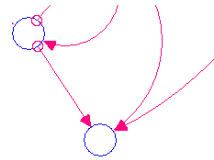
1. IThink 9.0.2.
2. File Open → ModelAirlift Airlift_1000L_sl_n_KCL.itm


“Model Window”.

The software has 4 windows on the left side, the first window that is shown when the AirLift_1000L_sl_nKCl file is opened is called "**model**". In this window the level variables, timers, flows are created, and the specifications required to run the model are defined.

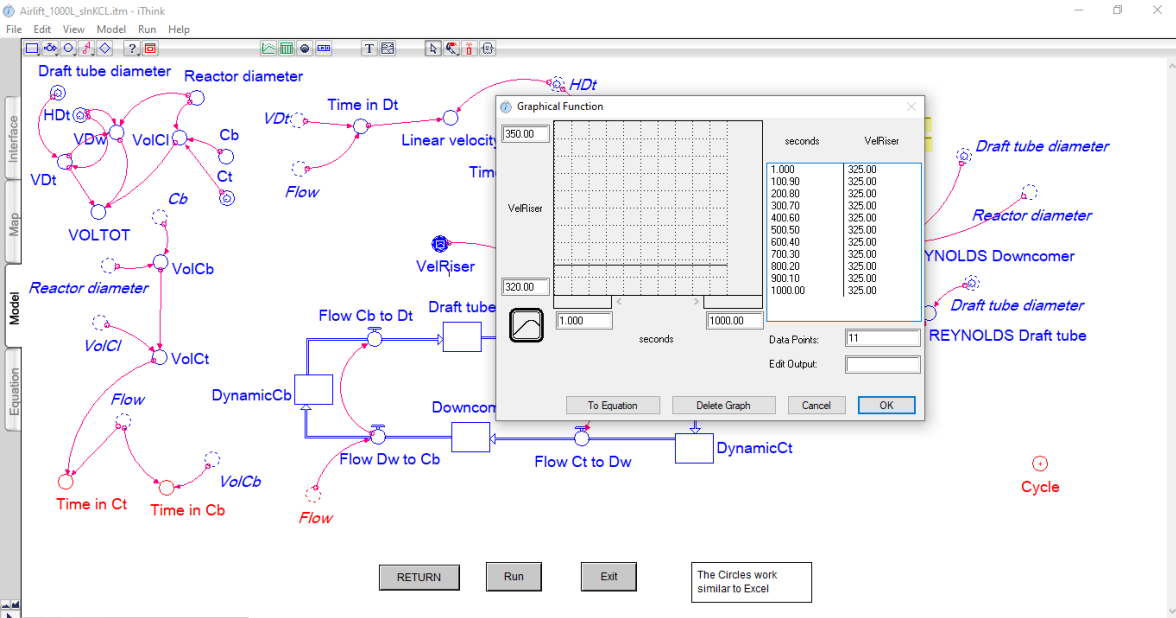


The screenshot shows the 4 commands that were used in this model, each of the circles and boxes defines the formulas and values that were described in numbers 6.4 and 7.3.4. To access each of them, double click on the command.

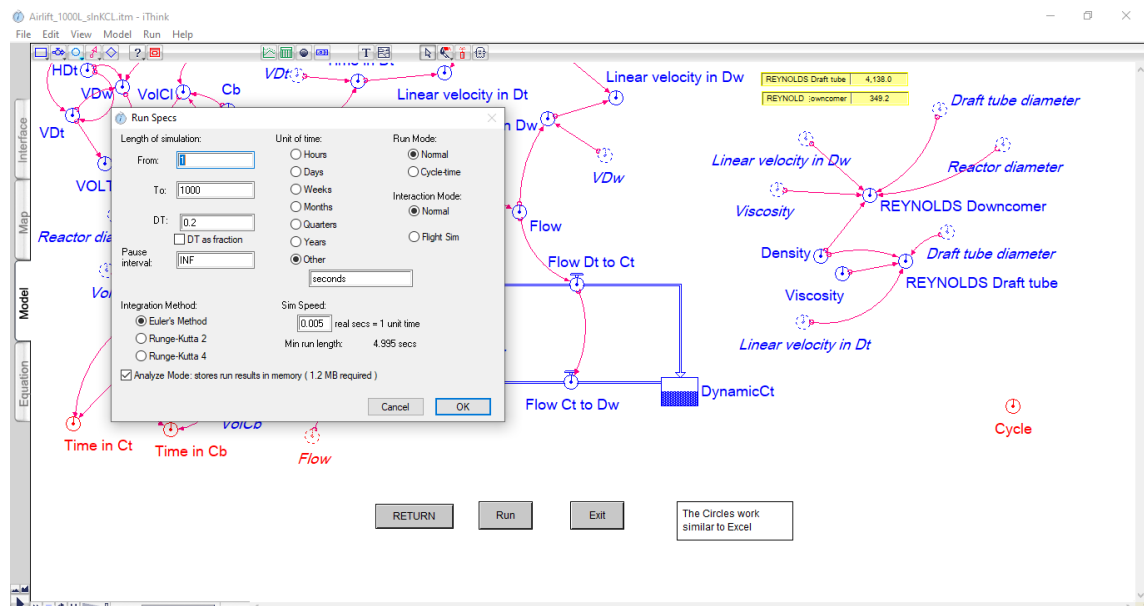
<p>Stock</p> 	<p>The Stock (tank) is a level variable, the tank values can change with the time, what makes the system dynamic are the level variables. This tank feeds with input or output flows that make this variable able to change its value through time.</p>
<p>Flow</p> 	<p>The flows (keys) are rates per time unit. The only thing that makes the level variable change the value is a flow. Keys opens or closes to increases or decreases the value over time. It is important to emphasize that level variables must have the same units as flow variables. The latter (flows) always over a unit of time.</p>
<p>Converter</p> 	<p>Then all that makes the key open or close are the signal converters.</p>
<p>Feedback loops (connector)</p> 	<p>Its function is to connect the commands between converters and flows, producing a cause – effect. Feedback occurs when outputs of a system are routed back as inputs as part of a chain of cause-and-effect that forms a circuit or loop.</p>
<p>Ghost</p>	<p>An additional command called ghost was used to copy a previously created variable that is</p>

	<p>required to be used in an additional calculation, such as diameters, velocities and volumes, by preventing so many connectors coming out of the same point.</p>
---	--

This window called " model " allows to classify a graphic function as an Excel sheet does. In the graphic function, the average velocity determined in flow characterization test (with flowmeter - numeral 7.3.1) was also used to set the velocity value in the riser (VelRiser or in the draft tube). The model, however, allows to modify this velocity in a range between 320 and 350 l/min or other desired range, simply use the mouse to set the desired value. In this case, the velocity was set at 325 l/min whose value is the average of the flow characterized during the tests and was set as a constant that does not change over time.



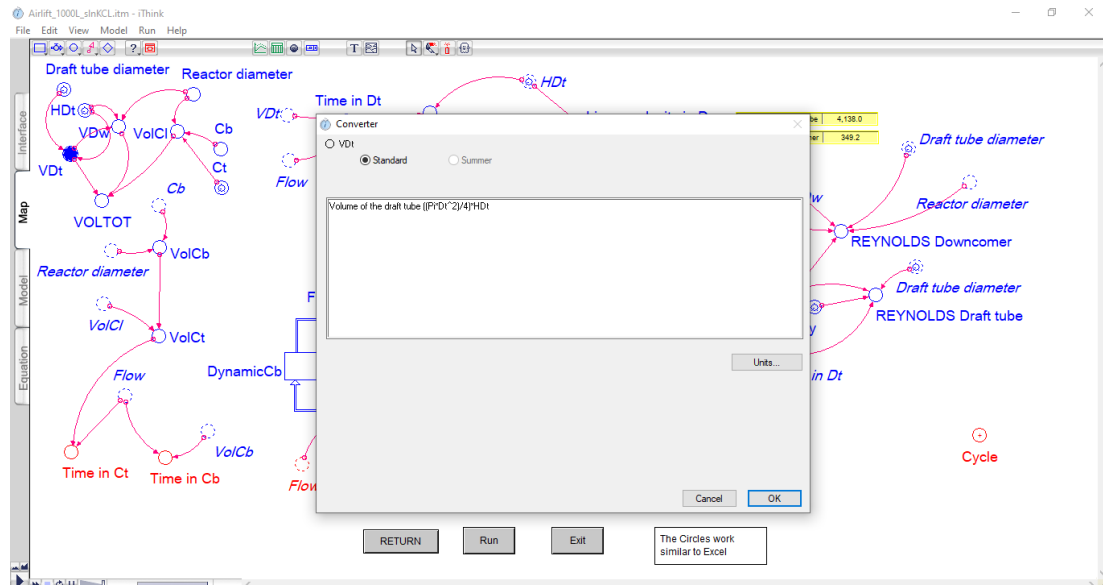
In the upper window called Run, the run specifications are defined for this model, in which a modeling interval between 1 and 1000 seconds was established. This means that the model was run in a time range greater than the mixing time previously determined in the theoretical mathematical model to achieve homogenization within the reactor (greater than 3.17 minutes or 190.49 seconds):



In these run specifications the unit of time was define in seconds, in a range between 1 to 1000 seconds of simulation; in the computer the model information is updated each time differential, in this case a differential of 0.2 was assumed, thas mean it is updated 5 times in 1 second. Finally, to run the model is possible to use the "Run" button.

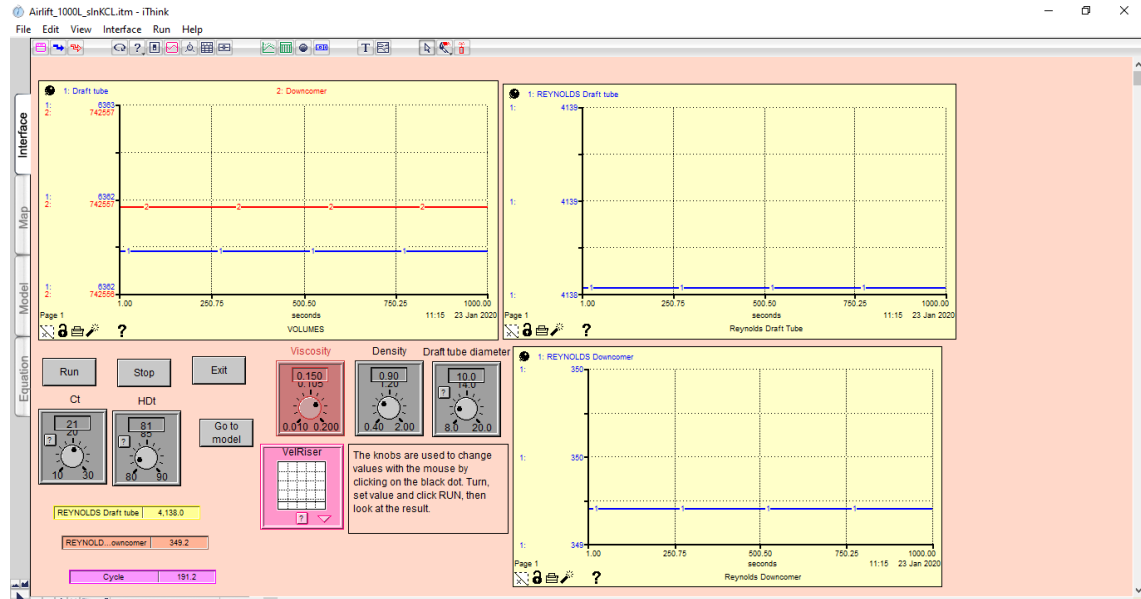
“Map Window”

In the window called “model” only allows to enter the values of the level variables or the converters, while in the “Map” window it is possible to make descriptions of those values, for example, explain the change of units to centimeters or the calculation of a specific converter as in the case of the calculation of the volume of the draft tube.



“Interface Window”

In this window the results of the variables of the model that are desired to know can be displayed graphically. It is called “interface” window because it is a control panel that allows to modify variables. In this case, the knobs or buttons that represent the variables that influence others were selected. For example, the height and diameter of the draft tube influence the linear velocity.

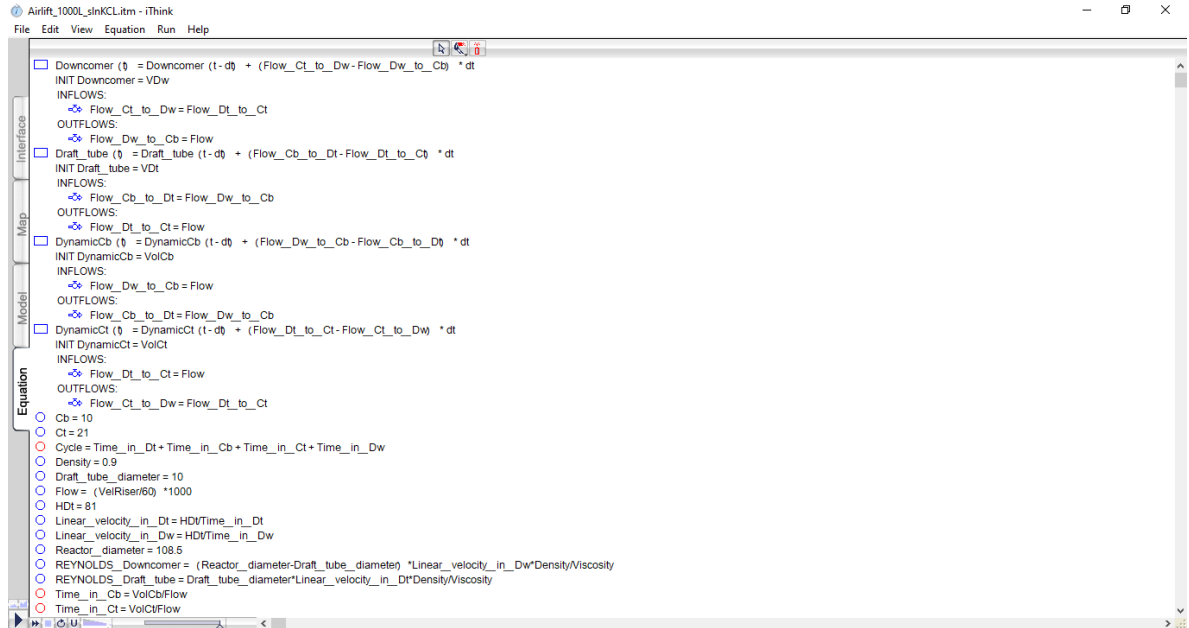


Likewise, the values of the viscosity can be modified to see how this type of reactor behaves in non-Newtonian fluids, even varying the velocity of the riser.

The final graphs show that the flow characterization values using the Reynolds number, which validate the exercise that was performed to know the flow characteristics in the draft tube and to know how the hydrodynamic behavior of the reactor would be.

Both in the experimental part and in the simulation, a laminar flow regime is presented in the downcomer zone, which negatively influences the sedimentation of particles in the bottom clearance.

“Equation Window”.



In this window, the finite difference equations are presented, it is something additional that is not include in all system dynamics software. In this case, Δt (DT) represents how often the values are updated and in this model as the level variable does not change drastically then the Euler’s method was selected. These are the equations:

$$\text{Downcomer}(t) = \text{Downcomer}(t - dt) + (\text{Flow_Ct_to_Dw} - \text{Flow_Dw_to_Cb}) * dt$$

$$\text{INIT Downcomer} = \text{VDw}$$

INFLOWS:

$$\text{Flow_Ct_to_Dw} = \text{Flow_Dt_to_Ct}$$

OUTFLOWS:

$$\text{Flow_Dw_to_Cb} = \text{Flow}$$

$$\text{Draft_tube}(t) = \text{Draft_tube}(t - dt) + (\text{Flow_Cb_to_Dt} - \text{Flow_Dt_to_Ct}) * dt$$

$$\text{INIT Draft_tube} = \text{VDt}$$

INFLOWS:

$$\text{Flow_Cb_to_Dt} = \text{Flow_Dw_to_Cb}$$

OUTFLOWS:

$$\text{Flow_Dt_to_Ct} = \text{Flow}$$

$$\text{DynamicCb}(t) = \text{DynamicCb}(t - dt) + (\text{Flow_Dw_to_Cb} - \text{Flow_Cb_to_Dt}) * dt$$

$$\text{INIT DynamicCb} = \text{VolCb}$$

INFLOWS:

$$\text{Flow_Dw_to_Cb} = \text{Flow}$$

OUTFLOWS:

$$\text{Flow_Cb_to_Dt} = \text{Flow_Dw_to_Cb}$$

$$\text{DynamicCt}(t) = \text{DynamicCt}(t - dt) + (\text{Flow_Dt_to_Ct} - \text{Flow_Ct_to_Dw}) * dt$$

$$\text{INIT DynamicCt} = \text{VolCt}$$

INFLOWS:

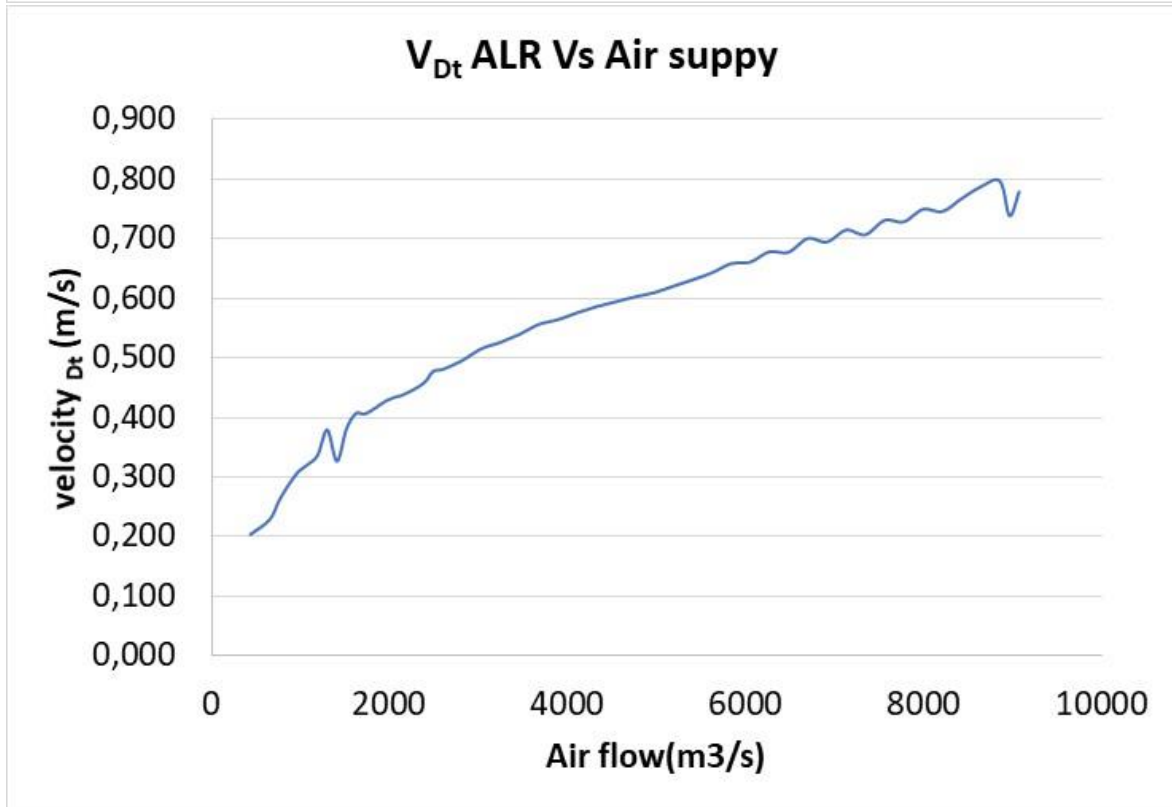
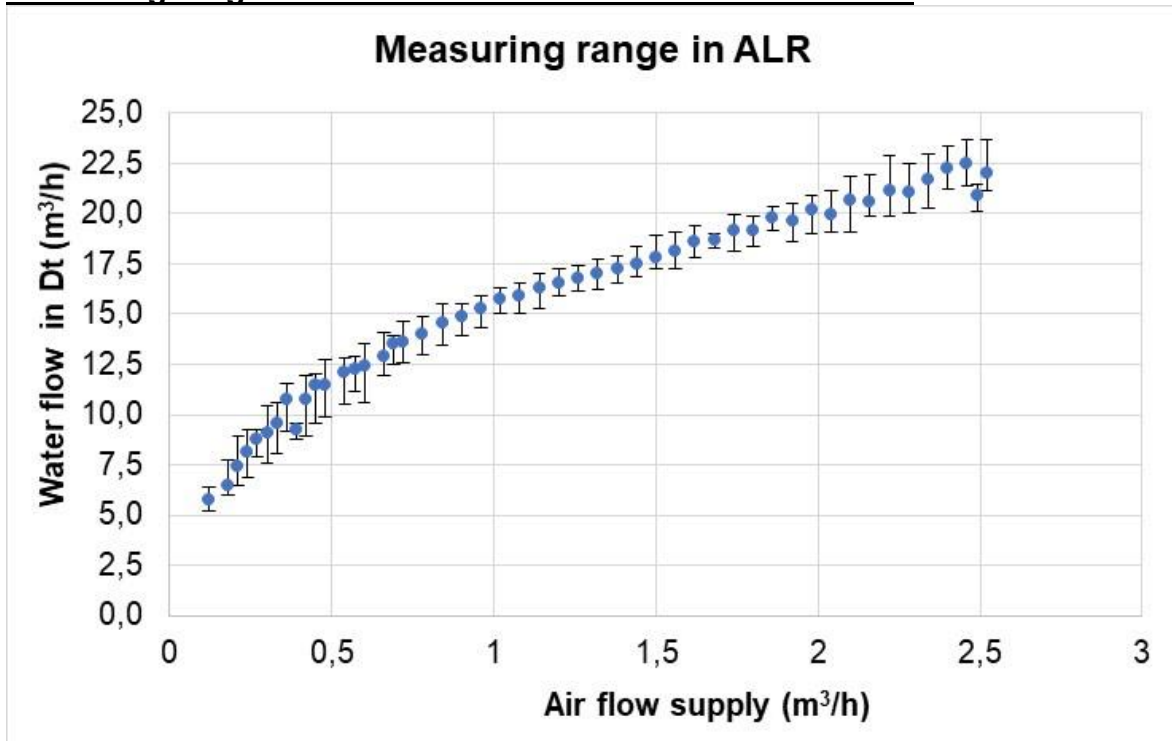
$$\text{Flow_Dt_to_Ct} = \text{Flow}$$

OUTFLOWS:

$$\text{Flow_Ct_to_Dw} = \text{Flow_Dt_to_Ct}$$

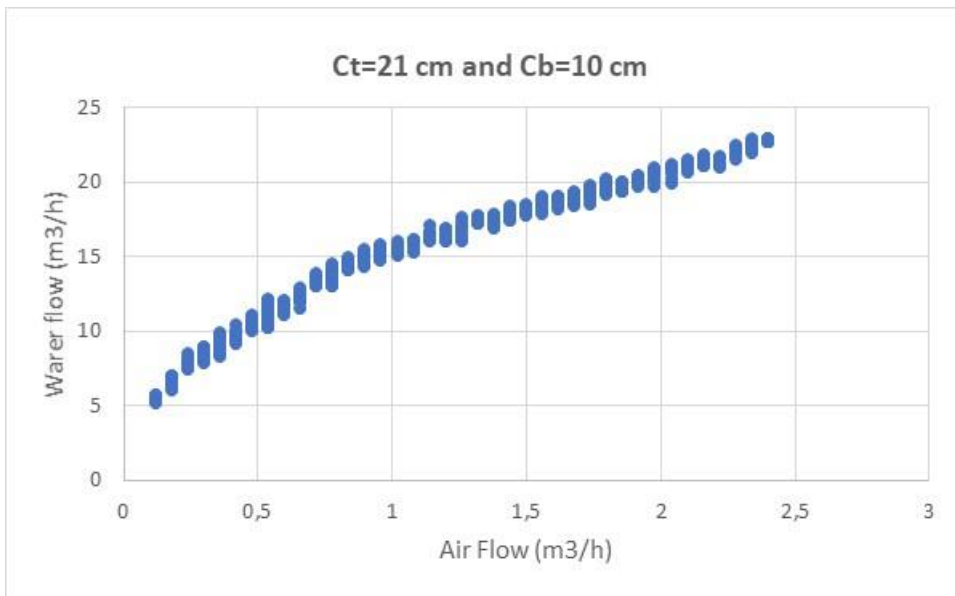
Annex 4 Graphics characterization flow in ALR

Measuring range in flowmeter and rotameter of ALR reactor

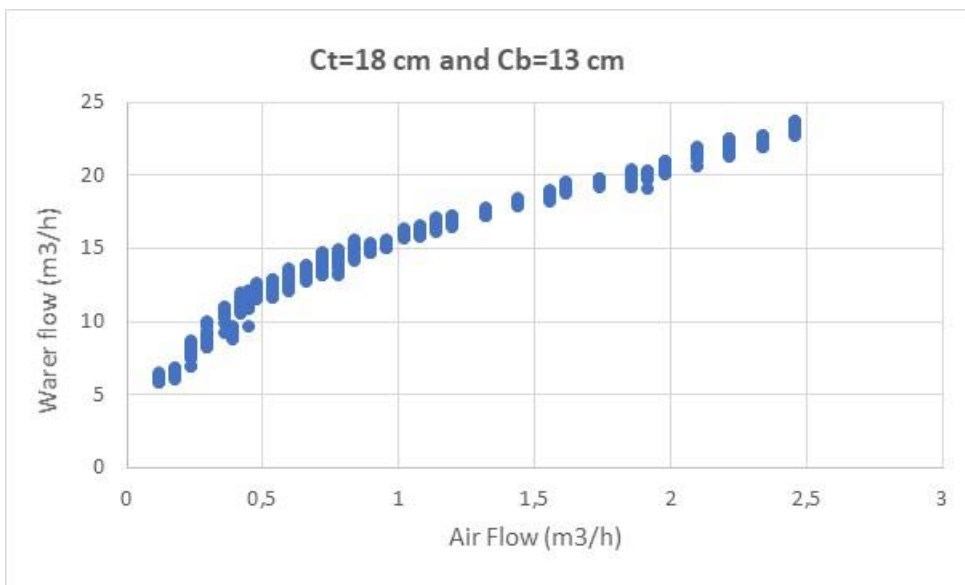


Graphs of the three draft tube positions in relation to the clearances region Ct and Cb

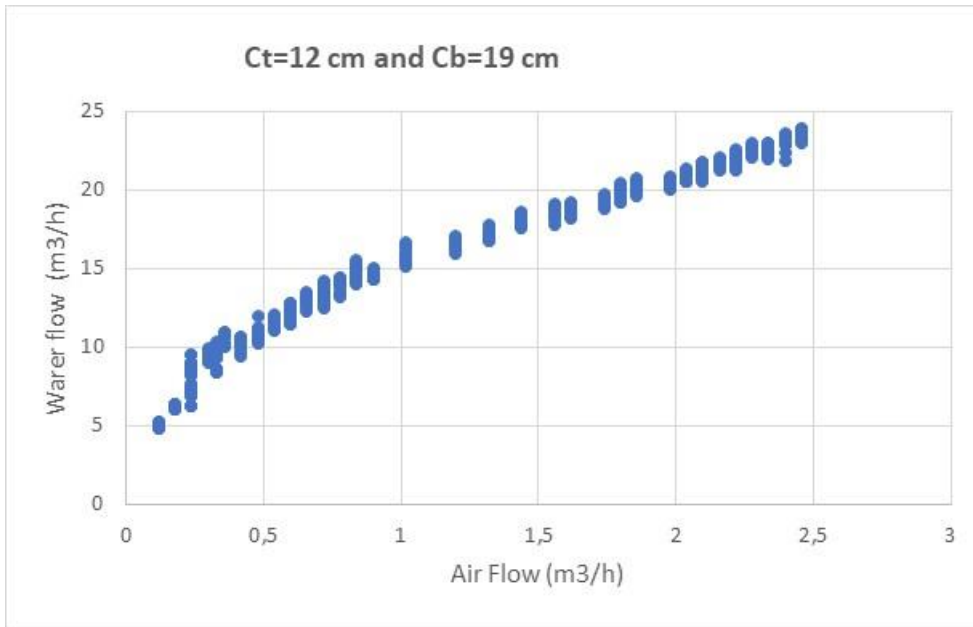
Water and air flow behavior for a top clearance (Ct:21 cm) and bottom clearance (Cb:10 cm).



Water and air flow behavior for a top clearance (Ct:18 cm) and bottom clearance (Cb:13 cm).



Water and air flow behavior for a top clearance (Ct:12 cm) and bottom clearance (Cb:19 cm).



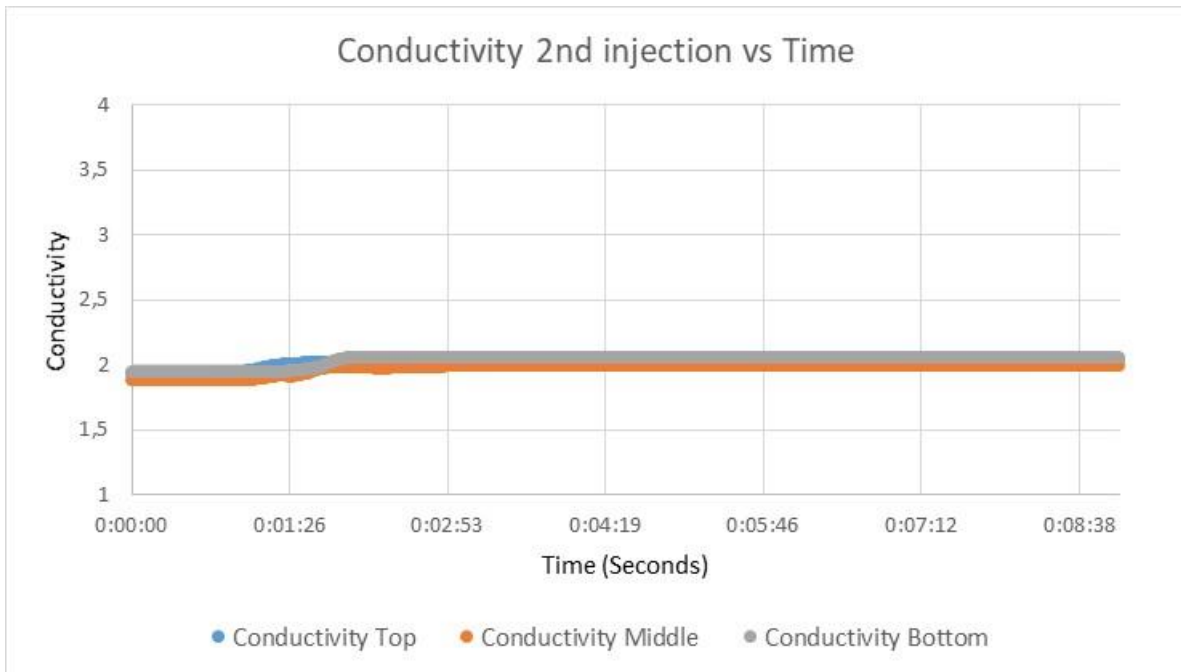
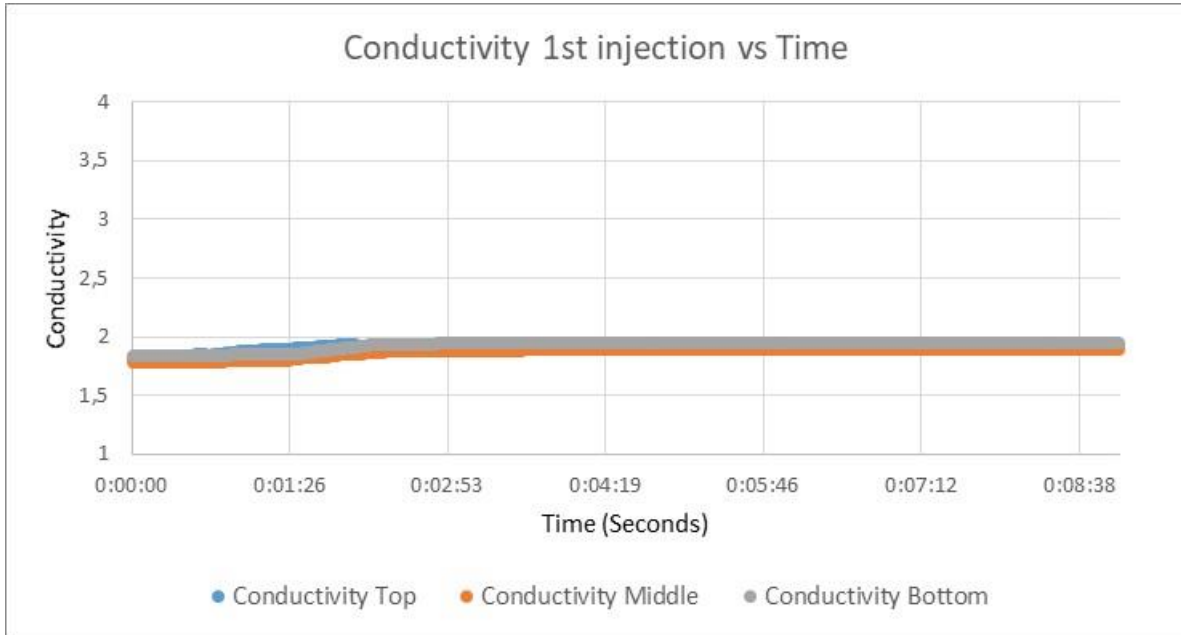
For measuring data see Annex 4.1 and Annex 4.2.

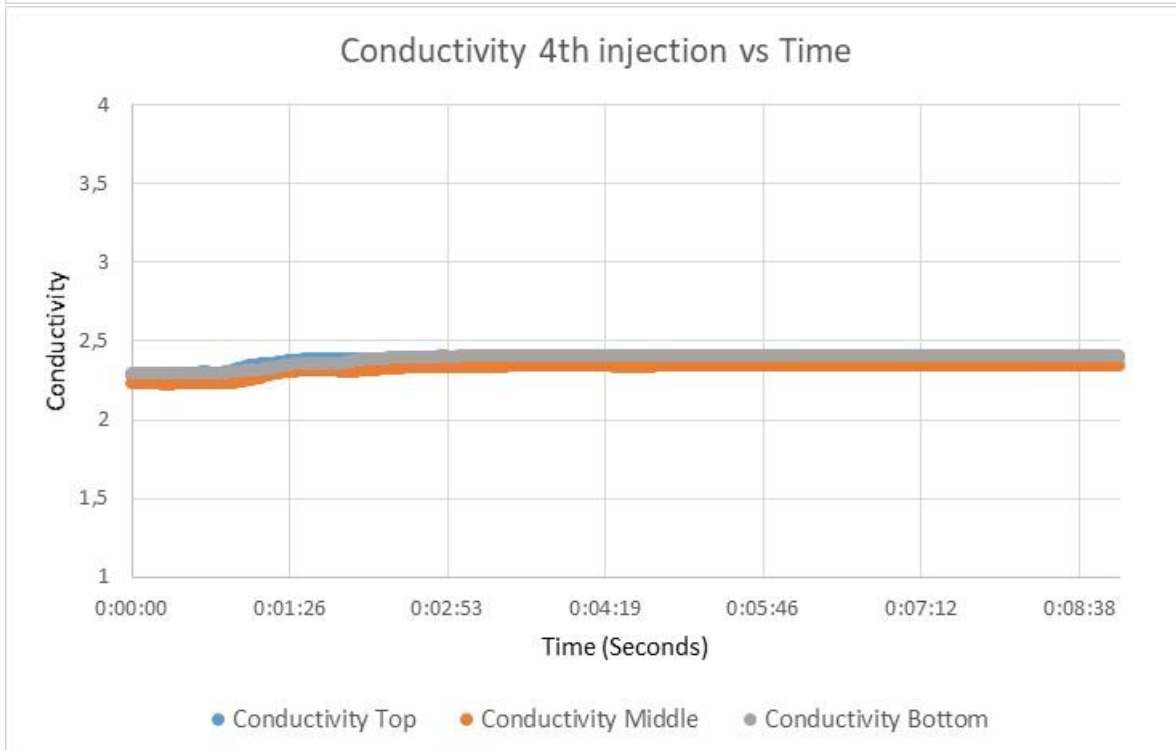
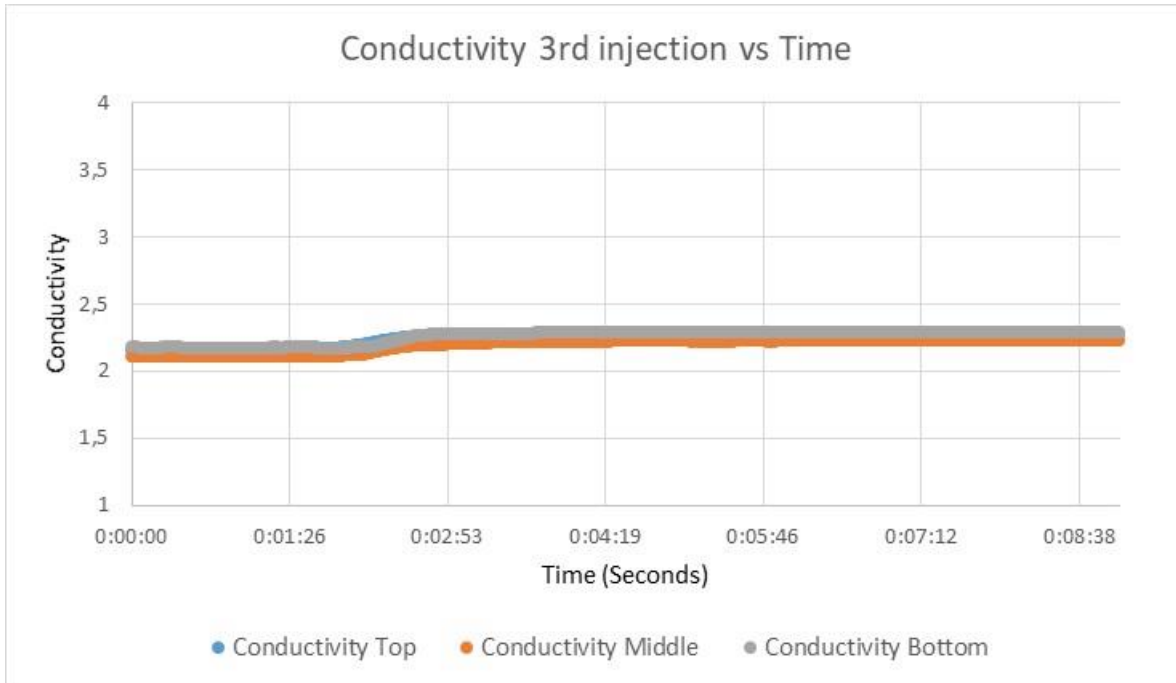
Annex 5 Conductivity and Homogenization data/graphics.

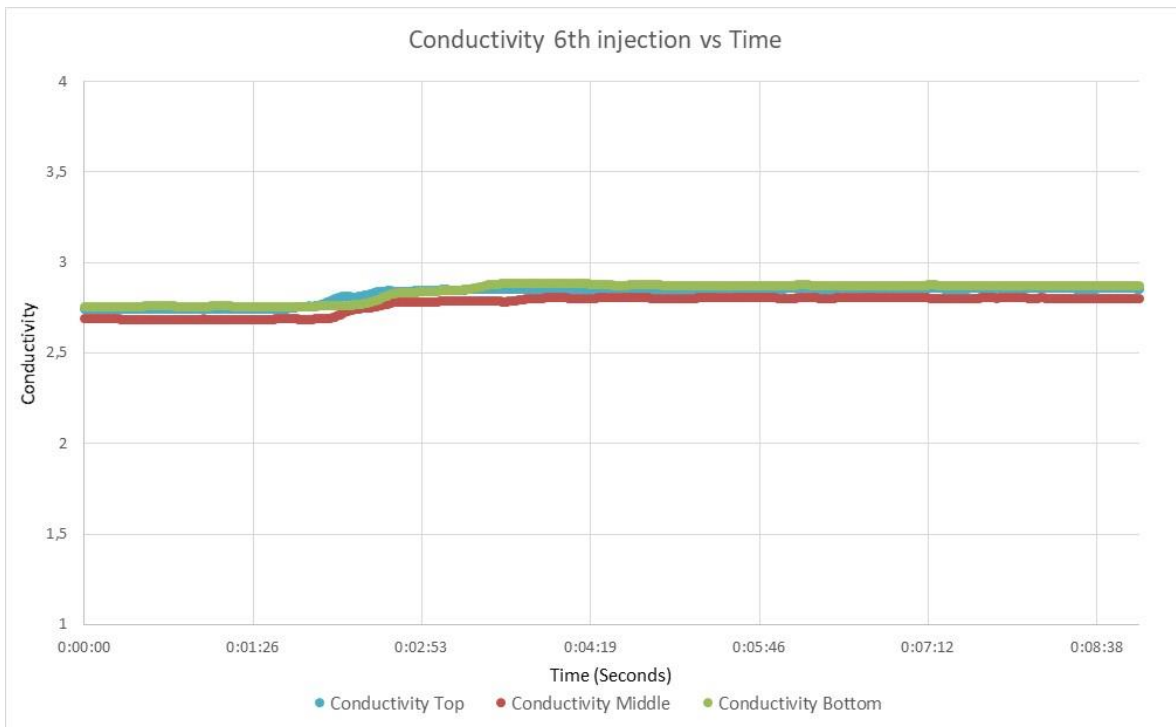
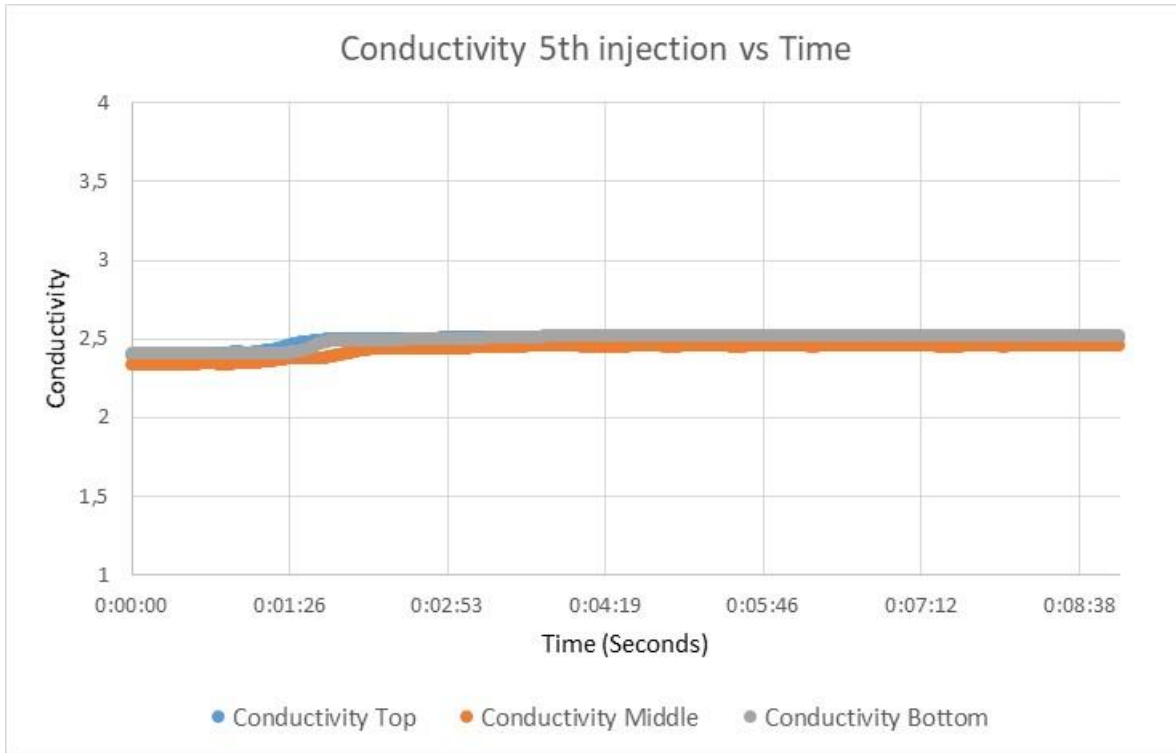
Mixing time in each injection of tracer test (KCL) in ALR

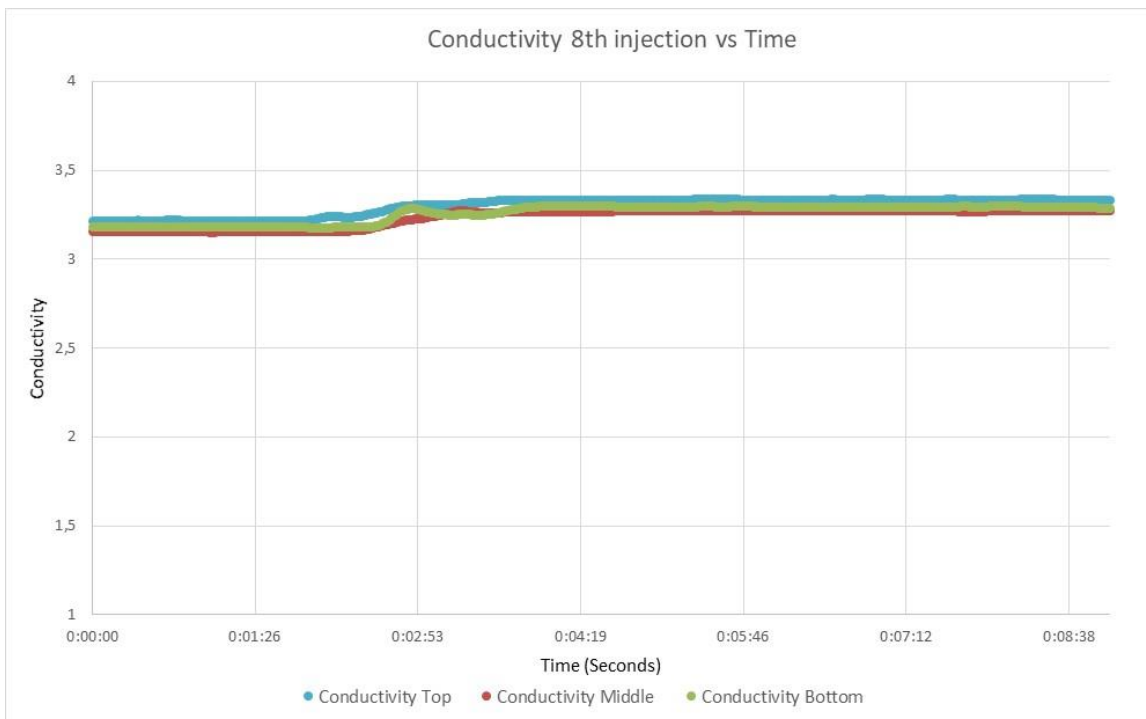
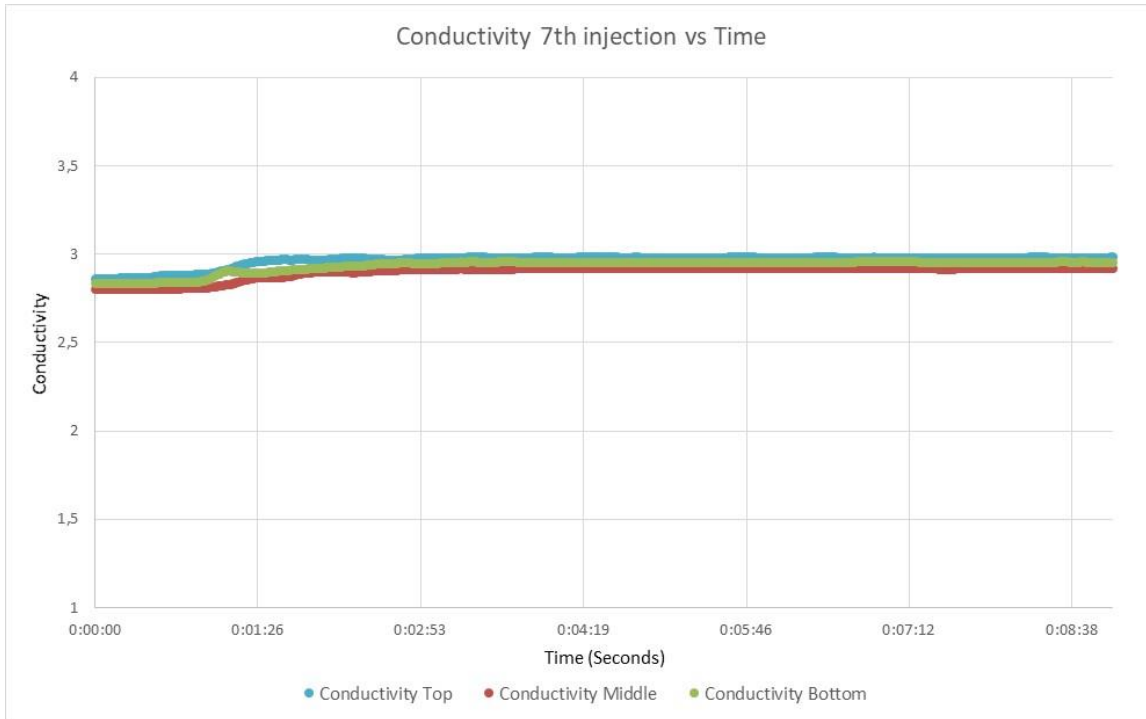
		Start	End	Delta time
1st injection	Top	00:01:02	00:03:39	00:02:37
	Middle	00:01:02	00:04:31	00:03:29
	Bottom	00:01:02	00:04:01	00:02:59
2nd injection	Top	00:10:18	00:13:13	00:02:55
	Middle	00:10:18	00:13:28	00:03:10
	Bottom	00:10:18	00:13:27	00:03:09
3rd injection	Top	00:44:17	00:48:11	00:03:54
	Middle	00:44:17	00:48:19	00:04:02
	Bottom	00:44:17	00:48:40	00:04:23
4th injection	Top	02:49:28	02:52:29	00:03:01
	Middle	02:49:28	02:52:50	00:03:22
	Bottom	02:49:28	02:52:54	00:03:26
5th injection	Top	03:02:06	03:05:05	00:02:59
	Middle	03:02:06	03:05:37	00:03:31
	Bottom	03:02:06	03:06:06	00:04:00
6th injection	Top	03:42:59	03:46:24	00:03:25
	Middle	03:42:59	03:46:48	00:03:49
	Bottom	03:42:59	03:46:28	00:03:29
7th injection	Top	04:25:01	04:28:06	00:03:05
	Middle	04:25:01	04:28:14	00:03:13
	Bottom	04:25:01	04:28:06	00:03:05
8th injection	Top	05:27:04	05:31:15	00:04:11
	Middle	05:27:04	05:30:17	00:03:13
	Bottom	05:27:04	05:30:58	00:03:54
9th injection	Top	00:28:13	00:30:43	00:02:30
	Middle	00:28:13	00:30:51	00:02:38
	Bottom	00:28:13	00:31:15	00:03:02

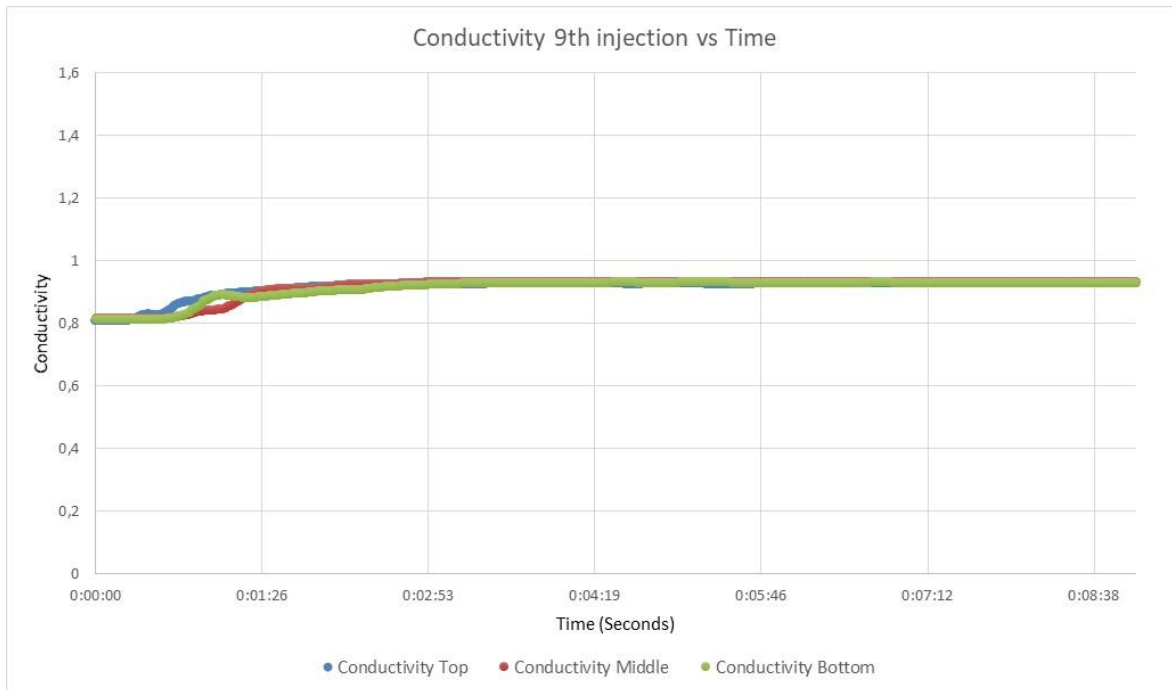
Injections from 1st to 9th Conductivity Graphics vs mixing time in seconds



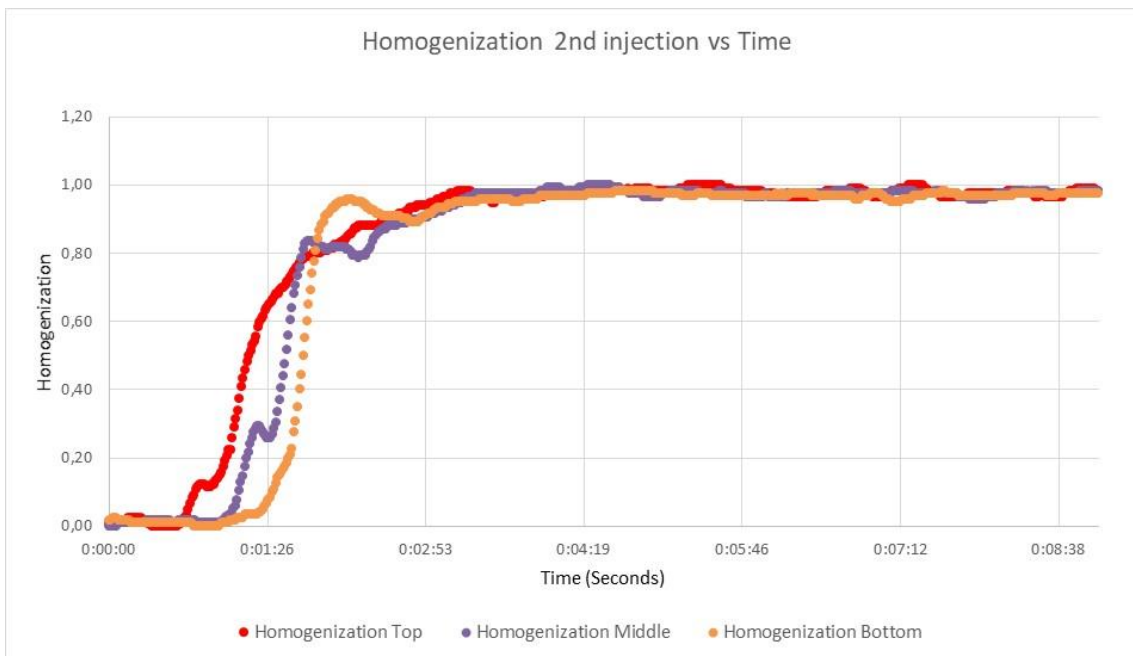
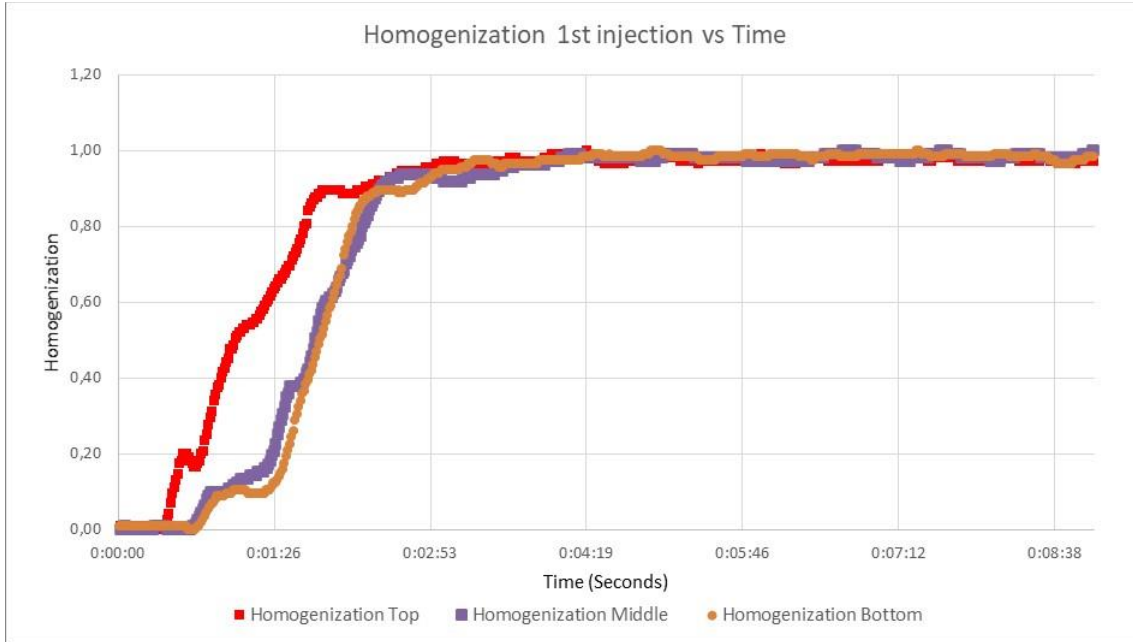


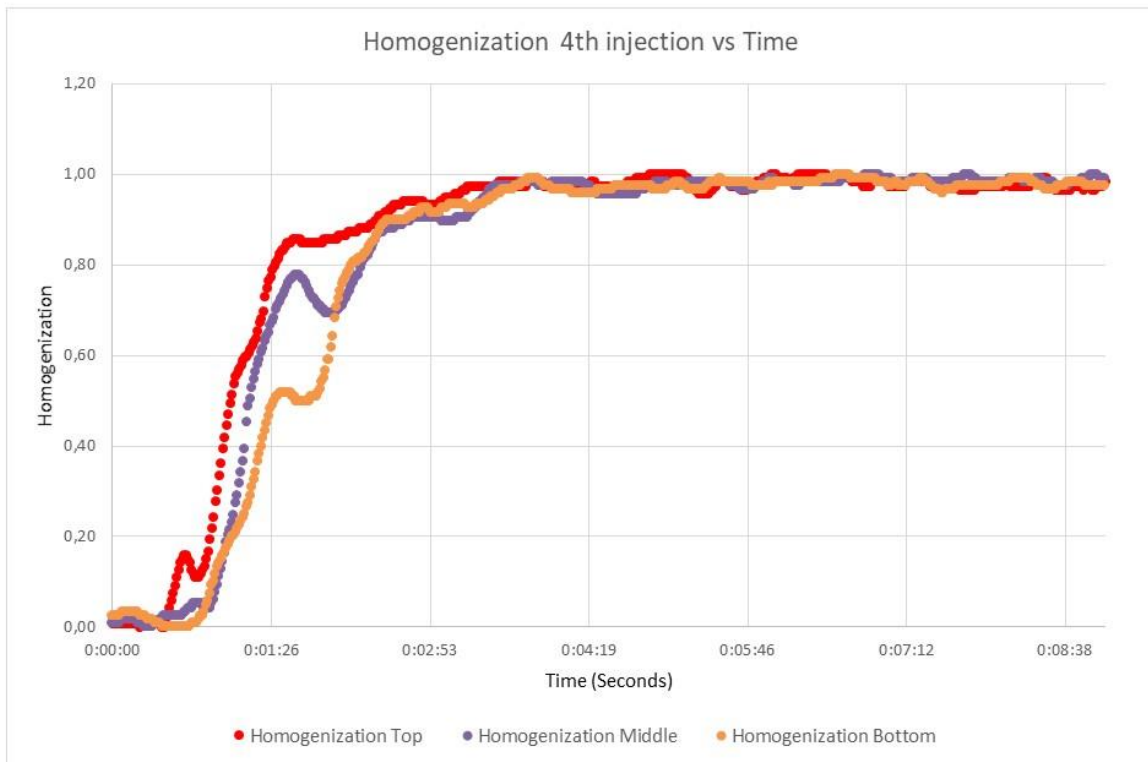
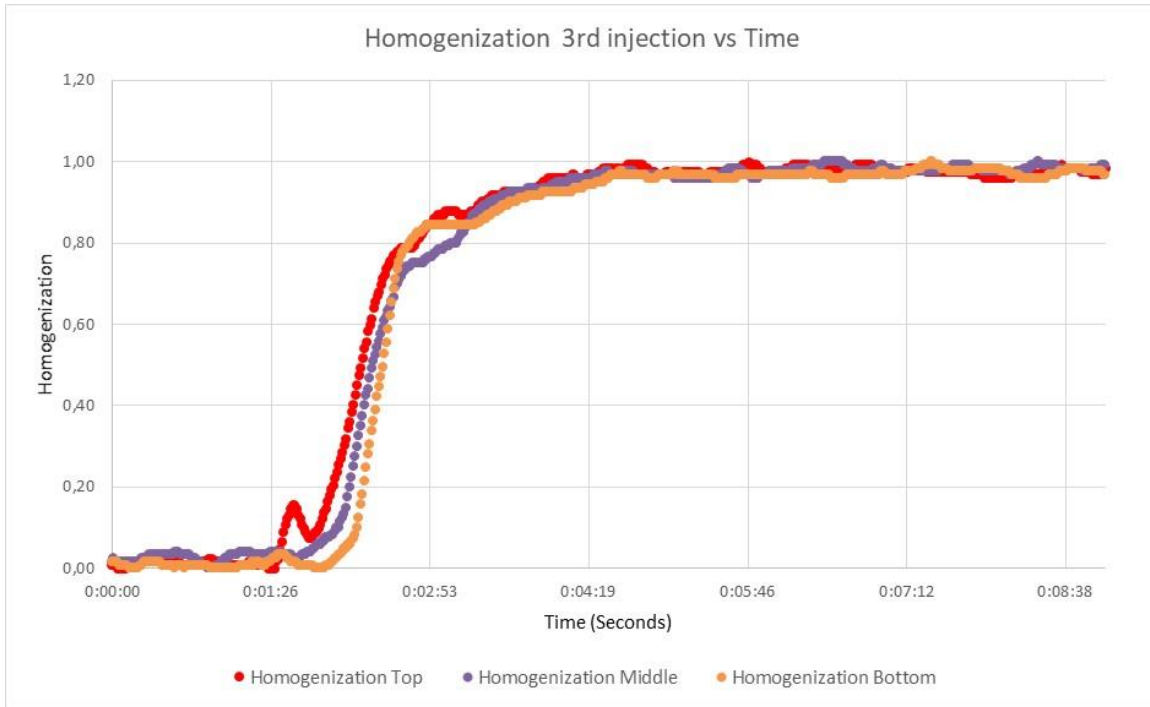


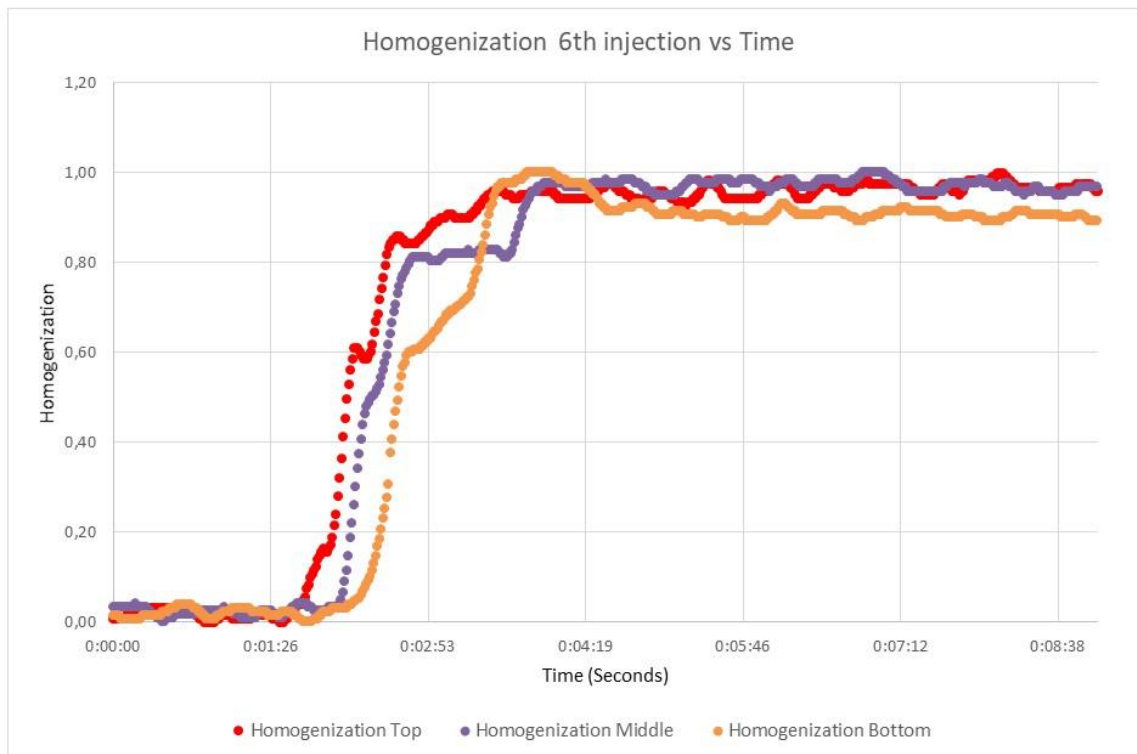
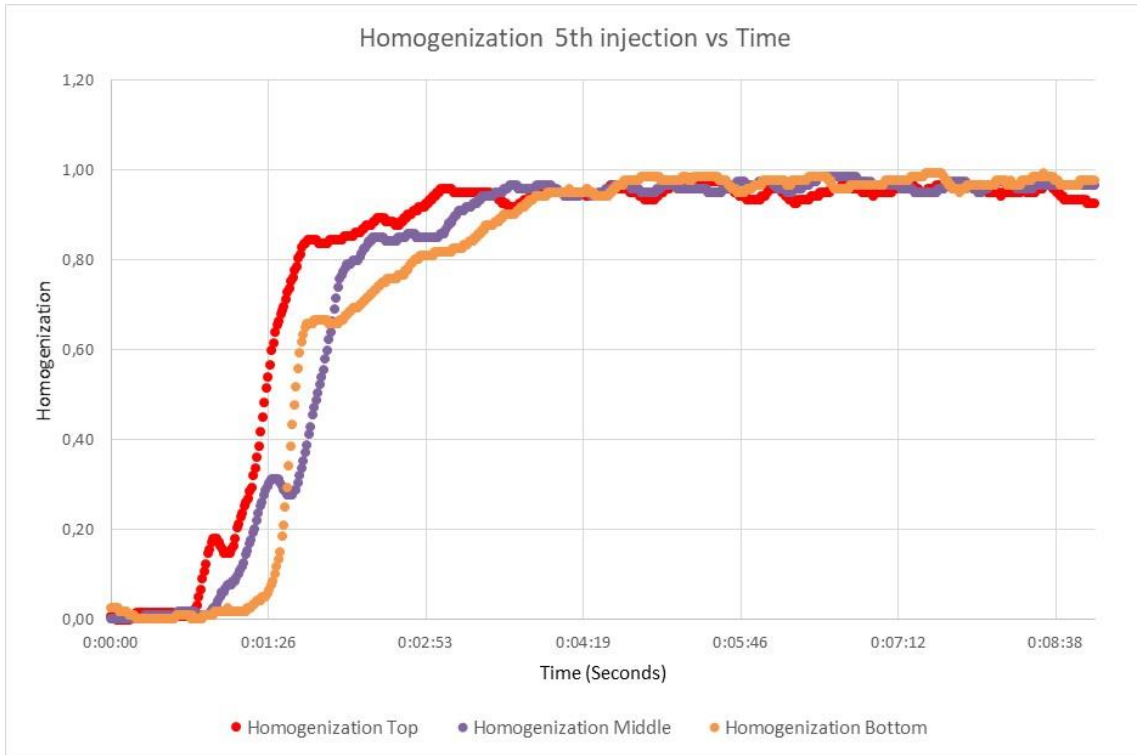


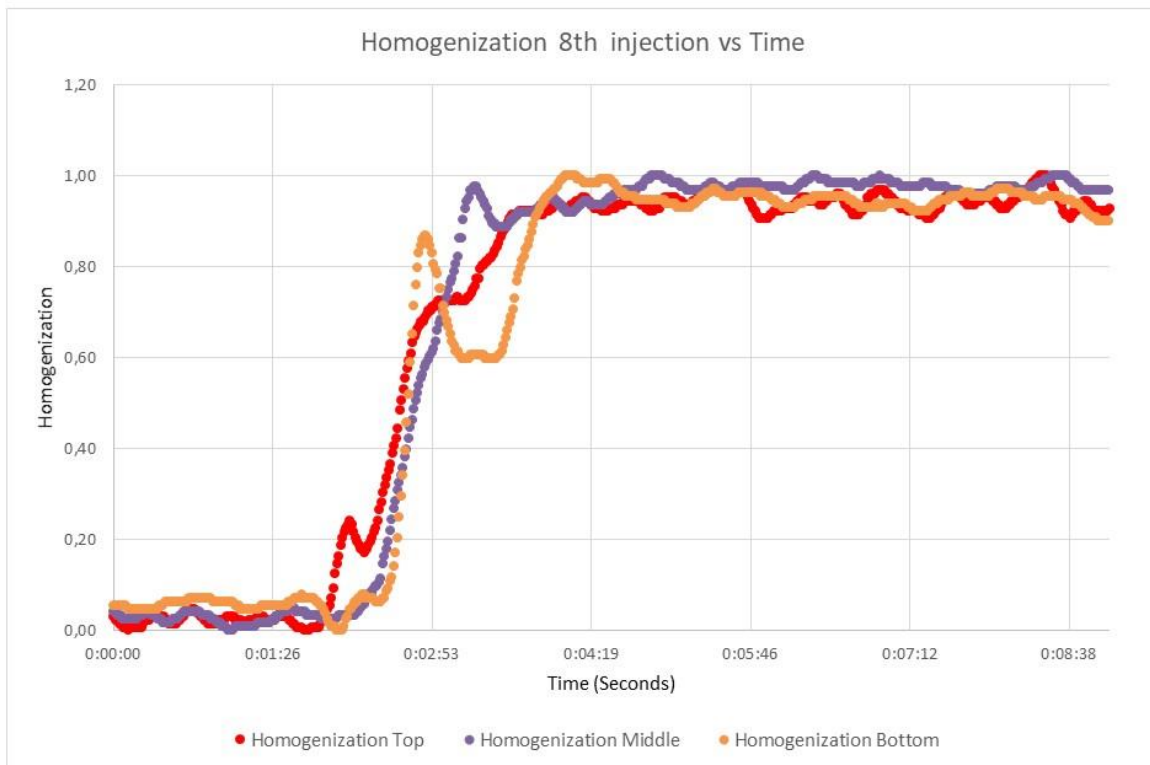
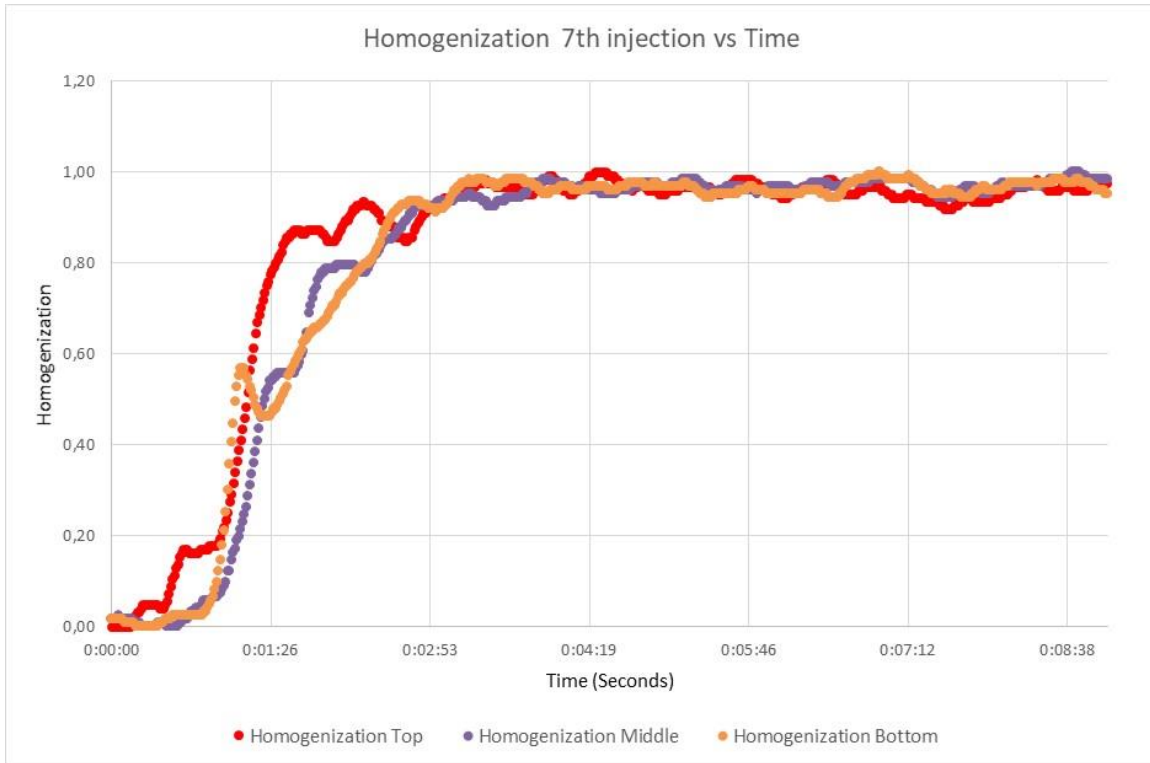


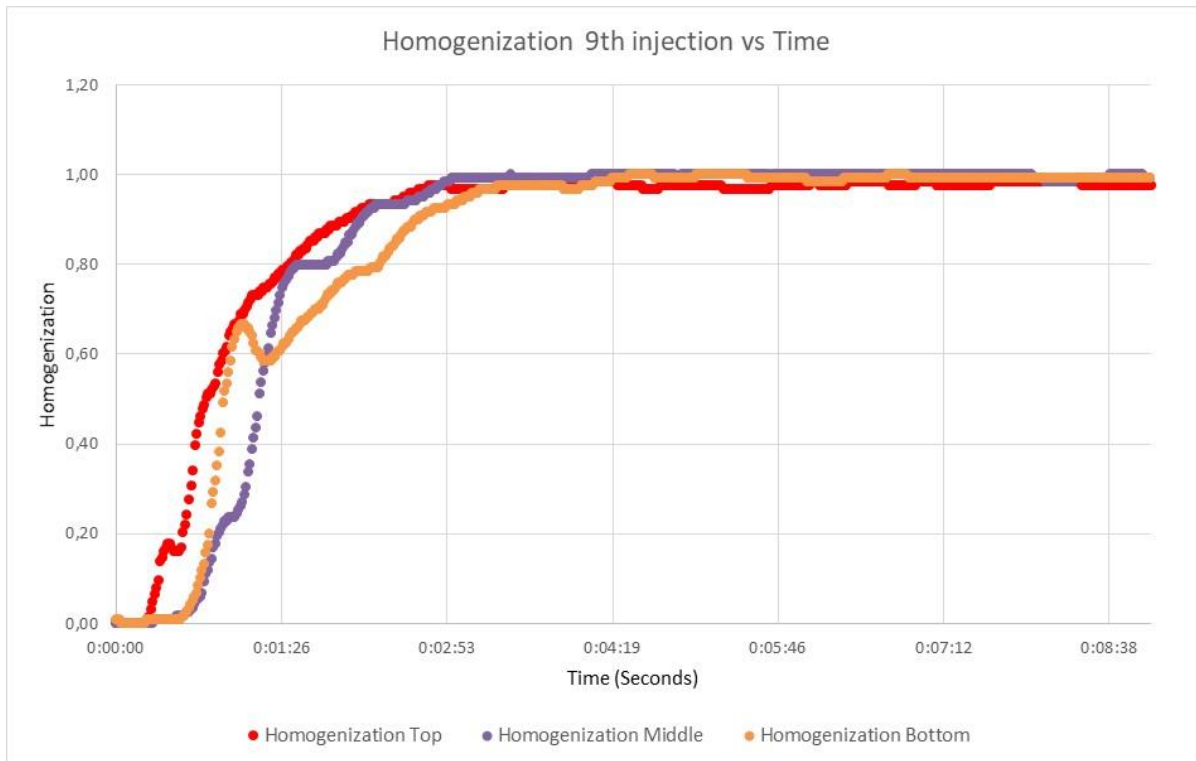
Injection from 1st to 9th Graphics Homogenization vs time to reach homogenization in seconds











For measuring data see Annex 5 -A.

For measuring data references see Annex 6, 7 and 8 in the appendix of this thesis

Annex 6 Reactors comparison methane and productivity yield

- Annex 6.1. Comparison KG ASBR
- Annex 6.2. Comparison ST ASBR

Annex 7 Dynamic viscosity database

Annex 8 Reactors comparison OTS and TS database

- Annex 8.1. Comparison OTS and TS - KG ASBR
- Annex 8.2. Comparison OTS and TS - ST ASBR